UNIVERSITY OF CALIFORNIA
RIVERSIDE

Regulation of the G Protein Alpha Subunits in Mutants Lacking the G Beta Subunit or a Cytosolic Guanine Nucleotide Exchange Factor in *Neurospora crassa.*

A Dissertation submitted in partial satisfaction
of the requirements for the degree of

Doctor of Philosophy

in

Genetics, Genomics and Bioinformatics

by

Alexander Vladimirovich Michkov

December 2014

Dissertation Committee:
Dr. Katherine A. Borkovich, Chairperson
Dr. Julia Bailey-Serres
Dr. Karine G. Le Roch

The Dissertation of Alexander Vladimirovich Michkov is approved:

_____

_____

_____

Committee Chairperson

University of California, Riverside

ACKNOWLEDGEMENTS

First and foremost, I deeply grateful to my supervisor, Dr. Katherine A. Borkovich, for guidance, encouragement and support throughout my graduate studies. Her passion for science, expansive knowledge, and great intuition always inspired me to become a good researcher and pursue an academic career. I am thankful to my dissertation committee members, Dr. Julia Bailey-Serres and Dr. Karine G. Le Roch, whose advice and patience helped make my dissertation possible.

I am also thankful to Dr. Reed Sorenson from the Dr. Julia Bailey-Serres laboratory for help with establishing the polysome-profiling protocol.

I thank Deidra Kornfeld from GGB program, as she is always helpful and cheerful.

The text of Chapter two of this dissertation is part of paper published in the *Eukaryotic Cell* and entitled, "Genetic and Physical Interactions between G alpha Subunits and Components of the G beta gamma Dimer of Heterotrimeric G Proteins in Neurospora crassa", with minor changes (173). The co-author Dr. Katherine A. Borkovich listed in that publication directed and supervised the research, which forms the basis for this dissertation.

Last but not least, I am very thankful to the members of the Dr. Borkovich laboratory, past and present, who became my good friends. They are Gyungsoon Park, Sara Wright, James Kim, Jackie Servin, Asharie Campbell, Shouqiang Ouyang, Patrick Schacht, Ilva Cabrera, Amruta Garud, Arit Ghosh, and Fitzgerald Diala. Thank you very much for your help and support.

DEDICATION

I dedicate this dissertation to my wife, Aynun,

for her enthusiasm for science, continuous support,

and sharing all my dreams and ideas.

ABSTRACT OF THE DISSERTATION

Regulation of the G Alpha Subunits in Mutants Lacking the G Beta Subunit or a Cytosolic Guanine Nucleotide Exchange Factor in *Neurospora crassa.*

by

Alexander Vladimirovich Michkov

Doctor of Philosophy, Graduate Program in Genetics, Genomics and Bioinformatics
University of California, Riverside, December 2014
Dr. Katherine A. Borkovich, Chairperson

Guanine nucleotide binding proteins (G proteins) and their cell surface G protein coupled receptors (GPCRs) regulate many cellular processes in filamentous fungi, including growth, sexual, and asexual development. Heterotrimeric G proteins are membrane-associated and composed of three subunits, alpha, beta, and gamma. The G alpha subunit is the most important, since through the exchange of bound GDP for GTP it activates G protein signaling pathways. This dissertation focuses on investigation of G alpha subunit genetic epistasis relationships, cytosolic protein-protein interactions and, regulation of G alpha protein level through translation or protein stability.

In this study, the three *Neurospora crassa* (*N. crassa*) G alpha subunits (GNA-1, GNA-2 and GNA-3) were analyzed for genetic epistasis relationships with the G beta subunit (GNB-1). Using appropriate genetic constructs and classical genetic epistasis analysis it was demonstrated that each of G alpha subunit genes has an epistatic

relationship with the G beta gene for at least one function. The genetic results are supported by finding that the G beta gamma dimer interacts with all three G alpha proteins (173).

Although there are known G alpha subunit membrane associated protein-protein interactions in *N. crassa* and other model organisms, little is known about interactions in cytosol. Therefore, Chapter 3 of this dissertation focuses on identification of cytosolic proteins that interact with the G alpha subunit protein GNA-1, as well as factors that influence the stability of GNA-1 *in vivo*. Using an endogenously tagged G alpha subunit (GNA-1), 46 proteins were found to be associated with GNA-1 in the cytosol. Six of the interacting proteins were identified in two independent CoIP/MS experiments, including the Tcp subunit theta chaperonin and the RIC8 protein. Four mutants deleted for genes corresponding to interactors from the Protein Fate category were checked for the level of the GNA-1 protein using western analysis. The results demonstrated that levels of GNA-1 were higher in mutants lacking the eukaryotic translation initiation factor, *eif-3f,* and the 19S regulatory proteasome subunits *sem-1* and *rpn13*.

Levels of G alpha subunit proteins in whole cell extracts isolated from submerged liquid cultures are decreased in the Δ*gnb-1* and Δ*ric8* strains relative to wild type, with GNA-1 showing the greatest reduction. Results from experiments involving treatment with protein degradation inhibitors suggested that accelerated protein turnover is not a major contributor to the low levels of the G alpha subunit proteins in the Δ*gnb-1* and Δ*ric8* backgrounds.

As mentioned above, GNB-1 and RIC8 positively influence levels of G alpha proteins, with RIC8 also affecting G beta protein levels. To determine whether RIC8 affects levels of G alpha proteins through GNB-1 or independently, appropriate genetic constructs were used to create strains for evaluation of GNA-1, GNA-2, and GNA-3 protein levels. The results showed that RIC8 controls levels of the GNA-1, GNA-2, and GNA-3 proteins independently from GNB-1. In sum, the data suggest that there are two independent G alpha protein levels regulatory pathways. It was hypothesized that GNB-1 and RIC8 maintained G alpha protein levels through a posttranscriptional mechanism.

To determine whether translation regulates G alpha protein levels in the Δ*gnb-1* and Δ*ric8* backgrounds, a ribosomal profiling protocol was established for *N. crassa*. During refinement of the protocol, it was found that cycloheximide pretreatment of living cells before harvesting and use of TRIzol to extract RNA are counter-indicated for *N. crassa*. It was also determined that the GNB-1 and RIC8 proteins associate with ribosomes or other elements of the translational machinery.

In conclusion, G alpha subunits were found to have epistatic relationships with the G beta and to interact with many cytosolic proteins involved in the protein life cycle. Moreover, the levels of G alpha proteins are regulated independently by GNB-1 and RIC8 on translational step.

Table of Contents

List of Tables

List of Figures

Chapter 1

Chapter 2

Chapter 3

Chapter 1

Introduction

Neurospora crassa as a model organism

Neurospora was discovered in the 1800's as the red bread mold that infested French bakeries (36). *N. crassa* (*Neurospora crassa*) is a filamentous fungus of the phylum Ascomycota and important eukaryotic model system used for more than 70 years in scientific research (36). *N. crassa* has a complex, but genetically and biochemically tractable life cycle (118;178). Research dedicated to *N. crassa* focuses on genetics, circadian rhythms, cell signaling, gene-silencing mechanisms, ecology, evolution, amino-acid metabolism, and many other areas. Nobel Prize laureates George W. Beadle and E.L. Tatum used *N. crassa* to discover their "one gene – one enzyme" theory (10). The most famous genetics method used to investigate meiosis, crossing over and gene conversion was tetrad analysis in *N. crassa* (24). *N. crassa* also proved to be ideal for genetic and phenotypic analysis of the circadian clock (13), which further fueled a new field – photobiology (27;92). *N. crassa* is an excellent model organism because it grows very quickly on inexpensive culture medium and most of life cycle is in the haploid stage, which makes genetic analysis simple since recessive traits will be revealed in the offspring (36). The whole genome of *N. crassa* has been sequenced (17;38;43). There are many molecular genetic tools, such as a full single nucleotide polymorphism maps (84),

helper strains that can shelter deleterious mutations and nonhomologous end-joining mutants, which allowed highly efficient gene replacement (107). There is a collection containing 4000 different strains from natural populations (154) and more than 8000 deletion mutants strains for the 9733 genes present in the ~40Mb haploid genome are available to the scientific community from the Fungal Genetics Stock Center (17).

The life cycle of *N. crassa*

Most isolates of *N. crassa* are from tropical and subtropical zones (154), but it has also been found in temperate forests of western North America and Europe (67;68). *N. crassa* vegetative hyphae are multicellular, divided into cells by internal perforated cross-walls called "septa", and these hyphae extend using highly polarized tip-based growth (36). Frequent fusion and branching among hyphae produces a complex multinucleate network (55). In response to oxygen or nutrient deprivation, elevated temperature or other environmental stresses, *N. crassa* produces multinucleate spores called macroconidia, formed on specialized aerial hyphae (15). Less is known about the pathway regulating production of uninucleate microconidia differentiated from microconidiophores or directly from the vegetative hypha (36;95;144). Limiting nitrogen induces the sexual cycle, with formation of multicellular female reproduction organs (protoperithecia) (158). *N. crassa* is heterothallic and has two mating types (*mat a* and *mat A*). Specialized hyphae (trichogynes) exhibit chemotropic growth from the protoperithecium towards male gametes, which could be any vegetative cells of the opposite mating type (14).After

fertilization, the protoperithecium forms a fruiting body (perithecium) containing sexual spores (ascospores) (17). Heat exposure and other environmental conditions lead to germination of ascospores to form vegetative hyphae.

G protein signaling system

Many sensory and chemical stimuli are recognized by specialized cell-surface receptors called G Protein Coupled Receptors (GPCRs), which transduce this information to intracellular signaling pathways via heterotrimeric G proteins (69). GPCRs are seven-helix membrane proteins, which in their ligand-bound form act as Guanine nucleotide Exchange Factors (GEFs) for G Protein alpha subunits (122). The GDP-bound alpha subunit associates with the beta-gamma dimer (Guanine nucleotide Dissociation Inhibitor – GDI) and the GPCR at the membrane (137). The principle of the signal transduction pathway is the alternation between binding of a guanosine diphosphate (GDP; inactive form) and guanosine triphosphate (GTP; active form) by the G alpha subunit. The GTP-bound alpha subunit dissociates from the beta-gamma dimer and GPCR, allowing both the alpha subunit and beta-gamma dimer to regulate downstream effectors (137). GTP hydrolysis by the alpha subunit results in reassociation of the GDP-bound alpha subunit with the beta-gamma dimer (GDI) and the GPCR, thus completing the cycle. The rate of GTP hydrolysis by the alpha subunit can be accelerated by Regulator of G protein Signaling proteins (RGS) (74;165) (Figure 1.1 A).

Until fairly recently, heterotrimeric G protein signaling was thought to be initiated solely by a GPCR in response to the presence of extracellular ligands. However, recent discoveries show that there are receptor-independent G protein mediated signaling pathways in which G alpha subunits are activated independently of the GPCR. This is facilitated by a non-GPCR GEFs (Figure 1.1 B) (150). Synembryn, or Resistance to Inhibitors of Cholinesterase 8 (RIC8), is an essential part of the asymmetrical cell division machinery (72) and extracellular ligand sensing (48) in animal cells. RIC8 was first discovered in *Caenorhabditis elegans* (101) and later confirmed in other organisms (152;170). In mammalian cells, Ric8A GEF activity has been characterized using two theoretical models. The first is that RIC8 binds the GDP-bound form of G alpha subunit, thus competing with the GDI (the beta-gamma dimer), releasing GDP and forming a stable nucleotide-free complex (148). In the second scenario, RIC8 binds the complex formed by the beta-gamma dimer and the GDP-bound alpha subunit and facilitates dissociation of the beta-gamma dimer and GDP, which yields a stable nucleotide-free complex (150). In both scenarios, RIC8 dissociates from the G alpha subunit after GTP binding. RIC8 has also been implicated in stabilization and localization of G alpha subunits (1;48;106). Interestingly, RIC8 is only found in animals and some fungi, including *N. crassa*, which is often used as a model for asymmetric cell division (50). All data shows that RIC8 play an important role in the G protein signaling pathway as a GEF and G alpha stabilization factor, and *N. crassa* is an ideal microbial model organism for further investigation.

G protein signaling system in *N. crassa*

The first heterotrimeric G protein in filamentous fungi was discovered in *N. crassa* in early 1990's (155). By now *N. crassa* has a well-characterized G protein signaling pathway (6;64;77;82). *N. crassa* possesses three G alpha subunits (GNA-1, GNA-2 and GNA-3), one G beta (GNB-1), and one G gamma (GNG-1). GNA-1 regulates many cellular processes, including mating, pheromone response and nutrient sensing (64;155). GNA-3 is responsible for sexual sporulation and nutrient sensing via cAMP-dependent pathways (77). GNA-1 and GNA-3 are highly conserved among fungi (88), and GNA-1 share homology with mammalian G alpha proteins (64). However, GNA-2 is not well conserved and is unique to fungi (88). GNA-2 has been shown to be required for carbon-source-dependent growth and play a compensatory role to GNA-1 and GNA-3 (87). In *N. crassa*, deletion of *gna-1* leads to female sterility, production of short aerial hyphae and higher resistance to stresses (64). Δ*gna-3* mutants have reduced fertility, short aerial hyphae, and defects in conidiation (77). Both mutants exhibit reduced mass accumulation on poor carbon sources (77;87). Δ*gna-2* mutants do not have a distinct phenotype, but also shows reduced mass accumulation on poor carbon sources. Loss of *gna-2* exacerbates the defects of Δ*gna-1* and Δ*gna-3* mutants due to compensatory role of GNA-2 (76). Mutating all three G alpha protein genes has been shown to severely restrict apical growth, and to cause dense, premature conidiation and female sterility (76).

N. crassa, like most filamentous fungi, has one G beta subunit (GNB-1) and one gamma subunit (GNG-1) (88). G beta subunits are highly conserved among filamentous fungi, and *N. crassa* GNB-1 is 65% identical to human G beta proteins (177). GNB-1 forms a tightly associated dimer with GNG-1 and is required for normal sexual and vegetative development and maintenance of normal levels of G alpha proteins (82). G beta and gamma deletion mutants are female-sterile, and have defects in conidiation, similar to the G alpha deletion mutant. This similarity can be explained by the observation that levels of all three G alpha proteins are very low in Δ*gnb-1* mutants (GNA-1 and GNA-2 are greatly reduced, GNA-3 is reduced approximately 50% in submerged culture) (82;173). We have postulated that the low level of G alpha proteins in *gnb-1* deletion mutants is likely due to increased protein turnover (82;177). In animals, there is a compensatory posttranscriptional mechanism which adjusts the levels of the G beta protein according to the level of G alpha proteins (98). However, in *N. crassa* loss of any G alpha does not affect the levels of other G alpha and G beta subunit proteins (66;77;177). Introducing GTPase-deficient alleles (constitutively activated) of the G alpha genes into the Δ*gnb-1* mutant restores the levels of G alpha proteins (82).

There is only one RIC8 protein in *N. crassa*. It acts as a non-GPCR GEF and shares 20% identity with mammalian RIC8 proteins (174). Δ*ric8* mutants are female-sterile; grow extremely slowly, have thin, hyperbranched hyphae, and defects in conidiation. Some of the observed phenotypes resemble those of Δ*gna-1* Δ*gna-3* double mutants and strains lacking all three G alpha genes. Similarly, in Δ*ric8* mutants, levels of all G alphas and G beta proteins are greatly reduced. This is the result of

posttranscriptional mechanisms, since mRNA levels were not affected (174). Introducing GTPase-deficient alleles of the G alpha proteins (GNA-1^{Q204L}, GNA-2^{Q205L}, and GNA-3^{Q208L}) in the Δ*ric8* mutant restores the levels of the G alpha, but not G beta, protein levels (174). Based on these results, the low levels of G alpha proteins in the absence of RIC8 and GNB-1 were hypothesized to be caused by posttranscriptional regulation.

Objectives and Major Conclusions

In this dissertation, I attempt to extend knowledge about one of the most important signaling pathways in the cell – G protein signal transduction. In the second chapter of this dissertation, I checked levels of the G alpha subunits (normal and overexpressed, constitutively active, GTPase-deficient alleles) in the Δ*gnb-1* background. Myself and Amruta V. Garud extended the work of a former M.S. student in the laboratory, Susan Won. I tested the genetic interactions between the G beta subunit gene and all three G alpha genes in *N. crassa*. Genetic analysis revealed that *gna-3* is epistatic to *gnb-1* with regard to negative control of submerged conidiation. *gnb-1* is epistatic to *gna-2* and *gna-3* for aerial hyphal height, while *gnb-1* appears to act upstream of *gna-1* and *gna-2* during aerial conidiation. None of the activated G alpha alleles restored female fertility to Δ*gnb-1* mutants. In sum, G alpha and G beta subunits have genetic epistasis relationships for least for one function. This chapter is a part of a published manuscript (173).

It has previously been reported that *N. crassa* GNA-1 regulates apical growth, conidiation, sexual fertility, and stress responses (64;65). Such a broad function for GNA-1 suggests also a wide spectrum of protein-protein interaction. Previous work in *N. crassa* and other model organisms showed membrane or membrane associated interactions with GPCRs, the G beta gamma dimer, and some effectors, but there is a gap in our understanding of the interactions between G alpha subunits and other proteins in the cytosol. In the third chapter, I focus on putative GNA-1 interacting cytosolic proteins. To discover potential GNA-1 interacting proteins in the cytosol, I used coimmunoprecipitation/mass spectrometry. I report many possible cytosolic interactors for GNA-1, which have predicted functions in protein translation and folding, signal transduction, metabolic pathways, and protein degradation. This preliminary results must be confirmed by other methods. I followed up on putative GNA-1 interactors involved in translation, degradation, and putative interactors affecting GNA-1 stability such as G beta subunit and RIC8. As mentioned above, the protein level of the G alpha subunits, especially GNA-1, are greatly reduced in the Δ*gnb-1* and Δ*ric8* backgrounds. The G alpha mRNA levels are similar in the deletion mutant and in wild type, suggesting post-transcriptional regulation. I investigated the possibility that GNB-1 and RIC8 could involve in protein degradation. However, treatment with protein degradation inhibitors did not restore levels of the G alpha proteins in the deletion mutant backgrounds. Taken together my results suggest that the low protein level of GNA-1 in the Δ*gnb-1* and Δ*ric8* backgrounds is not due to the protein turnover. Further investigation of other potential

interactors will result in better understanding of the regulation of G alpha protein levels and other novel functions for GNA-1.

The fourth chapter is focused on the translational regulation of G alpha subunits in genetic backgrounds lacking the G beta subunit or the cytosolic guanine nucleotide exchange factor (RIC8). I established a ribosome sucrose density gradient profiling protocol for *N. crassa* to study translational regulation. My preliminary results showed that G alpha subunit and actin mRNAs associated with polysomes were decreased in the Δ*gnb-1* and Δ*ric8* backgrounds compared to wild type. I detected GNB-1 and RIC8 proteins in sucrose density gradient fractions that contained ribosomes or ribosomal subunits. Although these preliminary results are interesting, questions regarding the nature of the translation control mechanism still need to be answered.

Altogether, the research presented in this thesis provided new insights into genetic and physical interactions, stability and regulation of G alpha subunits of heterotrimeric G proteins.

A.

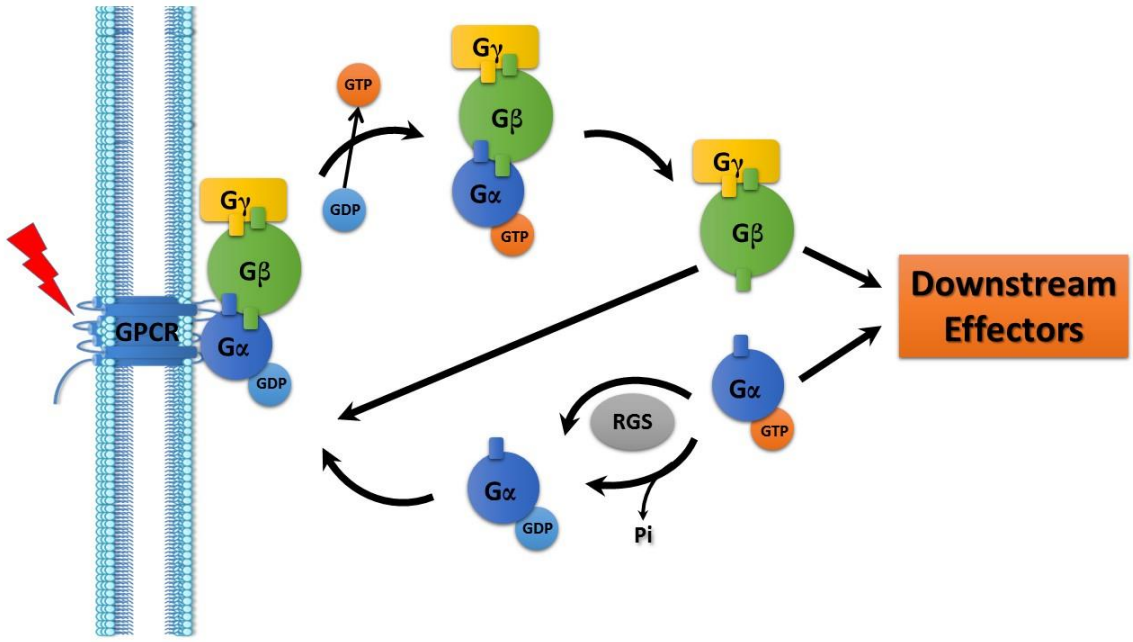

B.

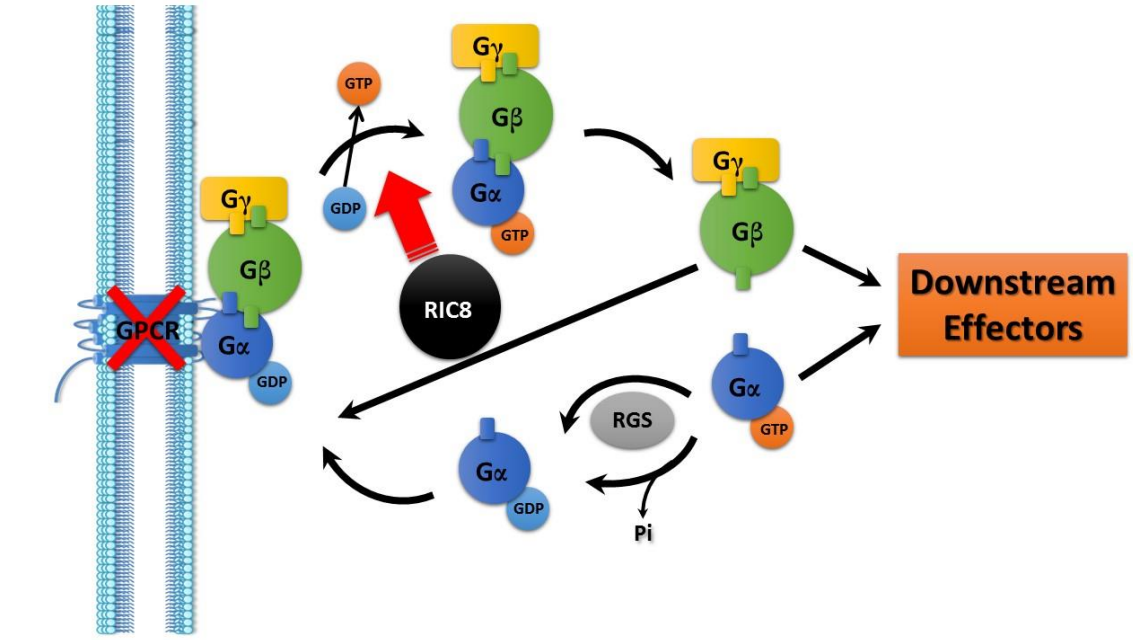

Figure 1.1 Heterotrimeric G protein signaling pathway. A. Canonical activation of the G protein signaling pathway through the G protein-coupled receptor (GPCR) in response to an extracellular stimulus. B. Receptor-independent activation of the heterotrimeric G protein signaling pathway through the cytosolic guanine exchange factor RIC8.

Chapter 2

Genetic interactions between G alpha subunits and components of the G beta gamma dimer of heterotrimeric G proteins in *Neurospora crassa*

Abstract

Heterotrimeric G proteins are critical regulators of growth and asexual and sexual development in the filamentous fungus *N. crassa*. Three G alpha subunits (GNA-1, GNA-2, and GNA-3), one G beta subunit (GNB-1), and one G gamma subunit (GNG-1) have been functionally characterized, but genetic epistasis relationships between G alpha and G beta subunit genes have not been determined. Tight physical association between G beta and G gamma subunits has been already demonstrated in *N. crassa*, but evidence of interaction between each G alpha subunits and the G beta gamma dimer is still lacking. Co-immunoprecipitation experiments using extracts from epitope tagged *gng-1*-Flag strain performed by coauthors Susan Won and Svetlana Krystofova showed that each of the three G alpha subunit proteins interacts with the G beta-gamma dimer.

Using a genetic approach, we investigated epistasis relationships between G beta and G alpha subunits genes in *N. crassa*. In this study, double mutants were created, each lacking one of the G alpha and G beta subunit genes. We also constructed strains with constitutively active, GTPase-deficient alleles for each G alpha subunit in the Δ*gnb-1* background. Phenotypic analysis of these strains demonstrated that *gna-3* is epistatic to

gnb-1 in a linear pathway to negatively regulate submerged conidiation. *gnb-1* is epistatic to *gna-2* and *gna-3* for aerial hyphal height. In the case of aerial conidiation, *gnb-1* acts upstream of *gna-1* and *gna-2*. The *gnb-1* deletion mutant does not form mature female reproductive structures and introduction of the activated G alpha alleles did not rescue female fertility. Moreover, introduction of the activated *gna-3*^{Q208L} allele inhibited formation of female reproductive structures in Δ*gnb-1* background. Taken together this study confirmed that G alpha subunits have an epistatic relationship with the G beta gene for at least one function. The information in this chapter is a part of publication (173).

Previous work in our laboratory showed that GNB-1 is required for maintenance of normal levels of G alpha subunit proteins (82), and *ric8* has an epistatic relationship with G alpha subunit genes and that loss of *ric8* results in low levels of not only G alpha subunits, but also GNB-1 (174). Therefore, using appropriate genetic constructs, the independent importance of RIC8 and GNB-1 in regulating G alpha protein level was addressed. It was found that GNB-1 and RIC8 independently regulate levels of GNA-1, GNA-2, and GNA-3.

Introduction

The filamentous fungus *N. crassa* possess three G alpha subunits: GNA-1, GNA-2, and GNA-3 (6;77;155). There is also one G beta protein (GNB-1) and one G gamma protein (GNG-1) (82;177). As already was discussed in Chapter 1, GNA-1 regulates multiple processes in the cell, including apical hyphae extension, carbon source sensing, aerial hyphae development, asexual sporulation (conidiation), female fertility, and adenylyl cyclase activity (64;66;66;87). GNA-3 also takes part in carbon source sensing, modulates the level of adenylyl cyclase and regulates conidiation and aerial hyphae formation (76;77;87). GNA-2 acts as a compensatory G alpha subunit, confirmed by intensification of phenotypes of Δ*gna-1* and Δ*gna-3* mutants by further deletion of *gna-2*, and Δ*gna-2* shows reduced mass accumulation on poor carbon sources (6;76;87). Major phenotypic defects were observed in *gna-1* and *gna-3* double mutants, especially in growth and differentiation (76).

G beta and G gamma subunits form the G beta gamma dimer, which is essential for asexual sporulation, female fertility, and G alpha protein levels. G beta and G gamma protein complex formation was confirmed by coimmunoprecipitation and the similar phenotypes of *gnb-1* and *gng-1* deletion mutants (82;173). During the sexual cycle, all single G protein subunit mutants form protoperithecia, but only Δ*gna-2* and Δ*gna-3* develop perithecia and ascospores. Phenotypes of single gene deletion mutants for each G protein subunit are presented in Table 2.1.

A major goal in biological research is to determine how genes act alone and together to regulate multiple processes in the cell. One of the classical and powerful tools is the genetic approach, which investigates the interaction between genes. In this work, we study epistasis (genetic interaction) between G protein subunit genes to control a single phenotype. Standard epistasis analysis involved comparison of mutants lacking one gene with a double mutant deleted for both genes. The gene whose phenotype persists in the double mutant is the epistatic gene, while the other gene is the hypostatic gene (5). G alpha subunits have three forms: GDP bound (passive), GTP bound (active) and nucleotide free. In our research we include constitutively active, GTPase deficient alleles for each G alpha gene (*gna-1*^{Q204L}, *gna-2*^{Q205L}, and *gna-3*^{Q208L}), which were created in previous studies (6;176). Ordering genes in a hierarchical way, we used the following rules: if the double mutant phenotype resembles the phenotype of the G beta subunit deletion mutant and activation of G alpha does not suppress G beta mutant phenotype, the G beta gene is epistatic to the G alpha. If a double mutant phenotype resembles that of the G alpha single mutant, and activation of the G alpha gene suppresses the G beta phenotype, the G alpha is epistatic to the G beta gene. Any other combination demonstrates partial or full functional independence (Figure 2.1). Together with my co-author Amruta Garud, we performed a series of phenotypic assays, which included conidiation in submerged cultures, aerial conidiation, aerial hyphae formation in standing liquid cultures, and sexual development. This work was combined with that of previous student Susan Won and postdoctoral fellow Svetlana Krystofova in the final manuscript.

Materials and Methods

Strains and media. *N. crassa* strains used in this study are listed in Table 2.2. For collection of asexual spores or vegetative growth in liquid or solid culture, strains were cultured in Vogel's minimal medium (VM) (159), with 1% agar added for solid medium (BBL; Becton, Dickinson and Co., Franklin Lakes, NJ). Sorbose medium (FGS) (25) was used to induce colony formation on plates. Female reproductive structures (protoperithecia) were formed on synthetic crossing medium containing 1% agar (167). Medium was supplemented with hygromycin at 200 µg/ml or histidine at 100 µg/ml, where indicated.

Macroconidia (conidia) were propagated in VM agar medium flasks by incubation at 30ºC for three days in the dark, followed by five days at room temperature in constant light. Conidia were harvested as previously described (35).

Phenotypic Analysis. All cultures were inoculated using conidia, except for the Δ*gnb-1*, *gna-3*^{Q208L} G3-C strain that produces very few conidia; in this case, cultures were inoculated with a small amount of aerial hyphae (200 mg). To determine aerial hyphae height, 13x100 mm glass tubes containing 2 ml of VM liquid medium were inoculated with the strains and then incubated for five days in dark and one day in light at room temperature. To analyze conidiation in submerged cultures, 30 ml of liquid medium was inoculated with conidia at a concentration of 10^6 cells/ml (except for strain G3-C, which

was inoculated using ~200 mg of packed aerial hyphae) and incubated with shaking at 200 rpm for 16 hr at 30°C.

Assessment of significant differences between strains with regard to the number of conidia and the height of aerial hyphae was determined using Student's t test ($P<0.05$) with StatView v 5.0.1 (SAS Institute Inc., Cary, NC) (Table 2.3 and 2.4).

Cultures were viewed and photographed at 60 x magnification, using a DIC (Differential Interference Contrast) oil immersion objective (N.A.=1.42) with an Olympus 1X71 inverted microscope (Olympus America, Center Valley, PA) and a QIClickTM CCD camera (QImaging, Surrey, British Columbia, Canada). Images were analyzed using Metamorph software (Molecular Devices Corporation, Sunnyvale, CA). For fertility assays, strains were inoculated onto SCM plates and incubated for 6 days in constant light at 25°C. Cultures were fertilized with males (macroconidia) of opposite mating type and incubated for 6 more days before being photographed using an SZX9 stereomicroscope (Olympus) with a Powershot G10 camera (Canon USA, Lake Success, NY) at a magnification of x57.

Western analysis. Since some of the strains did not produce a significant amount of conidia, submerged cultures to be used for isolation of the plasma membrane fraction were inoculated using aerial hyphae harvested from 1-day-old plate cultures using a sterile wooden stick. A mass of packed hyphae corresponding to 0.5 ml (200 mg) of tissue was added to a 125 ml flask containing 50 ml of liquid VM. The flasks were incubated for 16 hr at 30ºC in the dark with shaking at 200 rpm. Tissue was collected on

filter paper using a vacuum system and cell pads were flash-frozen in liquid nitrogen prior to storage at –80°C. Tissue was pulverized in liquid nitrogen using a mortar and pestle and then transferred into a medium-sized Bead-Beater chamber (Biospec Products, Bartlesville, OK) containing glass beads and extraction buffer (10 mM HEPES [pH 7.5], 0.5 mM EDTA, 1 M sorbitol, 0.5 mM PMSF and 0.1% fungal protease inhibitor cocktail; catalog no. P8215; Sigma-Aldrich, St. Louis, MO). The tissue was homogenized for 45 sec (repeated twice) at 4ºC. The homogenate was centrifuged in a JA-25.50 rotor (Beckman-Coulter, Inc., Brea, CA) at 15000xg for 30 min at 4ºC. The supernatant was removed and the protein concentration was determined using the Bradford protein assay (Bio-Rad). Samples were adjusted to the same total protein concentration using extraction buffer and centrifuged at 46,000xg for 60 min at 4ºC using the JA-25.50 rotor (Beckman-Coulter). The supernatant was collected and volume measured. The pellet was gently homogenized using a thin glass rod and resuspended in the same volume as the supernatant using a buffer containing 50 mM TrisCl [pH 7.5], 1 mM DTT, 0.5 mM PMSF, 10% glycerol and 0.1% fungal protease inhibitor cocktail (Sigma-Aldrich). Samples containing 100 µg of total protein were subjected to SDS-PAGE and then transferred to a nitrocellulose membrane as described previously (82).

The membranes were probed using primary antibodies for GNA-1, GNA-2, and GNB-1 at a final dilution of 1:1000 (6;64;82;174;177). GNA-3 polyclonal antibody was produced in rabbits by commercial source (Thermo Scientific Pierce Protein Research, Rockford, IL) and was diluted 1:2,000 (173). The secondary antibody (anti-rabbit horseradish peroxidase conjugate; Bio-Rad) was used at a 1:5000 dilution and

chemiluminescent detection was as described previously (82). Coomassie-stained gels served as the loading controls (data not shown).

Results

Introduction of activated G alpha alleles into the Δ*gnb-1* background restores G alpha protein levels.

As previously was shown, the *gnb-1* deletion mutant has reduced levels of G alpha proteins in *N. crassa* (82;177). Using western analysis, I assessed levels of GNA-1, GNA-2, GNA-3, and GNB-1 proteins in plasma membrane fractions isolated from submerged liquid cultures (Figure 2.2). Membrane fractions isolated from corresponding G alpha deletion mutants (Table 2.2) were used as a control for each G alpha antibody (Figure 2.2 ΔGα lines). As expected, negative controls for GNB-1 and all three G alpha proteins had no visible bands (Figure 2.2). Levels of GNA-1, GNA-2, and GNA-3 were lower in Δ*gnb-1* mutants than in wild type. GNA-1 was affected the most (80% decrease), and GNA-2, and GNA-3 were decreased by ~50% (Figure 2.2).

We also created strains expressing GTPase-deficient, constitutively activated G alpha alleles in the Δ*gnb-1* background using an *N. crassa* gene-targeting system that directs DNA sequences to the *his-3* locus (3). All three activated alleles were expressed using the *ccg-1* promoter (12;91) in order to eliminate the effects of different protein expression levels. Overexpression (using the *ccg-1* promoter) of the constitutively activated alleles, *gna-1*^{Q204L}, *gna-2*^{Q205L}, and *gna-3*^{Q208L}, not only restored levels of G alpha proteins, but also influenced levels of other proteins. For example, the *gna-1*^{Q204L}

and *gna-3*^{Q208L} alleles led to elevated GNA-2 protein levels in the Δ*gnb-1* background (Figure 2.2).

RIC8 and GNB-1 independently regulate G alpha protein levels.

It was previously shown that RIC8, similar to GNB-1, also is essential for maintenance of normal protein levels for GNA-1, GNA-2, and GNA-3 via a post-transcriptional mechanism (174). As for Δ*gnb-1* mutants, introduction of constitutively activated versions of the G alpha genes restored levels of the corresponding protein in the Δ*ric8* background. Moreover, loss of *ric8* caused a decrease not only in G alpha protein levels, but also in GNB-1 protein amount (Figure 2.6). Only in the case of GNA-3 did the data support regulation by RIC8 independently of GNB-1 (174).

To investigate the relationship between RIC8 and GNB-1 in regulation of G alpha protein levels, we created strains overexpressing *gnb-1* and *ric8* (using the *ccg-1* promoter) in wild type, Δ*gnb-1*, and Δ*ric8* backgrounds. Former student Dr. Sara J. Wright constructed strains with overexpressed *ric8*. I created strains that overexpressed *gnb-1* in the wild type and Δ*ric8* backgrounds. Overexpression of *ric8* did not affect protein levels for G alpha and G beta subunits in the wild type background (Figure 2.6) and did not restore normal levels of G alpha proteins in the Δ*gnb-1* mutant. Likewise, overexpression of *gnb-1* did not elevate G alpha protein levels in the wild type background and did not restore normal G alpha protein levels in the *ric8* deletion mutant (Figure 2.6). Thus, neither GNB-1 nor RIC8 can compensate for the loss of the other

protein when overexpressed, suggesting an at least partial independent mode of action in maintenance of G alpha protein levels.

GNA-3 and GNB-1 may operate in a linear pathway to negatively regulate submerged conidiation, while GNA-1 and GNA-2 are independent of GNB-1.

Previous work has demonstrated that heterotrimeric G proteins are essential for normal asexual and sexual development of *N. crassa* (64;79;82;177). The goal of this study was to identify the G alpha subunits that interact with the GNB-1/GNG-1 G beta gamma dimer in *N. crassa* during regulation of different cellular functions. We first utilized a genetic approach to determine whether there was evidence for an epistatic relationship between *gnb-1* and the three G alpha genes that would support a physical interaction between the encoded proteins in a heterotrimeric complex. Double mutants containing the Δ*gnb-1* and one G alpha deletion mutation were produced using sexual crosses between single mutants.

The results of the genetic analysis were interpreted as follows (see Figure 2.1 for diagrams). The observation that the Δ*gnb-1* ΔG alpha double mutant has the same phenotype as the *Δgnb-1* single mutant and that introduction of the constitutively activated G alpha allele does not suppress the Δ*gnb-1* phenotype shows that *gnb-1* is epistatic to the G alpha gene and supports GNB-1 acting downstream of the G alpha in a linear pathway (Figure 2.1 A). Conversely, the finding that the Δ*gnb-1* ΔG alpha mutant has the same phenotype as the ΔG alpha mutant and that the activated G alpha allele at

least partially bypasses the Δ*gnb-1* phenotype indicates that the G alpha gene is epistatic to *gnb-1* and suggests that the G alpha protein acts downstream of GNB-1 in a linear pathway (Figure 2.1 B). The interpretation of any other combination of results from genetic analysis was that the G beta and G alpha are at least partially independent and likely operate in different signaling pathways to regulate the cellular function being assayed.

We began by assessing several phenotypes during asexual growth and development in the strains. During the asexual phase of the life cycle, *N. crassa* grows by extension, branching and fusion of hyphae to form the network structure called the mycelium (143). The asexual sporulation pathway, macroconidiation/conidiation, begins with differentiation of aerial hyphae from the mycelium, followed by constriction of the aerial hyphal tips to form the mature conidia (143). Since conidiation is induced by exposure to air, wild-type cultures submerged in liquid do not normally produce conidia (143). We have previously demonstrated that Δ*gna-1*, Δ*gna-3*, and Δ*gnb-1* single mutants produce conidiophores in submerged cultures (65;76;177). Δ*gna-1* mutants do so in a cell density-dependent manner, forming conidiophores only at relatively high inoculation densities ($3x10^6$ cells/ml or greater (65). In order to increase the stringency of our screen, we assessed submerged cultures for the presence of conidiophores at an inoculation density of $1x10^6$ cells/ml, a condition that leads to conidiation in Δ*gna-3* and Δ*gnb-1*, but not Δ*gna-1*, mutants.

As previously shown (77;177), the only single mutants that produce conidiophores in submerged culture are those lacking *gnb-1* or *gna-3* (Figure 2.3 A).

Further deletion of any of the three G alpha genes in the Δ*gnb-1* background leads to a phenotype identical to that conferred by Δ*gnb-1* (Figure 2.3 A). Introduction of the constitutively activated *gna-1*^{Q204L} or *gna-3*^{Q208L} alleles into the Δ*gnb-1* background abolished inappropriate conidiation (Figure 2.3 A). In addition, hyphae in the Δ*gnb-1* *gna-3*^{Q208L} strain were whiter than in the other strains. The *gna-2*^{Q205L} allele yielded a partial correction, with some conidiophores present among the normal hyphae (Figure 2.3 A). These results suggest that *gna-3* is epistatic to *gnb-1*, since single and double mutants conidiate in submerged culture and *gna-3*^{Q208L} corrects the conidiation defect in the Δ*gnb-1* background. This is consistent with GNB-1 acting upstream of GNA-3 in a linear pathway to negatively regulate submerged conidiation. In contrast, the two genetic epistasis assays gave opposite results for *gna-1* and *gna-2*; the findings from double mutant analysis suggest that *gnb-1* is epistatic to *gna-1* and *gna-2*, while those from strains carrying the *gna-1*^{Q204L} or *gna-2*^{Q205L} allele support *gna-1* and *gna-2* being epistatic to *gnb-1*. Observation of opposite results for the two epistasis assays is most consistent with at least partial independence of GNA-1 and GNA-2 from GNB-1 during negative control of submerged conidiation.

Aerial hyphae height and production of conidia on solid medium involve different epistatic relationships.

We next investigated epistatic relationships between *gnb-1* and the three G alpha genes during aerial hyphae production in standing liquid cultures and conidiation on solid

medium (Figure 2.3 B, C). Student's t test was used to identify statistical differences between strains with regards to these two quantitative traits (Tables 2.3 and 2.4). As previously determined, Δ*gnb-1* and Δ*gna-3* strains have significantly shorter aerial hyphae than those of the wild type (77;177) (Figure 2.3 B), while Δ*gna-2* resembles the wild type in its aerial hyphae height (6) (Figure 2.3 B). In contrast to previous results (64;66;176), we did not detect a statistically significant difference between aerial hyphae height in wild type and Δ*gna-1* strains (Table 2.3). Deletion of a single G alpha gene in the Δ*gnb-1* background results in aerial hyphae heights similar to those of the Δ*gnb-1* mutant (Figure 2.3 B). Δ*gnb-1* strains carrying the *gna-2*- or *gna-3*-activated G alpha alleles have aerial hyphae heights similar to those of the Δ*gnb-1* mutant (Figure 2.3 B). Aerial hyphae are also denser in these strains (Figure 2.3 D and data not shown). These results are consistent with *gnb-1* being epistatic to (acting downstream of) *gna-2* and *gna-3* with respect to aerial hyphae height, as double mutants and Δ*gnb-1* strains carrying the activated *gna-2* or *gna-3* allele resemble the Δ*gnb-1* single mutant. In contrast, the relationship between *gnb-1* and *gna-1* is more consistent with at least partial functional independence, as the Δ*gnb-1 gna-1*^{Q204L} strain has an aerial hyphae height significantly greater than that of Δ*gnb-1*. (Table 2.3).

Δ*gnb-1* strains produced the greatest amount of conidia in plate cultures in our study, followed by Δ*gna-3* mutants (Figure 2.3 C). Δ*gnb-1* strains carrying any of the three activated G alpha genes resulted in significantly less conidia production than Δ*gnb-1* (Table 2.4), with levels in the Δ*gnb-1, gna-3*^{Q208L} near zero (Figure 2.3 C). This indicates that all three activated G alpha genes can negatively regulate conidia production in the

Δ*gnb-1* background. With regards to epistatic relationships between *gnb-1* and *gna-1* and *gna-2*, the observation that double mutants have levels of conidia similar to those of G alpha single mutants and that Δ*gnb-1* strains carrying *gna-1*^{Q204L} or *gna-2*^{Q205L} have levels significantly lower than Δ*gnb-1* mutants is most consistent with *gna-1* and *gna-2* being epistatic to *gnb-1*. In contrast, the epistatic relationship between *gnb-1* and *gna-3* is less clear, as conidium levels are significantly lower in Δ*gnb-1* Δ*gna-3* double mutants than in either single mutant, and lower still in Δ*gnb-1 gna-3*^{Q208L} strains (Table 2.4).

We also observed differences in orange pigmentation, indicative of carotenoid production, in the strains (Figure 2.3 D). The intensity of pigmentation roughly correlated with the extent of conidiation, with Δ*gnb-1 gna-1*^{Q204L} and Δ*gnb-1 gna-3*^{Q208L} strains much lighter than wild type. In the case of the Δ*gnb-1 gna-3*^{Q208L} strain, the suppression yielded a white hyphal mass (Figure 2.3 D).

Constitutive activation of G alpha proteins does not restore sexual fertility to Δ*gnb-1* mutants.

Nitrogen starvation induces the sexual cycle by leading to production of female reproductive structures (protoperithecia) (117). Protoperithecia produce specialized chemotropic hyphae (trichogynes) that grow towards male cells of opposite mating type (14;117). During the course of cell fusion, fertilization and meiosis, the protoperithecium enlarges to form the perithecium. Approximately 2 weeks after fertilization, sexual spores (ascospores) are ejected and can germinate to form vegetative hyphae (117).

During the sexual cycle, Δ*gnb-1* and Δ*gna-1* mutants are male-fertile, but female-sterile (177) (Figure 2.4 A). Although these strains produce protoperithecia and trichogynes, their trichogynes have a defect in chemotropism and are not attracted by male cells (64;79;82;177). In contrast, Δ*gna-2* and Δ*gna-3* mutants produce protoperithecia and develop perithecia after fertilization with wild-type males (6;77). In this study, we observed that all ΔG alpha Δ*gnb-1* double mutants resembled Δ*gnb-1* single mutants, forming protoperithecia, but not perithecia, after fertilization (Figure 2.4 A). The sexual cycle phenotypes of Δ*gnb-1 gna-1*^{Q204L} and Δ*gnb-1 gna-2*^{Q205L} strains were similar to those of the Δ*gnb-1* mutant (Figure 2.4 B), with the Δ*gnb-1 gna-1*^{Q204L} strain exhibiting a delay in protoperithecial development (data not shown). In contrast, the *gna-3*^{Q208L} allele completely inhibited protoperithecial formation in the Δ*gnb-1* background (Figure 2.4 B).

We have previously hypothesized that the block in fertility of Δ*gnb-1* mutants may be a consequence of low GNA-1 protein levels (177). The findings from the double mutant analysis presented here are consistent with this idea, as Δ*gnb-1* is epistatic to Δ*gna-2* and Δ*gna-3* and has the same phenotype as Δ*gna-1*. Furthermore, the results with the *gna-1*^{Q204L} allele corroborate those from a previous study showing that although GNA-1 is required for chemotropism of female trichogynes towards male cells, constitutive activation of *gna-1* cannot rescue the defect in chemotropism caused by loss of the pheromone receptor (79). The delayed perithecial development of Δ*gnb-1 gna-1*^{Q204L} strains and the complete inhibition of protoperithecial development by *gna-3*^{Q208L}

suggests that GNA-1 and GNA-3 must cycle through inactive and active forms during fertilization and protoperithecial development, respectively.

Discussion

We have previously demonstrated that GNB-1 is essential for the correct functioning of G alpha and G gamma protein subunits in *N. crassa* (82;177). In the absence of GNB-1, levels of the three G alpha proteins and GNG-1 are severely reduced (177). In this study, we explored the relationship between the GNB-1/GNG-1 dimer and the three G alpha proteins in signal transduction using genetic and biochemical approaches.

The genetic approach involved analysis of G alpha-*gnb-1* single and double mutants and Δ*gnb-1* strains carrying activated G alpha alleles. Models that summarize the different epistatic relationships are presented in Figure 2.5. The results indicate that *gna-3* is epistatic to *gnb-1* for negative regulation of submerged culture conidiation (Figure 2.5 A), while *gna-1* and *gna-2* are epistatic to *gnb-1* with regards to negative control of aerial conidiation (Fig 2.5 C). These observations suggest that GNB-1 is necessary for activation of the G alpha proteins, which then regulate conidiation. In contrast, *gnb-1* appears to act downstream of *gna-2* and *gna-3* to regulate aerial hyphal height (Figure 2.5 B), consistent with GNA-2 and GNA-3 as positive regulators of GNB-1 for this trait. A caveat to these conclusions is the reduced levels of G alpha proteins in a mutant lacking the G beta or G gamma subunit; this scenario complicates interpretation of the results from genetic analysis (82;177). However, all Δ*gnb-1* mutant phenotypes cannot be explained by reduced levels of G alpha proteins, as a mutant lacking all three G alpha genes has much more severe defects in asexual and sexual growth and development than

the Δ*gnb-1* strain (76). Finally, the observation that constitutive activation of any G alpha suppresses the hyperconidiation defects of Δ*gnb-1* mutants suggests that all three proteins are negative regulators of conidia production (Figure 2.5 A and C). This observation complements previous results establishing synergy between G alpha gene deletion mutations during regulation of conidiation in *N. crassa* (76). However, our previous finding that *gna-2* acts in a compensatory fashion to *gna-1* and *gna-3* to regulate conidiation suggests that the role of *gna-2* is relatively minor compared to the roles of the other two G alpha genes.

There was no clear epistatic relationship between *gnb-1* and *gna-3* with regards to aerial conidiation (Figure 2.3 B). Loss of *gna-3* leads to increased conidiation, while constitutive activation of *gna-3* in the Δ*gnb-1* background reduces conidiation to nearly zero, consistent with *gna-3* as a strong negative regulator of conidiation. However, levels of conidia are lower in the Δ*gnb-1* Δ*gna-3* double mutant than in either single mutant. The last observation may reflect the presence of low levels of constitutively active G alpha proteins in the strains lacking *gnb-1*. These strains lack the G beta gamma tether that prevents the G alpha proteins from signaling in the absence of an activated GPCR. In this scenario, the recently discovered cytosolic guanine nucleotide exchange factor (GEF) RIC8 may function to load GTP on the remaining free G alpha proteins. We have shown that RIC8 binds to and regulates GDP/GTP exchange on GNA-1 and GNA-3 in *N. crassa* (174).

Our results demonstrate that the three G alpha genes are epistatic to *gnb-1* for submerged (*gna-3*) or aerial (*gna-1* and *gna-2*) conidiation (Figure 2.5 A and C). This

indicates that the G alpha proteins are likely to interact directly with downstream effector proteins. Since elevated cyclic AMP (cAMP) levels correlate with suppression of conidiation in *N. crassa* (123), one probable effector is adenylyl cyclase (CR-1), which converts ATP to cyclic AMP. GTP (G alpha)-dependent adenylyl cyclase activity can be assayed in submerged liquid cultures of *N. crassa* (124). We have shown that loss of *gna-1* leads to reduced GTP-dependent adenylyl cyclase (CR-1) activity (but normal CR-1 protein levels) in extracts from submerged liquid cultures, supporting adenylyl cyclase as a downstream effector of GNA-1 (66). Δ*gnb-1* mutants have normal CR-1 protein levels, but reduced GTP-stimulatable adenylyl cyclase activity, consistent with decreased GNA-1 protein amount in these strains (177). In contrast, mutation of *gna-3* leads to reduced CR-1 protein levels, but does not influence GTP-dependent activity (77), and *gna-2* has no apparent effect on adenylyl cyclase protein levels or activity (66;76). The last point implies that GNA-2 and GNA-3 interact with another/additional downstream effector(s). These observations, in combination with the known conidiation defects of *N. crassa* mitogen-activated protein (MAP) kinase mutants (86;109;111), suggest that additional effectors (such as MAP kinase modules) operate downstream of GNA-1, GNA-2, GNA-3 and GNB-1 to regulate conidiation.

We observed differences in pigmentation in the strains during this study. Previous work in our laboratory and others has established an inverse relationship between levels of carotenoid pigments and cAMP (19;81;176). For example, loss of *gna-1* leads to increased carotenoid amount and lowered cAMP, while constitutive activation results in reduced levels of carotenoids and elevated cAMP (176). Furthermore, our previous work

indicates that *gna-3* has a more profound positive influence on cAMP levels than *gna-1* does (66;77). Taken together, these observations are consistent with our results showing that *gna-3*^{Q208L} strains are less pigmented than *gna-1*^{Q204L} mutants are. They also reinforce the notion that regulation of cAMP levels is an important downstream function of heterotrimeric G proteins in *N. crassa*.

Regulation of female fertility likely involves GNB-1 regulating protein levels of GNA-1, the active subunit during mating (Figure 2.5 D). GNA-3 plays a role in ascospore ejection and viability, as few ascospores are ejected and are viable from homozygous Δ*gna-3* crosses (77) (Figure 2.5 D). Female fertility was not restored by transformation of the Δ*gnb-1* mutant with any activated G alpha alleles. The observation that activation of GNA-1 is not sufficient to restore full mating in Δ*gnb-1* mutants is consistent with results from a similar experiment conducted in a strain background lacking a pheromone receptor gene (79). The inability to restore female fertility by expressing a GTPase-deficient *gna-1* allele may stem from a need for both GNA-1-GDP and GNA-1-GTP at different times during protoperithecial development, mating, meiosis and/or ascospore formation. Alternatively, GNB-1 may be absolutely necessary for normal sexual development and this requirement cannot be bypassed by activation of *gna-1* or the other two G alpha genes. The *gna-3*^{Q208L} allele completely inhibited development of female reproductive structures, suggesting that GNA-3 needs to be in the inactive GDP-bound form during at least some critical stages of this process in *N. crassa*. This observation is consistent with the relatively normal functioning of Δ*gna-3* mutants

(that completely lack GNA-3 protein) as females during crosses with wild-type males (77).

Our results can be compared to those of studies in *Aspergillus nidulans* and *C. neoformans*, where a single constitutively activated G alpha allele has been tested for its ability to suppress defects of a G beta mutant (60;121). The results showed that an activated Group I G alpha allele bypassed defects resulting from mutation of the G beta gene in *A. nidulans* (121), but not in *C. neoformans* (60). In *A. nidulans*, the authors conclude that the G alpha can function independently of G beta to regulate proliferative growth. In contrast, the findings from *C. neoformans* suggest interdependence of the G alpha and G beta for downstream signaling.

We have proposed that a protein turnover mechanism leads to low levels of the G alpha proteins in the Δ*gnb-1* and Δ*gng-1* backgrounds, as (i) mRNA levels for the three genes are normal in Δ*gnb-1* mutants (82;177), (ii) proteolysis of G alpha proteins is a regulatory mechanism observed in other fungi (22;75;163;175), and (iii) results from preliminary experiments analyzing chemicals that influence the proteasomal or vacuolar protein turnover pathways are consistent with proteolysis of at least one G alpha protein [GNA-1; (data not shown)]. Importantly, we were able to restore levels of the three G alpha proteins through overexpression of the activated alleles. This suggests either that the proteolysis machinery activated in the Δ*gnb-1* background cannot keep pace with the level of G alpha protein being produced or that the GTP-bound form of the G alpha proteins is resistant to the turnover mechanism. We have recently made similar

observations after expression of activated G alpha alleles in a mutant lacking the RIC8 GEF (174).

Previous work in our laboratory explored the epistatic relationship between *ric8* and the three G alpha subunit genes (174). RIC8 is a positive regulator and acts upstream of GNA-1 and GNA-3, but not GNA-2. Moreover, loss of *ric8* not only negatively impacts protein levels of the three G alpha subunits, but also leads to decreased amount of GNB-1 protein. In this work, we found that overexpression of *gnb-1* or *ric8* in the wild type background did not change protein levels of G alpha subunits, suggesting that levels of GNB-1 or RIC8 are already maximal in the wild type background, and further increase does not elevate G alpha protein levels. Overexpression of GNB-1 in the Δ*ric8* background or RIC8 in Δ*gnb-1* mutants did not change levels of G alpha subunit proteins, suggesting that GNB-1 regulates levels of GNA-1, GNA-2, and GNA-3 independently of RIC8 and *vice versa*. In sum, these results suggest that GNB-1 and RIC8 are likely operate in different pathways to regulate G alpha protein levels.

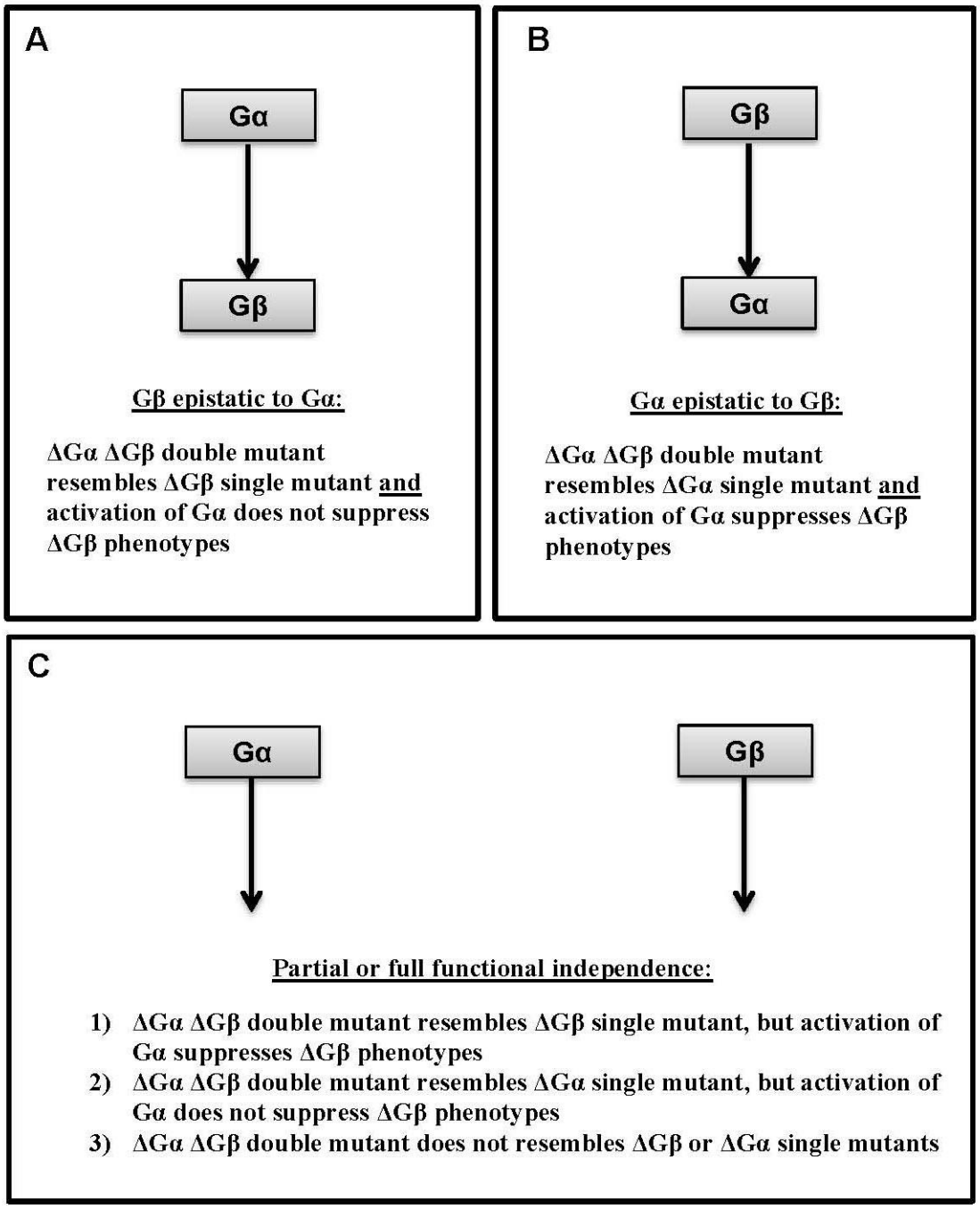

Figure 2.1 Diagram of epistasis analysis. A. G beta epistatic to G alpha, **B.** G alpha epistatic to G beta, **C.** Partial or full functional independence of G alpha and G beta.

TABLE 2.1. Phenotypes of heterotrimeric G protein subunit single gene deletion mutants[a]

Mutation	Submerged culture conidiation[b]	Aerial hyphal height	Aerial conidiation	Female fertility[c]
Δ*gna-1*	None	Slight reduction	Slight increase	Sterile (no perithecia or ascospores)
Δ*gna-2*	None	Normal	Normal	Normal
Δ*gna-3*	Yes	Greatly reduced	Greatly increased	Normal
Δ*gnb-1*	Yes	Reduced	Greatly increased	Sterile (no perithecia or ascospores)
Δ*gng-1*	Yes	Reduced	Greatly increased	Sterile (no perithecia or ascospores)

[a] Phenotypes known prior to this study. All are relative to the wild type.
[b] Inoculated at 10^6 cells/ml. The wild type does not conidiate under these conditions
[c] Fertility in heterozygous crosses with wild-type males.

TABLE 2.2. *N. crassa* strains used in this study

Strain	Relevant genotype	Source or reference
74 A-OR23-1A (74A)	Wild type, *mat A*	FGSC[a] 987
74 a OR8-1a (74a)	Wild type, *mat a*	FGSC 988
74-OR23-IVA	Wild type, *mat A*	FGSC 2489
[b]a^{ml}	*a^{ml} cyh-1 ad3B*	FGSC 4564
his-3a	*his-3 mat a*	(82)
1B4	Δ*gna-1::hph$^+$ mat A*	(66)
1B8	Δ*gna-1::hph$^+$ mat a*	(66)
Δ2	Δ*gna-2::hph$^+$ mat a*	FGSC 12377
3lc2	Δ*gna-3::hph$^+$ mat A*	(77)
hβJ	Δ*gnb-1::hph$^+$ his-3$^-$ mat A*	(77)
42-5-11	Δ*gnb-1::hph$^+$ mat A*	(173)
42-5-18	Δ*gnb-1::hph$^+$ mat A*	(177)
[c]5A	Δ*gng-1::hph$^+$ FLAG-gng-1::his-3$^+$ mat a*	(82)
G1-F	Δ*gnb-1::hph$^+$ his-3$^+$::gna-1^{Q204L} mat a*	(173)
G2-C	Δ*gnb-1::hph$^+$ his-3$^+$::gna-2^{Q205L} mat a*	(173)
G2-D	Δ*gnb-1::hph$^+$ his-3$^+$::gna-2^{Q205L} mat a*	(173)
G3-C	Δ*gnb-1::hph$^+$ his-3$^+$::gna-3^{Q208L} mat a*	(173)
G1-23	Δ*gna-1::hph$^+$* Δ*gnb-1::hph$^+$ mat a*	(173)
G2-5	Δ*gna-2::hph$^+$* Δ*gnb-1::hph$^+$ mat A*	(173)
G3-21	Δ*gna-3::hph$^+$* Δ*gnb-1::hph$^+$ mat A*	(173)
R81-5a	Δ*ric8::hph$^+$ mat a*	(174)
R8↑	*his-3$^+$::ric8 mat a*	This study
B1-R8↑	Δ*gnb-1::hph$^+$ his-3$^+$::ric8 mat a*	This study
B1↑	*his-3$^+$::gnb-1 mat a*	This study
R8-B1↑	Δ*ric8::hph$^+$ his-3$^+$::gnb-1 mat a*	This study

[a]FGSC, Fungal Genetics Stock Center, Kansas City, MO.
[b]Helper strain used for female-fertile heterokaryon production (113)
[c]Strain used for coimmunoprecipitation experiments (173)

TABLE 2.3. Unpaired t-test[a] for aerial hyphae height (cm)

Strains being compared[b]	Mean Difference	DF[c]	t-Value	P-Value	Significance ($p<0.05$)
Wild type; Δ*gnb-1*	-1.233	10	-5176	0.0004	S
Wild type; Δ*gna-1*	-0.417	10	-1.367	0.2017	
Wild type; Δ*gna-2*	-0.233	10	-0.695	0.503	
Wild type; Δ*gna-3*	-1.633	10	-5.973	0.0001	S
Wild type; Δ*gnb-1*, Δ*gna-1*	-1.367	10	-5.839	0.0002	S
Wild type; Δ*gnb-1*, Δ*gna-2*	-1.276	10	-5.11	0.0005	S
Wild type; Δ*gnb-1*, Δ*gna-3*	-1.4	10	-5.382	0.0003	S
Wild type; Δ*gnb-1*, *gna-1*^{Q204L}	-0.733	10	-3.078	0.0117	S
Wild type; Δ*gnb-1*, *gna-2*^{Q205L}	-1.45	10	-5.54	0.0002	S
Wild type; Δ*gnb-1*, *gna-3*^{Q208L}	-1.15	10	-4.331	0.0015	S
Δ*gnb-1;* Δ*gna-1*	0.817	10	3.389	0.0069	S
Δ*gnb-1;* Δ*gna-2*	1	10	3.583	0.005	S
Δ*gnb-1;* Δ*gna-3*	-0.4	10	-2.003	0.073	
Δ*gnb-1;* Δ*gnb-1*, Δ*gna-1*	0.133	10	0.945	0.3667	
Δ*gnb-1;* Δ*gnb-1*, Δ*gna-2*	0.033	10	0.205	0.842	
Δ*gnb-1;* Δ*gnb-1*, Δ*gna-3*	0.167	10	0.921	0.3789	
Δ*gnb-1;* Δ*gnb-1*, *gna-1*^{Q204L}	-0.5	10	-3.38	0.007	S
Δ*gnb-1;* Δ*gnb-1*, *gna-2*^{Q205L}	0.217	10	1.182	0.2646	
Δ*gnb-1;* Δ*gnb-1*, *gna-3*^{Q208L}	-0.83	10	-0.442	0.6682	
Δ*gna-1;* Δ*gna-2*	0.183	10	0.543	0.5991	
Δ*gna-1;* Δ*gna-3*	1.217	10	4.412	0.0013	S
Δ*gna-1;* Δ*gnb-1*, Δ*gna-1*	0.95	10	4.012	0.0025	S
Δ*gna-1;* Δ*gnb-1*, Δ*gna-2*	0.85	10	3.394	0.0068	S
Δ *gna-1;* Δ*gnb-1*, Δ*gna-3*	0.983	10	3.745	0.0038	S
Δ*gna-1;* Δ*gnb-1*, *gna-1*^{Q204L}	0.317	10	1.314	0.2181	
Δ*gna-1;* Δ*gnb-1*, *gna-2*^{Q205L}	1.033	10	3.912	0.0029	S
Δ*gna-1;* Δ*gnb-1*, *gna-3*^{Q208L}	0.733	10	2.737	0.0209	S
Δ*gna-2;* Δ*gna-3*	1.4	10	4.521	0.0011	S
Δ*gna-2;* Δ*gnb-1*, Δ*gna-1*	1.133	10	4.114	0.0021	S
Δ*gna-2;* Δ*gnb-1*, Δ*gna-2*	1.033	10	3.596	0.0049	S
Δ *gna-2;* Δ*gnb-1*, Δ*gna-3*	1.167	10	3.916	0.0029	S
Δ*gna-2;* Δ*gnb-1*, *gna-1*^{Q204L}	0.5	10	1.792	0.1035	
Δ*gna-2;* Δ*gnb-1*, *gna-2*^{Q205L}	1.217	10	4.064	0.0023	S
Δ*gna-2;* Δ*gnb-1*, *gna-3*^{Q208L}	0.917	10	3.029	0.0127	S
Δ*gna-3;* Δ*gnb-1*, Δ*gna-1*	-0.267	10	-1.37	0.2007	
Δ*gna-3;* Δ*gnb-1*, Δ*gna-2*	-0.367	10	-1.737	0.113	
Δ*gna-3;* Δ*gnb-1*, Δ*gna-3*	-0.233	10	-1.035	0.3248	
Δ*gna-3;* Δ*gnb-1*, *gna-1*^{Q204L}	-0.9	10	-4.506	0.0011	S
Δ*gna-3;* Δ*gnb-1*, *gna-2*^{Q205L}	-0.183	10	-0.807	0.4384	
Δ*gna-3;* Δ*gnb-1*, *gna-3*^{Q208L}	-0.483	10	-2.087	0.0634	
Δ*gnb-1*, Δ*gna-1*; Δ*gnb-1*, *gna-1*^{Q204L}	-0.633	10	-4.491	0.0012	S
Δ*gnb-1*, Δ*gna-2;* Δ*gnb-1*, *gna-2*^{Q205L}	0.083	10	0.469	0.6493	
Δ*gnb-1*, Δ*gna-3;* Δ*gnb-1*, *gna-3*^{Q208L}	-0.217	10	-1.182	0.2646	S

[a]Student's *t*-test performed using StatView *v*5.0.1 (SAS Institute Inc., Cary, NC).

[b]Two strains are separated by semicolon.

[c]Degrees of freedom (DF).

TABLE 2.4. Unpaired t-test[a] for conidia amount (% Wild type)

Strains being compared[b]	Mean Difference	DF[c]	t-Value	P-Value	Significance (p<0.05)
Wild type; Δ*gnb-1*	119.683	4	3.8	0.0191	S
Wild type; Δ*gna-1*	9.206	4	0.328	0.7596	
Wild type; Δ*gna-2*	-3.571	4	-0.48	0.656	
Wild type; Δ*gna-3*	69.841	4	8.315	0.0011	S
Wild type; Δ*gnb-1*, Δ*gna-1*	-19.921	4	-2.023	0.1131	
Wild type; Δ*gnb-1*, Δ*gna-2*	24.206	4	1.337	0.2523	
Wild type; Δ*gnb-1*, Δ*gna-3*	-3.889	4	-0.182	0.8646	
Wild type; Δ*gnb-1, gna-1*^{Q204L}	-50	4	-1.941	0.1242	
Wild type; Δ*gnb1, gna2*^{Q205L}	0.476	4	0.04	0.9702	
Wild type; Δ*gnb1, gna3*^{Q208L}	-92.857	4	-13	0.0002	S
Δ*gnb-1;* Δ*gna-1*	-110.476	4	-2.618	0.059	
Δ*gnb-1;* Δ*gna-2*	-123.254	4	-3.809	0.019	S
Δ*gnb-1;* Δ*gna-3*	-49.841	4	-1.529	0.2009	
Δ*gnb-1;* Δ*gnb-1*, Δ*gna-1*	139.603	4	4.231	0.0134	S
Δ*gnb-1;* Δ*gnb-1*, Δ*gna-2*	95.476	4	2.628	0.0583	
Δ*gnb-1;* Δ*gnb-1*, Δ*gna-3*	123.571	4	3.246	0.0315	S
Δ*gnb-1;* Δ*gnb-1, gna-1*^{Q204L}	169.683	4	4.171	0.014	S
Δ*gnb-1;* Δ*gnb1, gna2*^{Q205L}	119.206	4	3.539	0.024	S
Δ*gnb-1;* Δ*gnb1, gna3*^{Q208L}	212.54	4	6.582	0.0028	S
Δ*gna-1;* Δ*gna-2*	-12.778	4	-0.44	0.6829	
Δ*gna-1;* Δ*gna-3*	-60.635	4	-2.067	0.1076	
Δ*gna-1;* Δ*gnb-1*, Δ*gna-1*	29.127	4	0.978	0.3834	
Δ*gna-1;* Δ*gnb-1*, Δ*gna-2*	-15	4	-0.449	0.6769	
Δ *gna-1;* Δ*gnb-1*, Δ*gna-3*	13.095	4	0.371	0.7296	
Δ*gna-1;* Δ*gnb-1, gna-1*^{Q204L}	59.206	4	1.553	0.1953	
Δ*gna-1;* Δ*gnb1, gna2*^{Q205L}	8.73	4	0.286	0.7892	
Δ*gna-1;* Δ*gnb1, gna3*^{Q208L}	102.063	4	3.52	0.0244	S
Δ*gna-2;* Δ*gna3*	-73.413	4	-6.545	0.0028	S
Δ*gna-2;* Δ*gnb-1*, Δ*gna-1*	16.349	4	1.325	0.2557	
Δ*gna-2;* Δ*gnb-1*, Δ*gna-2*	-27.778	4	-1.419	0.2289	
Δ *gna-2;* Δ*gnb-1*, Δ*gna-3*	0.317	4	0.014	0.9895	
Δ*gna-2;* Δ*gnb-1, gna-1*^{Q204L}	46.429	4	1.732	0.1583	
Δ*gna-2;* Δ*gnb1, gna2*^{Q205L}	-4.048	4	-0.287	0.7881	
Δ*gna-2;* Δ*gnb1, gna3*^{Q208L}	89.286	4	8.66	0.001	S
Δ*gna-3;* Δ*gnb-1*, Δ*gna-1*	89.762	4	6.936	0.0023	S
Δ*gna-3;* Δ*gnb-1*, Δ*gna-2*	45.635	4	2.286	0.0842	
Δ*gna-3;* Δ*gnb-1*, Δ*gna-3*	73.73	4	3.207	0.0327	S
Δ*gna-3;* Δ*gnb-1, gna-1*^{Q204L}	119.841	4	4.424	0.0115	S
Δ*gna-3;* Δ*gnb-1, gna2*^{Q205L}	69.365	4	4.746	0.009	S
Δ*gna-3;* Δ*gnb-1, gna3*^{Q208L}	162.698	4	14.756	0.0001	S
Δ*gnb-1*, Δ*gna-1*; Δ*gnb-1, gna-1*^{Q204L}	30.079	4	1.091	0.3366	
Δ*gnb-1*, Δ*gna-2;* Δ*gnb1, gna2*^{Q205L}	-20.397	4	-1.317	0.2584	
Δ*gnb-1*, Δ*gna-3;* Δ*gnb1, gna3*^{Q208L}	72.937	4	5.996	0.0039	S

[a]Student's *t*-test performed using StatView *v*5.0.1 (SAS Institute Inc., Cary, NC).

[b]Two strains are separated by semicolon.

[c]*Degrees of freedom (DF).*

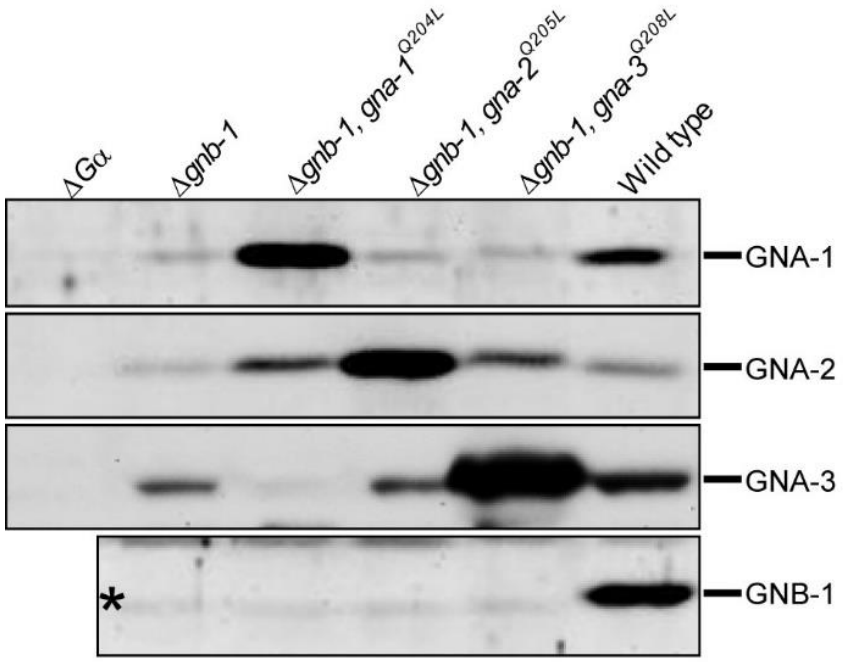

Figure 2.2 Analysis of G alpha and G beta protein levels. Strains are wild type (74a) and Δ*gnb-1* (42-5-11), Δ*gnb-1 gna-1*^{Q204L} (G1-F), Δ*gnb-1 gna-2*^{Q205L} (G2-D), Δ*gnb-1 gna-3*^{Q208L} (G3-C), Δ*gna-1* (1B8), Δ*gna-2* (Δ2), and Δ*gna-3* (31c2) mutants. The last three strains were used as negative controls for the corresponding G alpha antibody (ΔGα lanes). Strains were cultured in liquid VM medium with shaking at 200 rpm for 16 hours in the dark at 30˚C. The plasma membrane protein fraction was isolated, and 100 µg of total protein subjected to Western analysis using GNA-1, GNA-2, GNA-3, and GNB-1 antibodies as described in Materials and Methods.

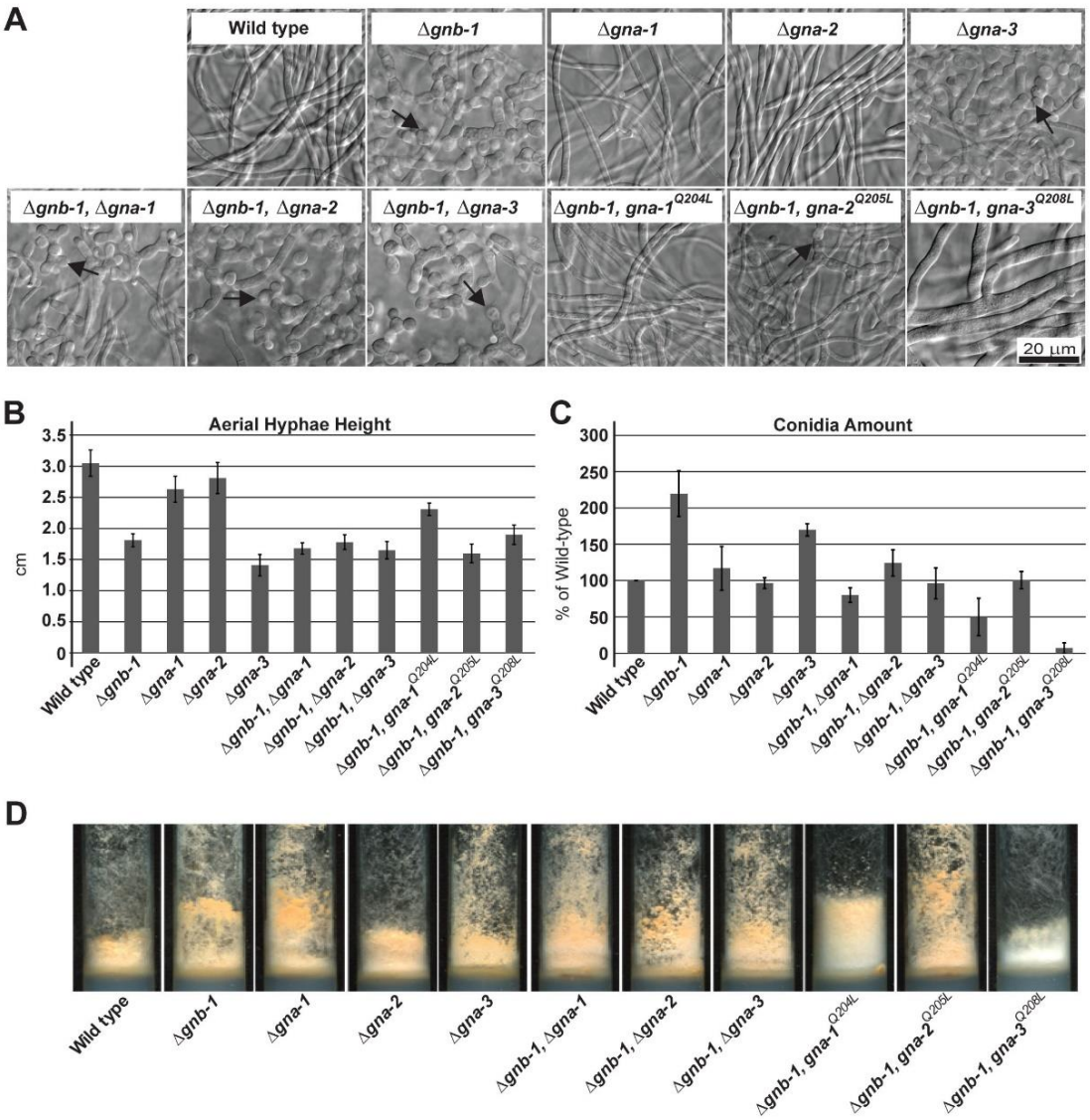

Figure 2.3 Phenotypes during asexual growth and development. Strains are wild type (74a) and Δ*gnb-1* (42-5-18), Δ*gna-1* (1B4), Δ*gna-2* (Δ2), and Δ*gna-3* (31c2), Δ*gna-1* Δ*gnb-1* (G1-23), Δ*gna-2* Δ*gnb-1* (G2-5), Δ*gna-3* Δ*gnb-1* (G3-21), Δ*gnb-1 gna-1*^{Q204L} (G1-F), Δ*gnb-1 gna-2*^{Q205L} (G2-C), Δ*gnb-1 gna-3*^{Q208L} (G3-C) mutants. **A. Submerged cultures.** Strains were cultured in VM liquid medium for 16 hours with shaking at 200 rpm in the dark at 30˚C. The arrows indicate conidiophores. **B. Aerial hyphal height.** To measure aerial hyphal height, liquid VM cultures were inoculated with the indicated strains and incubated statically for 5 days in the dark and 1 day in light at room temperature. Values are from six replicates, with error calculated as the standard error of the mean. **C. Amount of conidia.** VM agar flasks were inoculated with the indicated strains and incubated for 3 days in the dark at 30˚C and 5 days in light at room temperature. Conidia were harvested from flasks and quantitated using a hemacytometer. Values are expressed as percentages of the wild type from three independent experiments, with the error calculated as the standard error of the mean. **D. Strain morphology in VM agar tube cultures.** Strains were

cultured in tubes containing 2 ml of VM agar medium for 3 days in the dark at 30°C and 5 days in light at room temperature.

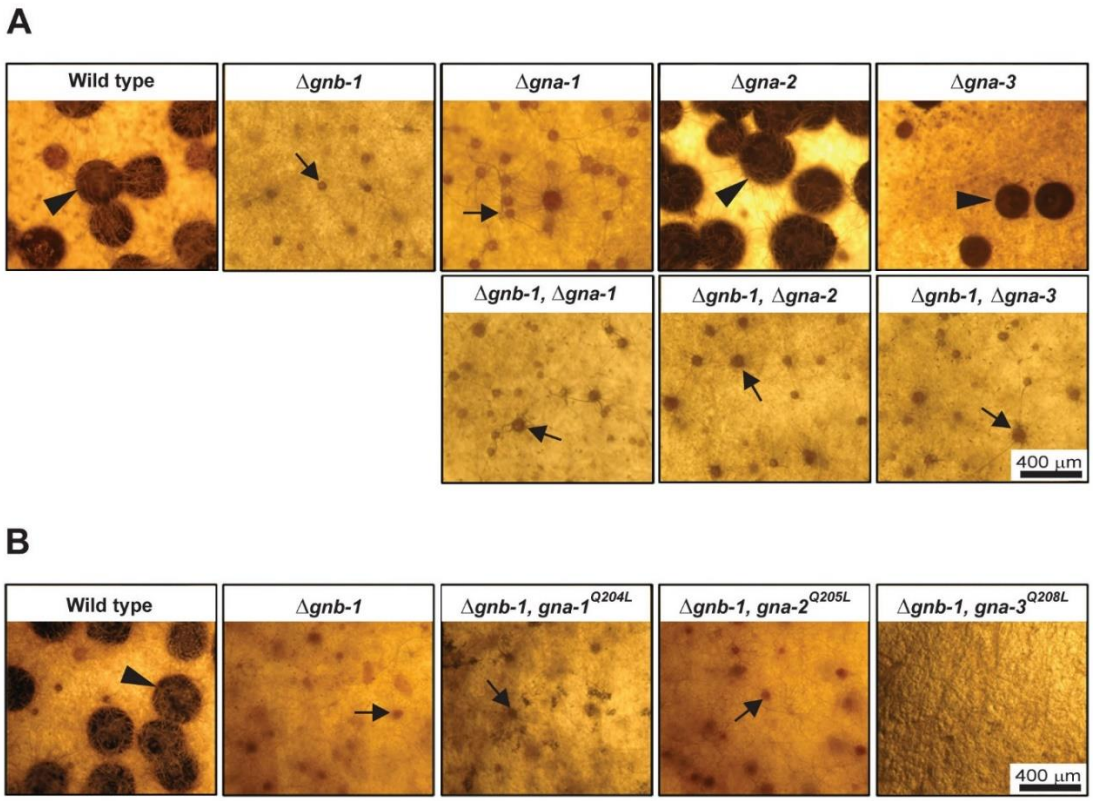

Figure 2.4 Sexual phase phenotypes. Strains were inoculated onto SCM plates to induce production of female reproductive structures (protoperithecia) and incubated for 6 days in constant light at 25˚C. Cultures were then fertilized with males (macroconidia) of opposite mating type and incubated for 6 more days before being photographed. Protoperithecia are indicated by black arrows, while perithecia are marked by black arrowheads. **A. Single and double mutants.** Strains are wild type (74a) and Δ*gnb-1* (42-5-11), Δ*gna-1* (1B4), Δ*gna-2* (Δ2), and Δ*gna-3* (31c2), Δ*gna-1* Δ*gnb-1* (G1-23), Δ*gna-2* Δ*gnb-1* (G2-5), Δ*gna-3* Δ*gnb-1* (G3-21) mutants. **B. Strains carrying G alpha-activated alleles.** Strains are wild type (74a) and Δ*gnb-1* (42-5-11), Δ*gnb-1 gna-1*^{Q204L} (G1-F), Δ*gnb-1 gna-2*^{Q205L} (G2-C), Δ*gnb-1 gna-3*^{Q208L} (G3-C) mutants.

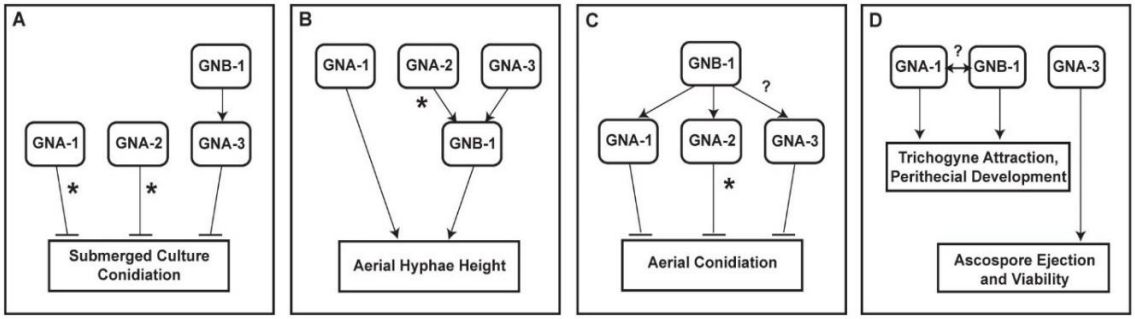

Figure 2.5 Models for interactions between G alpha proteins and G beta gamma dimers in *N. crassa*. A. Submerged culture conidiation. GNB-1 acts upstream of GNA-3 to suppress conidiation in submerged cultures. The independent action of GNA-1 and GNA-2 is observed only in Δ*gnb-1* strains that express constitutively activated *gna-1* or *gna-2* alleles (denoted by asterisks). **B. Aerial hyphal height.** GNA-2 and GNA-3 operate upstream of GNB-1 to positively modulate aerial hyphal height. The asterisk indicates that for *gna-2*, a phenotype is seen only upon constitutive activation in the Δ*gnb-1* background. GNA-1 positively regulates aerial hyphal height independently of GNB-1. **C. Aerial conidiation.** GNA-1 and GNA-2 are downstream of GNB-1 during negative regulation of conidiation on solid medium. The role for *gna-2* is revealed only by the presence of the *gna-2*^{Q205L} allele in the Δ*gnb-1* background (denoted by asterisk). GNA-3 is a strong negative regulator of aerial conidiation, but epistatic relationship between *gna-3* and *gnb-1* is not clear from our analysis (denoted by a question mark). **D. Female fertility.** Although GNB-1 and GNA-1 regulate trichogyne attraction and perithecial development, their epistatic relationship is unclear and the role of GNB-1 may be to maintain GNA-1 protein levels (denoted by the question mark above the double-ended arrow). GNA-3 is required for ascospore ejection and viability, while GNA-2 has no obvious function in regulating female fertility.

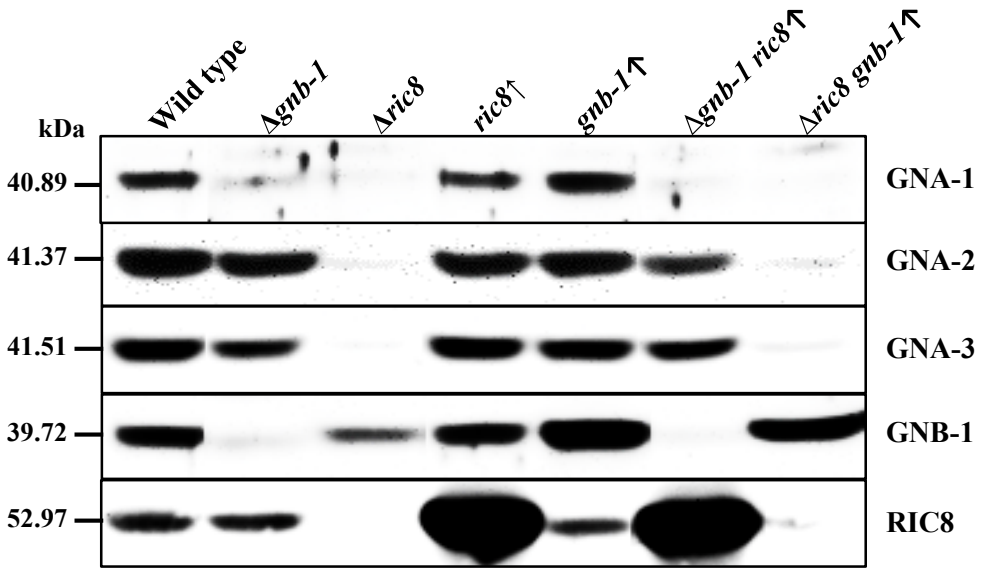

Figure 2.6 Analysis of G protein subunits protein levels. Strains are wild type (74-OR23-IVA) and Δ*gnb-1* (42-5-11), Δ*ric8* (R81-5a), *ric8*↑ (R8↑), *gnb-1*↑ (B1↑), Δ*gnb-1 ric8*↑ (B1-R8↑), Δ*ric8 gnb-1*↑ (R8-B1↑). Strains were cultured in liquid VM medium with shaking at 200 rpm for 16 hours in the dark at 30˚C. The whole cell extract was isolated and 100 µg of total protein subjected to Western analysis using GNA-1, GNA-2, GNA-3, GNB-1, and RIC8 antibodies as described in Materials and Methods.

Chapter 3

Identification of cytosolic proteins that interact with GNA-1 and investigation of GNA-1 protein stability

Abstract

Heterotrimeric G protein signaling pathways are very important for eukaryotic cell homeostasis and the proper response to various environmental signals. Many sensory and chemical stimuli are recognized by cell-surface G protein coupled receptors (GPCRs) that then use heterotrimeric G proteins to transduce this information to intracellular signaling pathways. Heterotrimeric G proteins consist of alpha, beta, and gamma subunits. Signal transduction is accomplished through the alternation between binding of GDP (inactive form) and GTP (active form) on the alpha subunit and dissociation of the alpha subunit and beta-gamma dimer. Duration and intensity of transducing signal are regulated by many factors; one of the most important of which is the amount of the signaling protein. The amount of signaling protein depends on protein synthesis and degradation, which are regulated by multiple protein–protein interactions in the cytosol.

GNA-1 is one of three G alpha subunits in *N. crassa*. Mutation of *gna-1* results in reduced apical growth, osmotic sensitivity, premature conidiation and female sterility. We constructed a *N. crassa* strain with epitope-tagged GNA-1, giving us the opportunity to isolate interacting proteins in the cytosol. Co-immunoprecipitation (CoIP) with V5

epitope tag antibody immobilized agarose beads followed by mass spectrometric (MS) analysis revealed ~46 putative proteins associated with GNA-1. Six GNA-1 protein-protein interactions (NCU07567, NCU07697, NCU09222, NCU11181, NCU02788 and NCU00502) were identified in two independent CoIP/MS experiments, including the Tcp/CCT chaperonin subunit theta (NCU07567) and RIC8 protein (NCU02788). Recovery of RIC8 in both experiments supports the ability of the method to detect true cytosolic interactors. However, it should be noted that one of the CoIP/MS experiments employed a tagged form of GNA-1 (^{V5}GNA-1) that did not show normal stability in Δ*gnb-1* and Δ*ric8* backgrounds (see Appendix B).

These results are preliminary and require follow up. Among the identified proteins from the CoIP/MS experiment using ^{V56His}GNA-1 are those involved in regulation of protein synthesis, protein folding and degradation. Protein synthesis interactors include five ribosomal subunits, one WD repeat-containing protein involved in ribosome biogenesis and one eukaryotic translational initiation factor, eIF-3f, which acts as negative regulator of translation through the mTOR/S6K signaling pathway (97). Follow-up analyses revealed that GNA-1 protein levels are higher in the *eif-3f* deletion mutant. Regarding interactors implicated in protein folding and degradation, we identified four 19S proteasome regulatory subunits. Analysis of knockout mutants lacking two candidates, *sem-1* and *rpn13*, supported a role for these 19S proteasome subunits in degradation of GNA-1.

GNB-1 and RIC8 were tested for positive regulation of GNA-1 protein levels using the inhibitors of protein degradation pathways. Treatment of Δ*gnb-1* or Δ*ric8*

strains with the proteasome inhibitor MG132 did not restore levels of GNA-1. Treatment with the lysosomal protease inhibitor phenylmethylsulfonyl fluoride (PMSF) also did not show any effect. In sum, the results did not support a mechanism involving higher rates of protein turnover in causing the low level of GNA-1 protein in Δ*gnb-1* and Δ*ric8* mutants.

Introduction

The correct and precise functioning of signaling pathways in transmitting signals from upstream receptors to downstream effectors involves multiple sequential and transient protein-protein interactions (PPIs) (168). Heterotrimeric G proteins, composed of alpha, beta and gamma subunits, associate with seven-helix transmembrane receptor proteins (G protein-coupled receptors; GPCRs) at the membrane. Upon activation, the G alpha subunit dissociates from the G beta gamma dimer and they both can activate downstream effectors, which either act as second messengers or direct physiological responses (108). Depending on GDP/GTP occupancy, G alpha subunits interact with a wide variety of proteins, including the G beta gamma dimer, guanine nucleotide exchange factors (GEFs) (both GPCRs and cytosolic GEFs), regulator of G protein signaling (RGS) proteins, and downstream effectors (137).

The G alpha subunit GNA-1 in *N. crassa* regulates multiple cellular processes, including growth, sexual development, asexual sporulation (conidiation) and stress responses (64;176). Previous work in our laboratory reported that *gna-1* has genetic interactions with *gnb-1* and that the GNA-1 protein physically interacts with the G beta gamma dimer (173). In addition, GNA-1 strongly interacts with the carboxyl terminus of the GPCR GPR-4 in the yeast two-hybrid assay (87). Another GEF, RIC8, is localized in the cytosol and interacts with GNA-1 (174). Adenylyl cyclase is a G protein effector in many eukaryotic organisms (31). GNA-1 specific antibody immuno-inhibits the enzymatic activity of CR-1, the membrane-associated *N. crassa* adenylyl cyclase, in

wild-type cell extracts, suggesting a direct interaction between GNA-1 and CR-1 (66). Taken together, the results show that the number of known GNA-1 membrane-associated interactions currently exceeds the number reported for cytosolic proteins.

The major methods used to predict protein-protein interactions are the yeast two-hybrid system (Y2H), fluorescence methods (BRET, FRET, BiFC), and co-immunoprecipitation with detection of interactors by western blot or mass spectrometry (119). Y2H allows the direct detection of interactions between protein pairs. Drawbacks of this method are the large numbers of false negative and positive hits. Ideally in the Y2H assay, the interacting proteins are localized in the nucleus, properly folded, and undergo all necessary posttranslational modifications in the yeast cell environment (63;130). Bimolecular fluorescence methods give the opportunity to detect protein-protein interactions in the live natural environment, but require extensive instrumentation (90). Co-immunoprecipitation followed by mass spectrometry reveals interactions between proteins in their native form in a complex mixture of existing cellular components. This detection method is sensitive enough to detect even transient protein-protein interactions (103).

In this study, we used co-immunoprecipitation combined with identification of the putative proteins by mass spectrometry for identification of cytosolic proteins associated with GNA-1. The results revealed known as well as novel interactions between GNA-1 and other proteins in *N. crassa*. Secondary confirmation of the putative new interactions is needed using CoIP and *in vivo* co-localization.

Materials and Methods

Strains and media. *N. crassa* strains used in this study are listed in Table 3.1. For collection of asexual spores or vegetative growth in liquid or solid culture, strains were cultured in Vogel's minimal medium (VM) (159), with 1% agar added for solid medium (BBL; Becton, Dickinson and Co., Franklin Lakes, NJ). Sorbose medium (FGS) (25) was used to induce colony formation on plates. Female reproductive structures (protoperithecia) were formed on synthetic crossing medium containing 1% agar (167). Medium was supplemented with hygromycin B (Calbiochem, #D00148746) at 200 µg/ml, nourseothricin (Jena Bioscience, #AB-101S) or cycloheximide at 150 µg/ml, where indicated.

Macroconidia (conidia) were propagated in VM agar medium flasks by incubation at 30ºC for three days in the dark, followed by the indicated number of days at room temperature in constant light. Conidia were harvested using water as previously described (35).

For work involving the proteasome inhibitor MG132, modified medium based on one used for *Saccharomyces cerevisiae* (*S. cerevisiae*) (89) was implemented: VM containing 0.5% L-proline and 0.003% sodium dodecyl sulfate (SDS).

For growth of *S. cerevisiae*, YPD medium contained 10 g yeast extract, 20 g peptone, 20 g dextrose, and 15 g agar dissolved in water to a final volume of 1 L (133). SC-Ura medium contained 26.7 g Drop-out Base with Glucose (US Biological,

Swampscott, MA) and 2 g Drop-out Mix Synthetic Minus Uracil w/o Yeast Nitrogen Base (US Biological) in 1 L of water.

Strain construction. The previously published high throughput detailed protocol (29;30;110) was adapted for single knock-in cassette production and transformation of *N. crassa*. A schematic of the knock-in cassette construction using yeast recombinational cloning is presented in Figure 3.1. Briefly, all fragments were amplified from *N. crassa* genomic DNA by PCR using a high fidelity polymerase (Phusion High-Fidelity PCR Master Mix, #F-531S, Thermo Scientific) with the oligonucleotides shown in Table 3.2. The nourseothricin-resistant marker gene (*nat*) under the control of the *Aspergillus nidulans trpC* promoter was excised from plasmid pGPD1-NAT1 (83) using *Eco*RI. All fragments were combined with linearized (digested with *Xba*I and *Xho*I) pRS426 shuttle vector containing the *URA3* marker (28;139) and transformed into *S. cerevisiae* strain FY834 (172), with selection on SC-Ura medium. Plasmids were extracted using the QIAprep Spin Miniprep kit (QIAGEN, #27104) with a user-adapted protocol (Isolation of plasmid DNA from yeast using the QIAprep Spin Miniprep Kit). Constructs were checked using restriction digestion and sequencing (UC Riverside Core Facility).

Confirmed correctly assembled vectors were transformed into a *N. crassa* Δ*mus-51* strain [FGSC #9718;(30)]. Briefly, 7-day-old conidia were collected using sterile water and agitation and filtered through a sterile layer of shop towels to remove all tissue types except conidia, which flow through. The conidial suspension was centrifuged at 2500 rpm for 5 min. The supernatant was removed, and the conidial pellet resuspended in

25 ml of sterile, cold sorbitol (1 M), and concentrated by centrifugation at 2500 rpm for 5 min, with the supernatant poured off again. A volume containing 1 ml of cold 1 M sorbitol was added, and the conidial concentration was determined using a hemacytometer. The concentration was adjusted to 2.0 10^9 conidia/ml using 1 M sorbitol. A volume containing 40 µl of conidial solution was pipetted into an electroporation cuvette along with 10 - 50 µg of linearized vector DNA and electroporated in an Eppendorf electroporator (model #2510). Immediately, 1 ml of cold sorbitol (1 M) was added to the electroporated conidial suspension. The suspension was pipetted into a 15 ml conical tube, to which 4 ml of VM liquid medium was added. The tube was placed in a shaker at 200 rpm for 2 hours at 30°C (recovery step). Then the contents were well-mixed and gently poured on top of petri plates containing 20 ml of FGS + nourseothricin medium (for 100 ml of media: 2 ml of 50x Vogel's, 1 g agar, 88 ml of H_2O, and 10 ml of 10x FGS). The plates were incubated at 30°C in the dark. After approximately 48 hours, single colonies could be visualized; these were picked off the plate with a sterile Pasteur pipet and into a slant tube containing 2 ml of VM-agar supplemented with nourseothricin. The slants were incubated at 30°C in the dark for 2 days. The cultures were then moved to room temperature with ambient lighting conditions and allowed to grow for 3 more days.

To confirm that the transforming DNA was integrated at the native locus, genomic DNA from each of the strains was extracted (Qiagen Fungal Tissue DNA Extraction kit (Qiagen) and subjected to PCR, using screening primers (V5 screening fw

and rv), which produce a product that includes the epitope tag, open reading frame (ORF), and part of the *nat* selectable marker gene (Table 3.2).

N. crassa macroconidia usually contain more than one nucleus and not all of them take up DNA during transformation. This results in formation of heterokaryons. To obtain homokaryons and also eliminate the Δ*mus-51* background, transformants were crossed to the wild-type strain of opposite mating type, 74-OR23-IVA (Table 3.1). Ascospores from the crosses were plated on FGS plates supplemented with nourseothricin. Progeny were screened for the integrated DNA using PCR. All homokaryons were screened for the Δ*mus-51* mutation by spot-testing for Ignite resistance, as described previously (110). Finally, all homokaryons were also checked for production of V5 tagged GNA-1 ($^{V5\ 6His}$GNA-1) using western analysis with GNA-1 specific and epitope tag (V5) antibodies (see below).

Western analysis and immunoprecipitation of tagged GNA-1 protein from *N. crassa*. Western analysis and detection of GNA-1 using a polyclonal antibody was as described in Chapter 2. For detection of the V5 tag, the primary antibody (Mouse anti-V5, Invitrogen) was used at a dilution of 1:2000 in 5% BSA in TBST (Tris-Buffered Saline, 0.1% Tween-20) at 4°C with agitation on a rotating shaker overnight. The secondary antibody (anti-rabbit horseradish peroxidase conjugate; Bio-Rad) was used at a 1:5000 dilution and chemiluminescent detection was as described previously (82).

In order to obtain tissue for co-immunoprecipitation (CoIP) experiments, conidia (harvested as mentioned in Chapter 2) were inoculated in 200 mL VM liquid medium in a

500 mL baffled flask at a concentration of $3x10^6$ conidia/ml, and cultured at 30˚C for 16 hours with shaking (200 rpm). Tissue was collected on filter paper using a vacuum system and cell pads were flash-frozen in liquid nitrogen prior to storage at –80°C. Tissue was pulverized in liquid nitrogen using a mortar and pestle and then transferred into a medium-sized Bead-Beater chamber (Biospec Products, Bartlesville, OK) containing glass beads and Cell Lysis Buffer (50 mM Tris-Cl [pH 7.5], 1 mM EDTA, 250 mM NaCl, 5 mM $MgCl_2$, 0.5 mM PMSF and 0.1% fungal protease inhibitor cocktail; P8215; Sigma-Aldrich, St. Louis, MO, and 0.5% Nonidet P40; NC 9375914, Fisher Scientific). The tissue was homogenized for 45 sec with 60 sec rest (repeated twice) at 4ºC. The homogenate was centrifuged in a JA-25.50 rotor (Beckman-Coulter, Inc., Brea, CA) at 12000xg for 30 min at 4ºC. The supernatant was transferred to a 1.5 ml microcentrifuge tube (for 0.5 ml CoIP reaction volume) or 15 ml conical tube (for 5 ml CoIP reaction volume). After adding 25 µl of an -agarose-antibody slurry (agarose immobilized goat anti-V5 antibody, S190-119, Bethyl laboratories, Montgomery, TX.) to the supernatant, tubes were incubated on a rotating shaker for 3 hours at room temperature or overnight at 4°C. Samples were centrifuged at 200xg for 5 min and the supernatant discarded. The beads were washed three times with cold Cell Lysis Buffer. Each sample was immunoprecipitated in duplicate. One of duplicates was immediately submitted for mass spectrometry analysis, while the other was subjected to western analysis. For elution of the protein complexes from the beads, 80 µL of 1X TBS and 20 µL or 4X Laemmli buffer were added the beads and incubated for 10 min at 85°C. For all experiments after elution, 50 µl fractions were subjected to SDS PAGE, with gels stained using GelCode

Blue Reagent (Thermo Scientific, #24590) or for western blot analysis, as described above and in Chapter 2.

Negative controls. Two different negative controls were used for the CoIP experiments. First, extracts from a wild type strain containing untagged GNA-1 were immunoprecipitated using the protocol outlined above. The results from this control would identify proteins that bind to the V5 tag itself. Second, extracts containing tagged GNA-1 were immunoprecipitated using nonspecific IgG-coupled agarose beads (Bethyl laboratories, #S50-100). This control would identify proteins that bind nonspecifically to IgG and/or agarose beads. Both types of negative control samples were submitted for mass spectrometry analysis.

Mass spectrometry analysis. Samples were submitted for mass spectrometry analysis in the UC Riverside Core Facility. The samples were digested with trypsin and processed as described previously (23). The sample digest was analyzed using a nano-liquid chromatography-electrospray ionization-tandem mass spectrometry (LC-MS-MS) instrument with a Waters nano-Acquity UPLC/Q-TOF Premier system (Waters, Milford, MA). An LC-MS-MS survey scan method was used for analyzing all peptide precursor ions in the samples. The raw data-dependent acquisition from the survey scan was then processed by Protein Lynx (Waters, Milford, MA) software to generate pkl text files that were used to search the NCBI *N. crassa* database with the MASCOT algorithm for protein identification (23;111) . Protein identifications were accepted if they could be

established at 95.0% probability and contained at least two unique identified peptides. The quantitative analysis of protein abundance for the samples was carried out with LC-MS-MS experiments as described in a prior study (120).

Identification of ^{V56His}GNA-1 interacting proteins by MS. A total of 203 proteins were identified from sample containing ^{V56His}GNA-1 CoIP products. After subtracting all proteins that were found in either of the two negative control samples described above, 46 proteins were identified that were specific to ^{V56His}GNA-1 CoIP samples (Table 3.3).

Results

Epitope-tagged GNA-1 is more abundant in the cytosol than wild type and complements most defects of the Δ*gna-1* mutation.

One of the goals of my dissertation research was to identify proteins that interact with GNA-1 in the cytosol. Therefore, I chose to fuse an epitope tag at the amino terminus of GNA-1, since the C-terminus is typically required for interaction with GEFs and other proteins. The N-terminus of G alpha proteins is important for interaction with G beta subunits and G protein coupled receptors (61;70).

We used a "knock-in" method to replace the endogenous *gna-1* ORF with the tagged version. Expression of the full-length GNA-1 protein was checked using V5 tag and GNA-1 specific antibodies. ^{V56His}GNA-1 was recognized using both antibodies (Figure 3.2A). The predicted molecular mass of wild type GNA-1 is 40.89 kilodaltons, while ^{V56His}GNA-1 is 43.57 kilodaltons, and these molecular masses correlate with the band sizes in Figure 3.2A. The wild type GNA-1 protein was previously detected by pertussis toxin labeling in whole cell extracts and the particulate (membrane) fraction (64;155), and by GNA-1 specific antibody in the particulate fraction (64;65;176). In my experiments, wild type GNA-1 was present in the particulate fraction, and practically undetectable in the cytosol, while ^{V56His}GNA-1 was detected in cytosol and particulate (membrane) fractions in 1:1 proportion. The presence of significant amounts of tagged

GNA-1 in the cytosol presented the opportunity to explore cytosolic GNA-1 interactors (Figure 3.2 B).

Higher accumulation in the cytosol could result in less GNA-1 available to be activated by GPCRs, leading to partial or complete lack of function. Previous work has demonstrated that loss of *gna-1* leads to a slower rate of hyphal apical extension and female-sterility (64). Thus, it was necessary to determine whether the ^{V56His}GNA-1 strain possessed any growth or developmental defects that might suggest issues with proper folding of the tagged protein. Phenotypic analysis of the ^{V56His}GNA-1 strain showed that it has growth rate 60% of wild type, better than Δ*gna-1* mutants, which grow only 40% of wild type, and has no other visible defects in comparison to wild type. The Δ*gna-1* mutant is female sterile, but the ^{V56His}GNA-1 strain is female fertile, similar to wild type. Taken together the results demonstrate that the ^{V56His}*gna-1* allele complements most phenotypes (except growth) of the Δ*gna-1* mutant. Introduction of the ^{V56His}*gna-1* allele into the Δ*ric8* background resulted in a strain with Δ*ric8* defects, including low GNA-1 protein levels. On the other hand, another variant of *gna-1* with only V5 epitope tag showed similar phenotypes as wild type, except protein levels in *gnb-1* or *ric8* deletion mutants are not affected and have the same level as in wild type background (Appendix B).

Identification of 46 unique cytosolic GNA-1 interactors distributed in 17 functional categories.

A direct CoIP with V5 antibody agarose beads was used to identify cytosolic GNA-1 interactors. After adjusting all experimental conditions, including the amount of total protein and duration of reaction, two methods were used to visualize the quality of co-immunoprecipitation: gel staining and western blot (Figure 3.3). ^{V56His}GNA-1 protein was easily detectable after staining gels with the GelCode Blue Reagent (Figure 3.3 A) and by probing the western blots with V5 antibody (Figure 3.3 B). To identify proteins that were non-specifically bound to agarose beads and/or IgG, extracts from wild type and ^{V56His} GNA-1 strains were incubated with IgG agarose beads. Proteins that nonspecifically bind to the V5 tag were detected by immunoprecipitating the extract of a wild type strain with V5 agarose beads.

Trypsin digested peptides were analyzed by LS-MS-MS. The acquired data was used to search the *N. crassa* genome database at the Broad Institute with the MASCOT algorithm to identify protein hits. A total of 203 proteins were identified in the CoIP from the ^{V56His}GNA-1 strain. After subtracting hits that were found in the control experiments described above, 46 unique proteins were specifically identified in ^{V56His}GNA-1 CoIP samples (Table 3.3). The bait ^{V56His} GNA-1 protein was identified as the highest score only in extracts of the ^{V56His} GNA-1 strain immunoprecipitated using V5 agarose beads (Table 3.3), which suggests successful CoIP and MS identification. There were no hits to the other G alpha subunits or components of the G beta gamma dimer, perhaps reflecting

the membrane association of these other proteins. It will be important to detect and identify interactions of GNA-1 with membrane-associated proteins using ^{V56His}GNA-1 CoIP/MS of the solubilized particulate (membrane) fraction. The combination of these two methods will allow us to build the complete GNA-1 interactome.

Even though our results are preliminary and still require confirmation by additional experiments, we were interested in identifying GNA-1 protein – protein interactions (PPI), which might affect the level of GNA-1 protein. GNA-1 cytosolic PPIs were functionally distributed using the MIPS Functional Catalog into 17 categories (FunCat, http://mips.helmholtz-muenchen.de/funcatDB/) (127) (Figure 3.4), with protein sequences obtained from the Broad Institute *N. crassa* genome database. Four proteins were in the Unclassified Protein category (NCU00059, NCU04254, NCU02006, and NCU09222). The most entries were in the Protein Fate, Metabolism, and Cellular Transport categories (Figure 3.4).

Deletion of *eif-3f*, *sem-1*, and *rpn13* affect GNA-1protein levels.

Putative GNA-1 associated proteins from the Synthesis and Protein Fate categories would be protein-protein interactions most likely to affect the G alpha protein life cycle. GNA-1 has 12 entries in the Protein Synthesis category, suggesting that GNA-1 may uniquely regulate translational processes. Among Protein Synthesis category interactors are five 40S and 60S ribosomal subunit proteins (NCU04552, NCU06226, NCU06210, NCU08627, NCU03150), one WD repeat containing protein (NCU07885)

involved in ribosome biogenesis, and one eukaryotic translation initiation factor 3, eIF-3f (NCU01021). eIF-3f plays an important role in regulation of the TOR signaling pathway in mammals (33;97). The majority of proteins in the Protein Synthesis and Protein Fate categories are high abundance proteins. Demonstration that these are specific GNA-1 interactors requires confirmation by additional methods, including CoIP using protein-specific antibodies.

The 26S proteasome, the macromolecular degradation machine of the ubiquitin-proteasome pathway, consists of a self-compartmentalized 20S protease core that is capped at one or both ends by the 19S regulatory particle (115;140;161). The 20S core particle is responsible for proteolytic activities, while the 19S regulatory complex is required for ATP-dependent recognition of the substrate proteins (156;161). 26S proteasome -mediated protein degradation is very important to the regulation of many cellular processes, including DNA repair, transcriptional activation, metabolism, signal transduction, stress responses, etc. (49;71;115). Among the GNA-1 interactors, we identified four proteasome regulatory subunits: *rpt-3* (NCU2260), *sem-1* (NCU07913), *rpn-3* (NCU02224), and *rpn13* (NCU02634). All of these are predicted components of the 19S regulatory complex.

At the time of this study, viable deletion mutants were available for *sem-1*, *rpn13*, *rpn-3*, and *eif-3f*. Using GNA-1 specific antibodies, I checked GNA-1 protein levels in these four deletion mutants (Figure 3.5). Three different fractions were evaluated: whole cell extract, cytosol, and particulate (membrane) fractions. In whole cell extract and cytosolic fractions, there are background bands just above the GNA-1 species. These

background bands are absent from the particulate fraction. The level of GNA-1 protein in whole cell extracts and cytosol of wild type is very low due to membrane association of the G alpha protein (Figure 3.5). In contrast, we observed accumulation of GNA-1 in the cytosolic and particulate fractions in Δ*sem-1* and Δ*rpn13*, but not Δ*rpn-3* mutants, presumably due to disruption of protein turnover in the first two strains. This result suggests that *sem-1* and *rpn13* are components of the protein degradation machinery for GNA-1 in *N. crassa*. Interestingly, we observed the same pattern for Δ*eif-3f* mutants as for strains lacking Δ*sem-1* or Δ*rpn13* (Figure 3.5), suggesting possible translational regulation of GNA-1 by eif-3f.

GNA-1 protein stability and turnover in *N. crassa*

GNA-1 protein stability and protein turnover were investigated using different inhibitors: cycloheximide (CHX) to halt protein biosynthesis (138), MG132 to inhibit the 26S proteasome (85;85) and (PMSF) to block degradation of proteins by multiple vacuolar proteases (73;85) (Figure 3.6). Use of MG132 in fungi is problematic due to impermeability of the cell wall and/or membrane and MG132 is effective only in *S. cerevisiae* mutants (Δ*erg4*, Δ*pdr5*) with increased drug permeability or reduced drug efflux (41;85). However, these mutations may indirectly or directly affect many cellular processes (42;166), including those regulated by G-proteins (40). To avoid the problems we used a *S. cerevisiae* protocol adapted for *N. crassa*, which included medium with L-proline as the nitrogen source and treatment with sodium dodecyl sulfate (SDS; 0.003%).

These conditions have been shown to increase the permeability of wild type *S. cerevisiae* cells to MG132 (89).

CHX treatment over 36 hours did not lead to a significant decrease in the GNA-1 level in wild type *N. crassa*. Combined treatment for 36 hours with CHX and MG132 increased the level of GNA-1 by 25%. CHX and PMSF treatment resulted in a similar level of GNA-1 at every time point (Figure 3.7). Some of the values exceed 100%, which indicates that CHX treatment did not completely stop biosynthesis, even though a protocol was used that previously demonstrated effectiveness of more than 80% in *N. crassa* (114) To confirm these results would require further a pulse-chase experiment using a labeled amino acid to determine whether CHX was effective in halting production of total protein. Taken together with the results indicating that higher levels of GNA-1 were observed in *sem-1* and rpn13 19S proteasome regulatory deletion mutants, these experiments support degradation of GNA-1 via the 26S proteasome in wild type *N. crassa*.

As already mentioned above, the GNA-1 protein level is low in Δ*gnb-1* and Δ*ric8* backgrounds (Figure 3.8), which could be explained by higher rates of protein turnover. To override GNA-1 degradation, we used protein degradation inhibitors during a time course of 48 hours. Addition of CHX was not necessary, since the GNA-1 level could not be detected at time point 0 in these genetic backgrounds. Treatment with MG132 or PMSF did not restore the level of GNA-1 at any time over 48 hours (Figure 3.8). These results suggest that GNB-1 and RIC8 do not regulate degradation of GNA-1 or that treatment with these two degradation inhibitors does not halt turnover of GNA-1 in these

mutant backgrounds. To investigate the last possibility, it will be useful to check whether the GNA-1 protein level is restored in 19S proteasome regulatory subunit deletion mutants in the Δ*gnb-1* and Δ*ric8* genetic backgrounds.

Discussion

The focus of this work was to identify cytosolic protein-protein interactions and investigate the stability of GNA-1 in different genetic backgrounds. I created a strain expressing epitope-tagged GNA-1, which complements most defects of the Δ*gna-1* mutation. In comparison with wild type GNA-1, which is present in very low amount in the cytosolic fraction, ^{V56His}GNA-1 was equally distributed (1:1) in both cytosolic and particulate fractions (Figure 3.2 B). G alpha subunits are subject to several types of lipid modifications, such as myristoylation and palmitoylation (32). Fully mature Gpa1p is membrane associated most of the time and only small amounts of Gpa1p are released from the membrane due to depalmitoylation in *Saccharomyces cerevisiae* (96). The higher amount of ^{V56His}GNA-1 in the cytosol in *N. crassa* could be explained by higher rates of depalmitoylation. However, the combination of complementation of the most defects of the Δ*gna-1* mutation and the greater amount of GNA-1 in the cytosol made this strain perfect for identification of cytosolic interacting proteins.

Using CoIP/Mass-spectrometry analysis, I preliminary identified 46 unique hits, which represent putative proteins interacting with GNA-1 in the cytosol (Table 3.3). Cytosolic proteins associated with GNA-1 were functionally distributed into 17 categories (Figure 3.4).

It is of interest that GNA-1 protein-protein interactions in the Protein Synthesis category included eukaryotic translation initiation factor 3, eIF-3f (NCU01021) (Table 3.3). The *N. crassa* eIF-3f subunit has no homolog in *S. cerevisiae*, but is highly

conserved in mammals, the fruit fly *Drosophila melanogaster*, the worm *Caernorhabditis elegans*, the plant *Arabidopsis thaliana* and the fission yeast *Schizosaccharomyces pombe* (4;53). My results showed that the level of GNA-1 in the Δ*eif-3f* background is higher than in wild type, which may result from higher rates of translation in the mutant (Figure 3.5). In mammalian cells, ribosome profiling assays show that ectopic expression of subunit eIF-3f inhibits translation and overall cellular protein synthesis (134;135). The mechanism of eIF-3f translational inhibition in *N. crassa* is unknown. In mammalian systems, it has been shown that eIF-3f regulates translation via physical interactions with mTOR and inactive S6K1 (51;59). In turn, mTOR and activated (phosphorylated) S6K promote assembly of eIF3-preinitiation complexes, recruitment of other initiation factors, and the translation of mRNAs encoding proteins (59). The role of mTOR is to control translation of proteins according to available cell resources, such as nutrients, energy, oxygen, etc. In animals, upstream mTOR signaling components include small GTPases proteins or their effectors (52). For example, the small GTPases protein Rheb is a molecular target of the TSC complex that regulates mTOR signaling in mammalian cells (149). mTOR also can be activated by inhibition of the TSC complex through the MAPK/ERK pathway, which is regulated by heterotrimeric GTPases (99).

The Protein Fate category has the most entries for putative GNA-1 associated proteins. Among them are four 19S proteasome regulatory subunits: *rpt-3* (NCU2260), *sem-1* (NCU07913), *rpn-3* (NCU02224), and *rpn13* (NCU02634). In *S. cerevisiae sem-1* plays an important role during proteasome lid biogenesis (16;141;151). The 19S proteasome regulatory subunits RPT-3, RPN-3, and RPN13 have functions in recognition

and proteolysis of ubiquitinated substrates in *S. cerevisiae* (8;47;62;126). During this work, I checked the GNA-1 protein level in three 19S proteasome regulatory subunit deletion mutants (Figure 3.5). Δ*sem-1* and Δ*rpn13* showed higher levels of GNA-1, especially in the cytosolic fraction, suggesting a scenario in which GNA-1 is recognized as a substrate for proteolysis by these 19S regulatory subunits. In the case of the Δ*rpn-3* strain, the level GNA-1 was not affected, suggesting that RPN-3 is not involved in recognizing and degrading GNA-1 in *N. crassa*. However, since the most of hits in the Protein Fate category are abundant proteins, their GNA-1 interactions must be confirmed by other methods before definitive conclusions can be reached.

Interestingly *S. cerevisiae* Gpa1p protein-protein interactions did not include any chaperones, but among *S. cerevisiae* G beta subunit interactors were four CCT chaperonin subunits (BioGRID). In this work, I identified four putative GNA-1 proteins that are chaperones or co-chaperones in other systems: *dnj1* (NCU07414), *tcp8* (NCU07567), *tcp5* (NCU03980), and *ric8* (NCU02788). TCP8 and RIC8 were proteins that I identified as GNA-1 associated in both CoIP/MS experiments (Table 3.3, highlighted). TCP8 and TCP5 are subunits of the cytosolic chaperonin ring complex Tcp/CCT is required for assembly of actin, tubulin and many other proteins *in vivo* (146). The *S. cerevisiae* G beta subunit Ste4p has been demonstrated to interact with four chaperonin CCT ring complex subunits (57). RIC8 interacts with G protein alpha subunits and acts as cytosolic GEF in many organisms, including *N. crassa* (1;102;150;152;174). DNJ1 is a HSP40 co-chaperone, involved in cellular stress responses and protein folding and refolding by regulating functions of HSP70 and HSP90

(34;80;93). Tcp/CCT ring complex, HSP70/HSP90, and RIC8 have been proposed as the chaperones for nascent G alpha subunits in mammalian systems (26;147). Confirmation that RIC8 is a chaperone in *N crassa* requires further investigation. One of the methods will be to construct structurally unstable G alpha variants using a protein modeling suite (Medusa) (153). The destabilized G alpha variant will not fold properly in any background and will accumulate during treatment with the MG132 proteolysis inhibitor.

GNA-1 physically interacts with GNB-1 as a component of the G beta gamma dimer (173) and with RIC8 (174), and the level of GNA-1 protein is low in Δ*gnb-1* and Δ*ric8* mutants, without affecting the mRNA amount (82;174). We proposed that the low GNA-1 protein level in Δ*gnb-1* and Δ*ric8* backgrounds is due to higher rates of protein turnover. According to our hypothesis, inhibition of protein degradation should restore GNA-1 protein levels in the deletion mutants (*gnb-1* and *ric8*) to those seen in wild type (Figure 3.6). During our study, we found that *N. crassa* GNA-1, in contrast to *S. cerevisiae* Gpa1p, is stable, as levels of GNA-1 decreased only by 9% over 36 hours of CHX treatment (Figure 3.7). In order to confirm these results, I would need to perform further experiments to measure the effectiveness of CHX in blocking protein synthesis. Our results show that there was no restoration of GNA-1 levels in Δ*gnb-1* and Δ*ric8* backgrounds when treated with inhibitors of proteasome or vacuolar degradation pathways (Figure 3.8). Taken together, our results suggest that GNB-1 and RIC8 do not regulate degradation of GNA-1 and that the low levels of G alpha proteins in Δ*gnb-1* and Δ*ric8* backgrounds result from other cellular processes in *N. crassa*.

Interestingly, overexpression of constitutively active, GTPase deficient alleles for each G alpha gene (*gna-1*^{Q204L}, *gna-2*^{Q205L}, and *gna-3*^{Q208L}) in Δ*gnb-1* and Δ*ric8* backgrounds restored levels of the corresponding proteins (82;173;174). This suggests that processes that lead to reduced G alpha protein levels in Δ*gnb-1* and Δ*ric8* backgrounds have a low capacity and can be overcome by a higher level of gene expression. In this case, there is a high probability that the increased amount of mRNA causes higher rates of translation. Experiments that support translational regulation are discussed in Chapter 4.

TABLE 3.1 *N. crassa* strains used in this study

Strain	Relevant genotype	Source or reference
74-OR23-IVA	Wild type, *mat A*	FGSC[a] 2489
ORS-SL6a	Wild type, *mat a*	FGSC 4200
1B4	Δ*gna-1::hph*$^+$ *mat A*	(66)
1B8	Δ*gna-1::hph*$^+$ *mat a*	(66)
42-5-11	Δ*gnb-1::hph*$^+$ *mat A*	(173)
42-5-18	Δ*gnb-1::hph*$^+$ *mat A*	(177)
R81-5a	Δ*ric8::hph*$^+$ *mat a*	(174)
mus-51 a	Δ*mus-51::hph*$^+$ *mat a*	FGSC 20277
mus-51 A	Δ*mus-51::hph*$^+$ *mat A*	FGSC 20278
NCU02634	Δ*rpn13::hph*$^+$ *mat a*	FGSC 12855
NCU02224	Δ*rpn-3::hph*$^+$ *mat a*	FGSC 11585
NCU07913	Δ*sem-1::hph*$^+$ *mat a*	FGSC19348
NCU01021	Δ*eif-3f::hph*$^+$ *mat a*	FGSC16510
[b]G1	$^{V5\ 6His}$*gna-1 mat a*	This study

[a]FGSC, Fungal Genetics Stock Center, Kansas City, MO.
[b]Strain used for coimmunoprecipitation experiments.

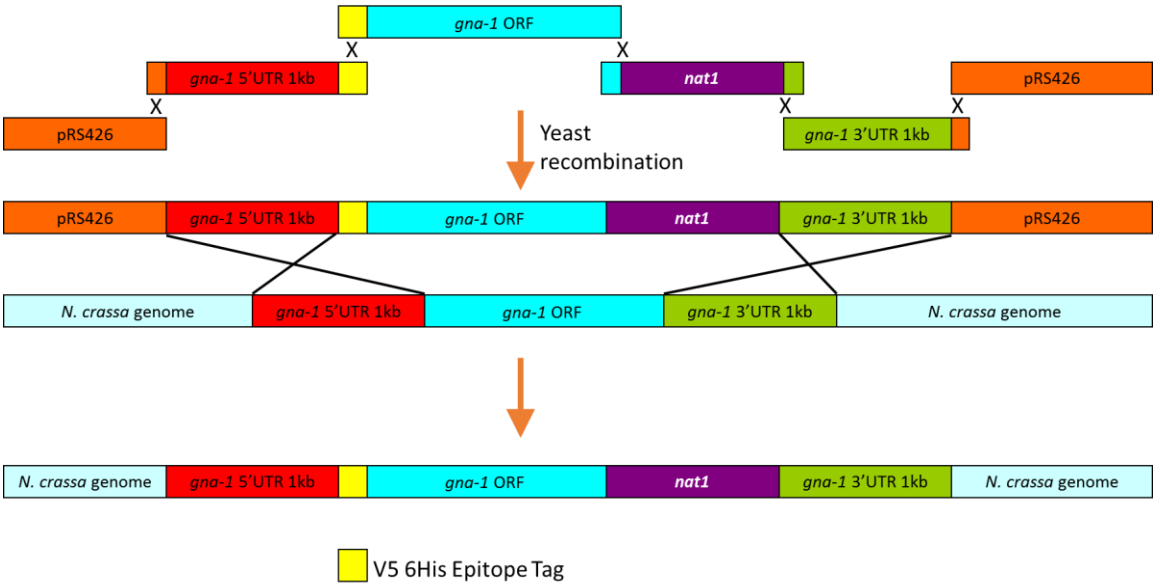

Figure 3.1 Scheme for tagging *gna-1* at the endogenous locus under control of the native promoter. Individual DNA fragments were amplified using the high fidelity polymerase and constructs produced utilizing yeast recombinational cloning. Construct was sequenced and used for electroporation into *Δmus-51* strain.
Abbreviations: pRS426 is the linearized shuttle vector; *nat1* - nourseothricin resistant marker gene under *trpC* promoter of *Aspergilus nidulans*. *N. crassa* genome – Δ*mus-51* strain.

TABLE 3.2 Oligonucleotides used in this study

Name	Sequence
[b]G1 5'UTR YR fw	GTAACGCCAGGGTTTTCCCAGTCACGACGAGTGCCGTCT AGCGTAGTGCC
[a]G1 5'UTR V5 6H rv	ACCGGTACGCGTAGAATCGAGACCGAGGAGAGGGTTAG GGATAGGCTTACCCATTTTGGCGACTTGTTGTAGCTCGT AGC
[a]G1 orf V5 6H fw	CTCCTCGGTCTCGATTCTACGCGTACCGGTCATCATCACC ATCACCATATGGGTTGCGGAATGAGTACAGAGG
[c]G1 orf YR rv	CCTGCGTCTCTGCGGTTTGATTTGAAGATCTTTGCCCGGT GTATGAAACCGGAA
[c]G1 3'UTR YR fw	CGCTCTACATGAGCATGCCCTGCCCCTGAGCACTGAACG CAATCTTTCTAATTTTTTCATCAG
[b]G1 3'UTR YR rv	GCGGATAACAATTTCACACAGGAAACAGCAGACAAATC CAACCGTTGCGTTGCCC
[d]V5 Screening fw	CTATCCCTAACCCTCTCCTCGGTCTCGA
[e]V5 Screening rv	TCGAGACCGAGGAGAGGGTTAGGGATAG

[a]V5 and 6His tags and 5 poly glycine included in oligonucleotide sequence for yeast recombination
[b]pRS426 sequences included in oligonucleotide sequence for yeast recombination with shuttle vector
[c]Nourseothricin resistant gene sequences included in oligonucleotide sequence for yeast recombination
[d]Screening primer forward, include V5 tag sequence
[e]Screening primers reverse, include Nourseothricin ORF sequence

A.

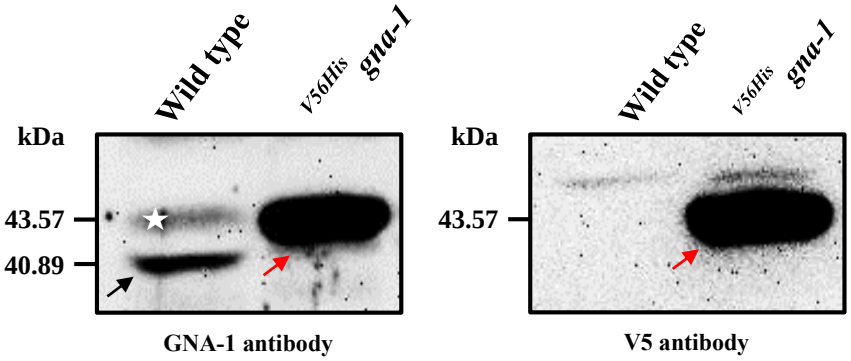

B.

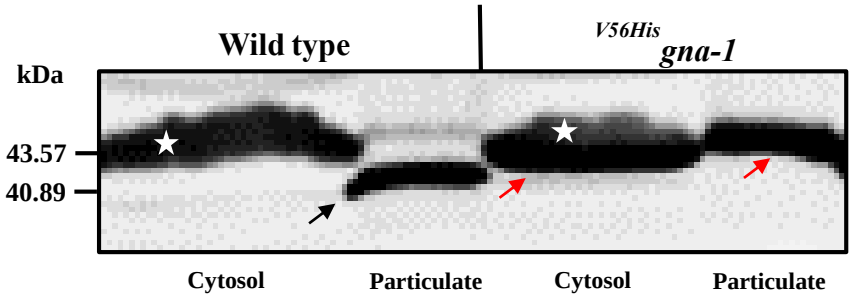

Figure 3.2 Expression and Localization of ^{V56His}GNA-1 protein. A. Detection of the ^{V56His}GNA-1 protein. Strains are wild type (ORS-SL6a) and ^{V56His}GNA-1 (G1). Strains were cultured in liquid VM medium with shaking at 200 rpm for 16 hours in the dark at 30˚C. Whole cell extracts were used for western analysis using GNA-1 antibody. **B. Localization of the ^{V56His}GNA-1 protein in cytosol and particulate fractions.** Strains were cultured as described in (A). Cytosolic and particulate (membrane) fractions were isolated, and 100 µg of total protein subjected to western analysis using GNA-1 antibody. White stars denotes background bands, black arrows indicate wild type GNA-1 protein, and red arrows indicate ^{V56His}GNA-1 protein.

A.

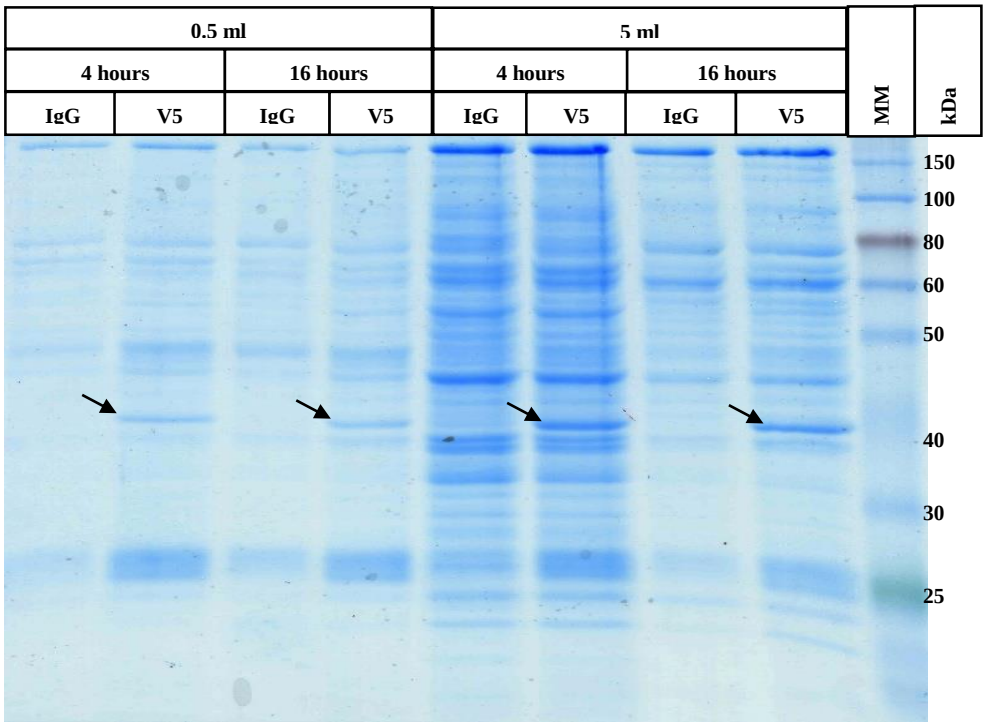

B.

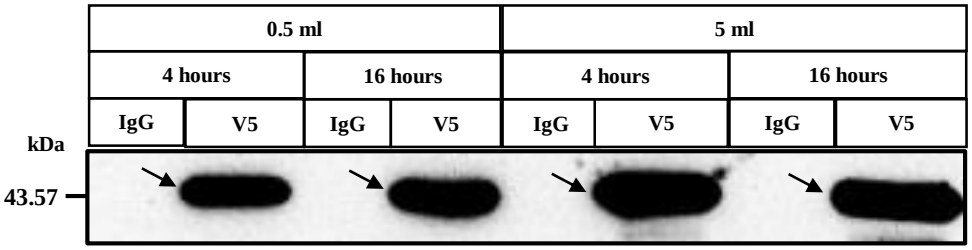

Figure 3.3. Coimmunoprecipitation conditions. CoIP reaction volumes were 0.5 and 5 mL (Total protein concentration 20 mg/mL) with incubation time 4 and 16 hours in 4°C, using two types of agarose beads: IgG and V5 antibody immobilized. **A. Gel stained using GelCode Blue Reagent. B. Western blot reacted with V5 monoclonal antibody.** ^{V56His}GNA-1 bands are denoted by black arrows

TABLE 3.3 Putative ^{V56His}GNA-1 cytosolic interacting proteins identified from preliminary CoIP/MS

Nº	NCU	Protein	Score
1	**NCU06493**	**guanine nucleotide-binding protein alpha-1 (354 aa)**	**2315**
2	NCU07567	T-complex protein 1 subunit theta (548 aa)	125
3	NCU00775	isocitrate dehydrogenase subunit 1 (386 aa)	103
4	NCU07697	isocitrate dehydrogenase subunit 2 (380 aa)	102
5	**NCU05007**	**spindle poison sensitivity protein Scp3 (667 aa)**	**101**
6	NCU12059	hypothetical protein (639 aa)	100
7	NCU09222	hypothetical protein (117 aa)	99
8	NCU03020	IdgA domain-containing protein (783 aa)	98
9	**NCU04100**	**vacuolar sorting protein 1 (707 aa)**	**97**
10	**NCU03387**	**vesicular-fusion protein SEC18 (854 aa)**	**86**
11	NCU02006	hypothetical protein (774 aa)	85
12	NCU07286	related to membrane-associated progesterone receptor component 1 (174 aa)	79
13	NCU04552	40S ribosomal protein S26E, cytoplasmic ribosomal protein-5 (120 aa)	78
14	NCU08627	40S ribosomal protein CRP7, cytoplasmic ribosomal protein-7 (88 aa)	74
15	**NCU11181**	**Ras superfamily GTPase (190 aa)**	**72**
16	NCU02634	hypothetical protein (394 aa)(proteasome Rpn13 superfamily)	67
17	**NCU06419**	**MAP kinase kinase, MAPK/ERK kinase (519 aa)**	**62**
18	NCU06226	60S ribosomal protein L25 (157 aa)	62
19	NCU02224	26S proteasome non-ATPase regulatory subunit 3 (553 aa)	56
20	NCU03606	replication factor-A protein 1 (611 aa)	55
21	NCU04254	hypothetical protein (1647 aa)	54
22	NCU03857	isocitrate dehydrogenase NADP+, tca-5 (463 aa)	46
23	NCU02605	DNA-directed RNA polymerase I/II/III subunit 10 (85 aa)	45
24	NCU07913	hypothetical protein (92 aa)(26 proteasome complex subunit Sem1)	45
25	**NCU02354**	**RSC complex subunit, porin-binding domain protein-1 (1207 aa)**	**44**
26	**NCU09377**	**protein phosphatase PP2A regulatory subunit B-1 (482 aa)**	**44**
27	NCU03838	transcription elongation factor spt-4 (121 aa)	43
28	NCU00636	ATP synthase subunit D (174 aa)	42
29	NCU04459	Transcription coactivator, SAGA complex subunit (523 aa)	40
30	**NCU02788**	**Ric8 like (480 aa)**	**37**
31	NCU08776	hypothetical protein (1189 aa)	36
32	**NCU09269**	**GTP-binding nuclear protein GSP1/Ran (216 aa)**	**36**
33	NCU01501	mitochondrial peptidyl-tRNA hydrolase Pth2 (331 aa)	35
34	NCU01021	eukaryotic translation initiation factor 3 subunit, eIF-3f (370 aa)	34
35	NCU02677	carbamoyl-phosphate synthase large subunit, arginine-3 (1169 aa)	33
36	NCU02657	s-adenosylmethionine synthetase, ethionine resistant-1 (396 aa)	30
37	NCU03150	60S ribosomal protein L24 (157 aa)	28
38	NCU00059	hypothetical protein, rRNA processing/ribosome biogenesis (830 aa)	26
39	NCU08024	mannan polymerase II complex ANP1 subunit (482 aa)	24
40	NCU07414	DnaJ family protein, hypothetical protein similar to protein mitochondrial targeting protein Mas5 (415 aa)	23
41	NCU06210	hypothetical protein (151 aa)(Ribosomal L28e protein family)	22
42	NCU02260	26S protease regulatory subunit 6B (422 aa)	21
43	NCU00502	ATP synthase subunit 4 (242 aa)	20
44	NCU08956	MSP domain-containing protein (280 aa)	20
45	NCU00090	pH-response transcription factor pacC/RIM101 (622 aa)	18
46	NCU07885	WD repeat containing protein 82 (378 aa)	15

Score threshold for Mascot >30, which indicate identity or extensive homology ($p<0.05$)
Score threshold for Mascot >15, which indicate homology ($p<0.05$)
Proteins that are low abundance indicated in bold
Proteins identified in both ^{V56His}GNA-1 and ^{V5}GNA-1 CoIP/MS (Appendix B, Table B.3) highlighted in yellow

A.

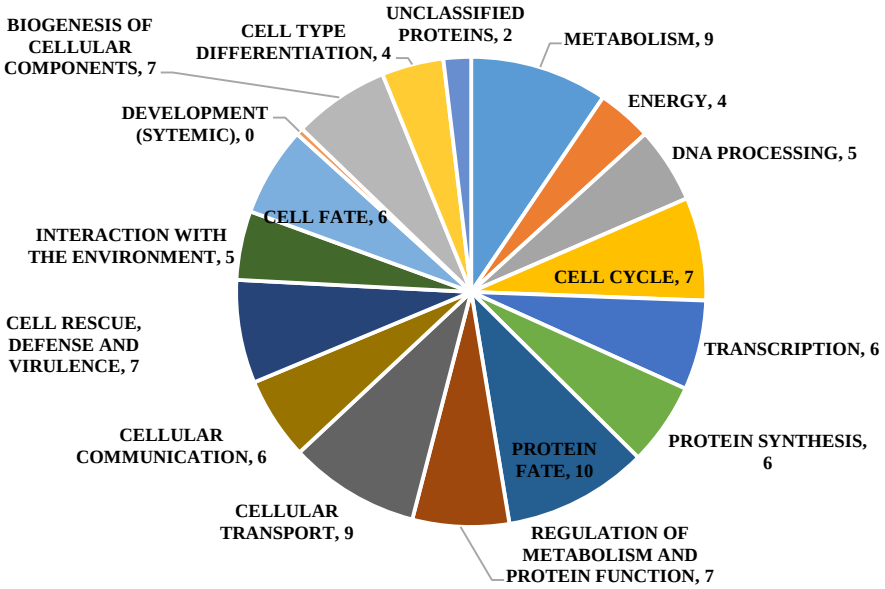

Figure 3.4. Functional distribution of the GNA-1 interaction dataset. Distribution is shown as percentage of total protein entries using MIPS FunCat (http://mips.helmholtz-muenchen.de/funcatDB/).

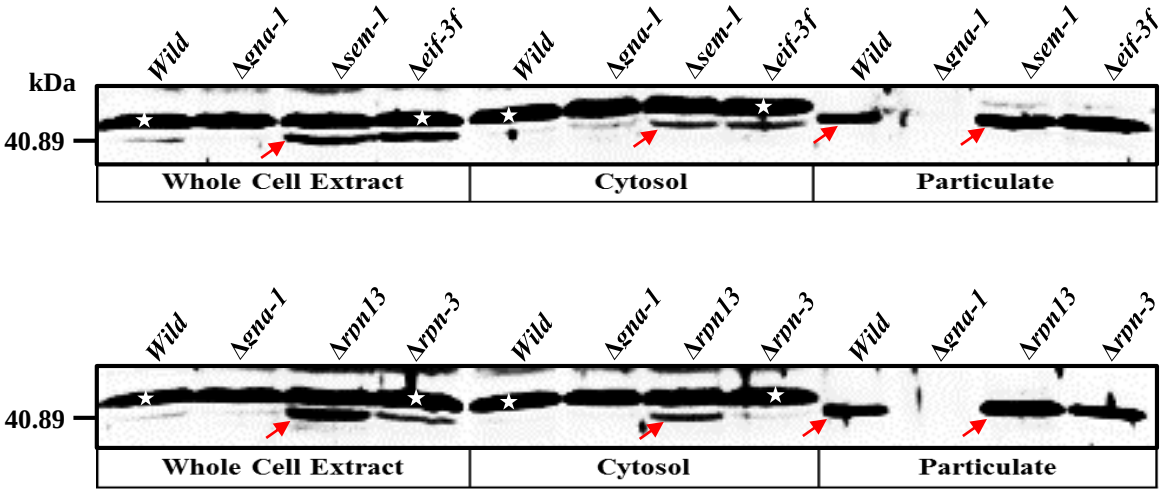

Figure 3.5. Level of GNA-1 protein in mutants lacking 19S proteasome regulatory subunits deletion mutants or eukaryotic translation initiation factor 3f. Strains are wild type (ORS-SL6a), Δ*gna-1* (1B4), Δ*sem-1* (NCU07913), Δ*rpn-3* (NCU02224), Δ*rpn13* (NCU02634), and Δ*eif-3f* (NCU01021). Strains were cultured in liquid VM medium with shaking at 200 rpm for 16 hours in the dark at 30˚C. Whole cell extract, cytosol and particulate (membrane) fractions were isolated, and 100 µg of total protein subjected to western analysis using GNA-1 antibody. Red arrows denote GNA-1 protein bands. White stars denote background bands.

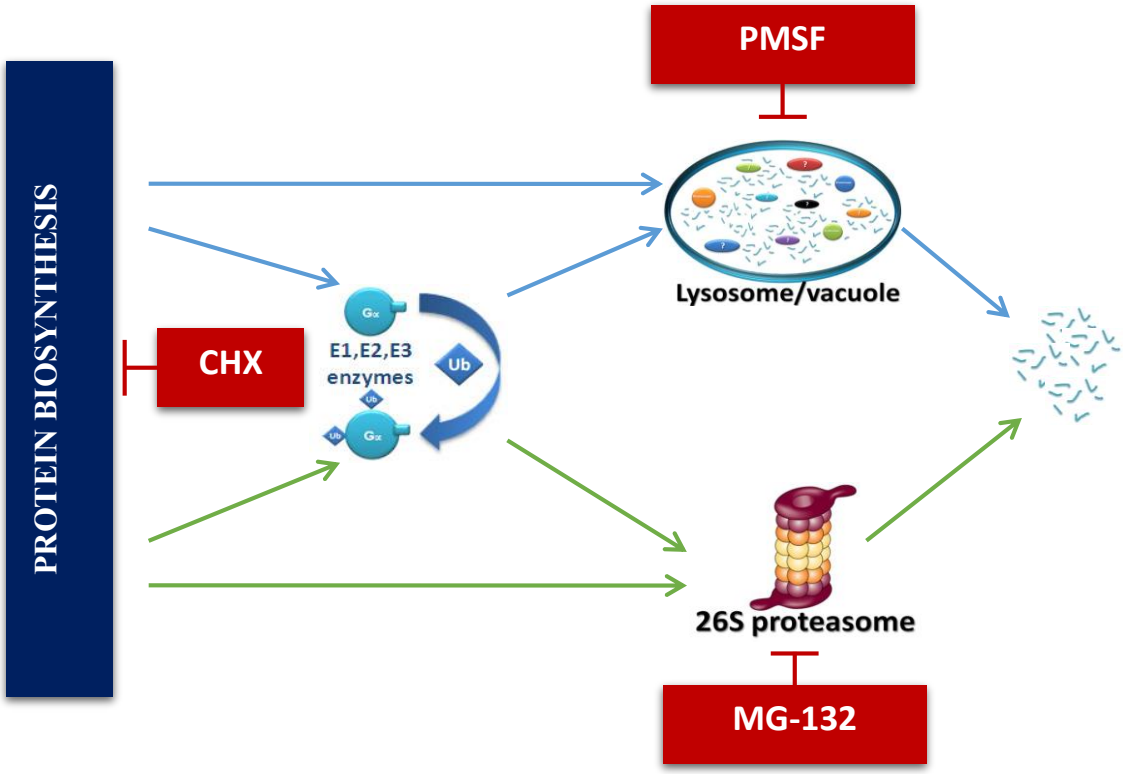

Figure 3.6. CHX is cycloheximide used to stop protein biosynthesis. MG-132 is inhibitor of proteolysis. PMSFis phenylmethylsulfonyl fluoride to block protein degradation by multiple vacuolar proteases. E1, E2, and E3 ubiquitination enzymes. Ubi is ubiquitin.

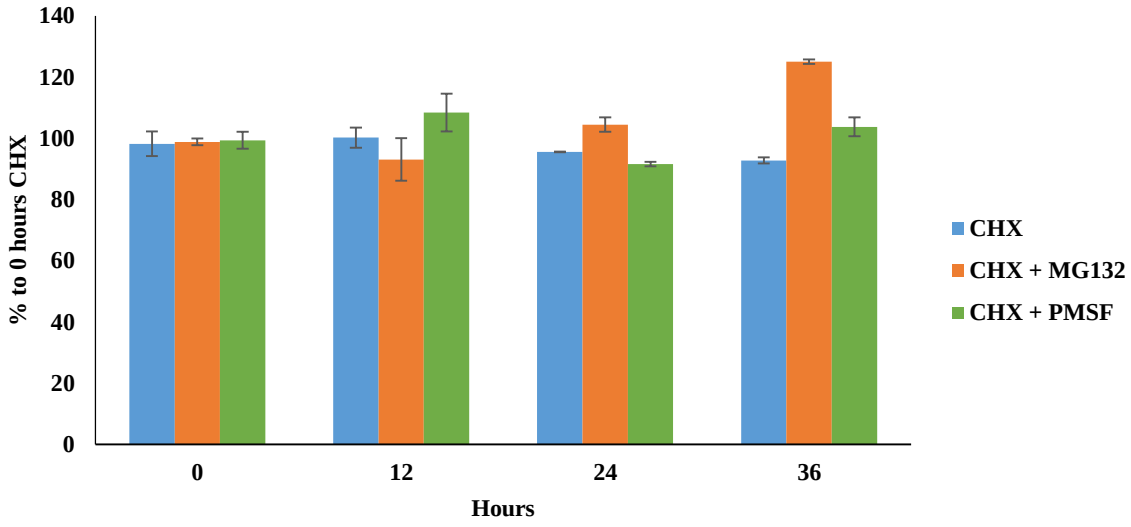

Figure 3.7. Stability of GNA-1 protein over 36 hours in wild type background. The wild type strain was cultured in modified liquid VM medium with L-proline as the nitrogen source and containing 0.003% sodium dodecyl sulfate (SDS) with shaking at 200 rpm in the dark at 30˚C. Cells were treated with cycloheximide (CHX), CHX + MG132, and CHX + PMSF for the indicated times. Whole cell extracts were isolated, and 100 µg of total protein subjected to western analysis using GNA-1 antibody. Intensity of the bands was determined using ImageJ 1.47v (NIH). Values are normalized at time 0 hours CHX treatment.

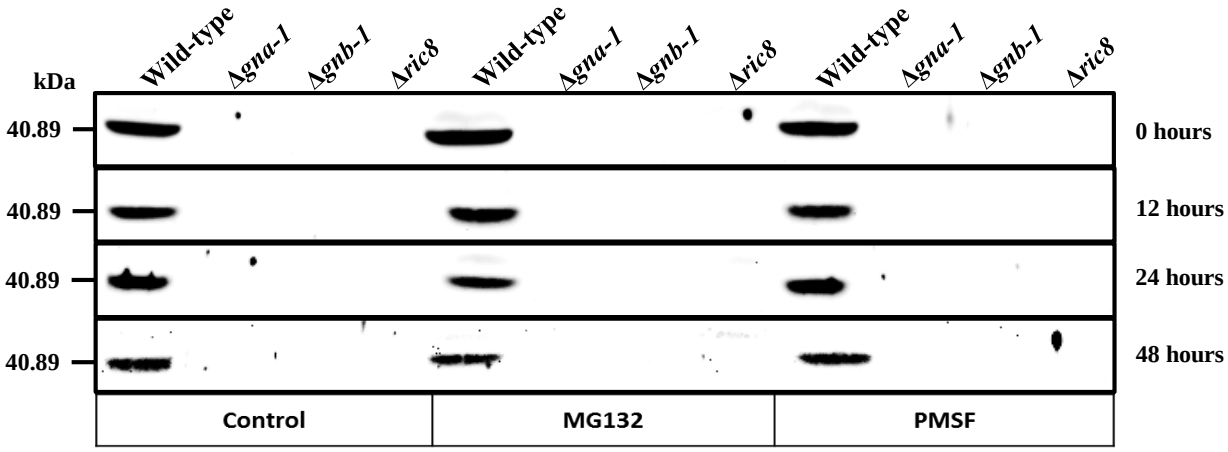

Figure 3.8. GNA-1 protein levels after treatment of wild type, Δ*gnb-1*, and Δ*ric8* strains with protein degradation inhibitors. Strains are wild type (ORS-SL6a), Δ*gna-1* (1B4), Δ*gnb-1* (42-5-18) and Δ*ric8* (R81-5a). Strains were cultured in modified liquid VM as described in the legend to Figure 3.7 for 0-48 hours. Cells were treated with MG132 or PMSF, as indicated. Whole cell extracts were isolated, and 100 µg of total protein subjected to western analysis using GNA-1 antibody.

Chapter 4

Translational regulation of G alpha subunits in mutants lacking the G beta subunit or a cytosolic guanine nucleotide exchange factor (RIC8) in *Neurospora crassa*

Abstract

The focus of the work in this chapter was to establish a reliable ribosome sucrose density gradient profiling protocol and to study aspects of translational control and their connection with G protein signal transduction in *N. crassa*.

Heterotrimeric G proteins regulate numerous processes in eukaryotic cells, including gene expression. Previous work in our laboratory demonstrated that low levels of G alpha proteins in mutants lacking the G beta subunit (*gnb-1*) or a cytosolic guanine nucleotide exchange factor (*ric8*) are due to posttranscriptional regulation, since levels of the corresponding mRNAs are similar in wild type and the deletion mutants. After confirmation of these results, my ribosome sucrose density gradient profiling experiments showed that G alpha subunit and actin mRNAs were dramatically decreased in Δ*gnb-1* and Δ*ric8* backgrounds compared to wild type. However, I could not detect redistribution of mRNA from polysomes to non-polysomal mRNPs. After intensive experiments and troubleshooting, I established a reliable ribosome sucrose density gradient profiling protocol that eliminated high RNAse activity and RNA extraction method specific bias in Δ*gnb-1*, and Δ*ric8* backgrounds.

I also found that GNB-1 and RIC8 proteins could be detected in sucrose gradient fractions that contained ribosomal populations. GNB-1 is found in 80S and polysome fractions in wild type. In Δ*ric8*, GNB-1 is shifted to the 40S and 60S ribosomal subunit fractions. In the case of RIC8, I detected this protein in all ribosomal fractions in wild type and Δ*gnb-1*strains.

Introduction

Expression of protein coding genes during the life cycle in eukaryotes is a complex process that includes several important steps, such as transcription, mRNA processing, translation, protein post-translational modifications, folding, and degradation. All of these steps require energy, and translation by ribosomes is the largest energy consumer, estimated to use around 30% of all cell energy in differentiating mammalian cells (21). The most energy efficient way to control the cellular level of proteins is to regulate steps prior to full translation of protein. In addition, due to the quite long half-lives of eukaryotic mRNA (the half-lives of stable mRNAs in yeast are more than 1.5 hours, and in mammalian cells exceed 24 hours) (116;136;162), control of transcription and mRNA processing does not allow rapid regulation of cellular protein levels, with the exception of enhanced mRNA turnover (54). Translational regulation, on other hand, can quickly tune up cellular protein levels by controlling mRNA translational efficiency (44;160) or elements of the translational machinery.

Depending on the number of mRNAs affected, two general types of control have been defined – global control, in which the majority of mRNAs are affected; and mRNA-specific regulation, in which translation of a single mRNA, or a small group of mRNAs is modulated without changing the translational status of the entire cellular transcriptome (58). Global regulation is often based on the activation or inhibition of elements of the translational machinery or common elements shared by many mRNAs (54), whereas

mRNA-specific control is driven by the action of regulatory complexes, which can include *trans*-acting RNA binding proteins (45), or microRNAs (125).

Translational efficiency of specific mRNAs can be determined by the transcript sequence itself, which has inherent regulatory elements usually located within the UTRs. Such structural regulatory elements can include, but are not limited to, a start-site consensus sequence, secondary structure, upstream open reading frames (uORFs), terminal oligopyrimidine (TOP), and internal ribosomal entry sites (IRES) (169). RNA binding proteins recognize and interact with these secondary structure and sequence elements. The mechanism by which RNA binding proteins regulate translation may involve competition with the ribosome for RNA or direct binding to the mRNA, promoting an RNA structure that inhibits ribosome binding (7).

Translation may also be regulated globally by modulating elements of the translational machinery. One of the most studied is phosphorylation of initiation factors, which often are targets of signal transduction pathways. For example, phosphorylation of eIF2 alpha results in reduced translational initiation (56). Numerous other translation factors undergo posttranslational modification, which can also be a part of translational control (125).

The process of translation can be divided into four stages: initiation, elongation, termination, and ribosome recycling (54). The majority of known translational regulatory mechanisms target the first stage: translational initiation, which involves more than 25 assisting proteins (142). The majority of mRNA-specific regulation and global translational rate changes happen at the initiation stage (7;56;142). There is also some

evidence that the elongation and termination stages are targets of translational regulation (37). One example of a protein that regulates translational elongation is the *S. cerevisiae* protein Stm1p, which inhibits translation by stalling the 80S ribosome on a target mRNA (9). Another example of a protein that regulates elongation is phosphorylated eEF2, which acts as a general inhibitor of translational elongation (128). A severe heat stress can trigger global pausing of translational elongation through altered activity of the Hsp70 protein (131). Termination in eukaryotes is catalyzed by two protein factors, eRF1 and eRF3 (145;179).

Typically, the total levels of mRNA are not rate-limiting for global protein synthesis, except for limiting mRNA accessibility during nutrient starvation or external chemical and physical stress (104;132). Global translation may be severely down regulated under stress conditions by sequestration of mRNA in stress granules or P-bodies (20;78;112).

The translational status of an mRNA can be identified by association with ribosomes. Actively translated mRNAs are associated with multiple ribosomes, forming large complexes – polysomes. Slowly translated or translation-inactive mRNAs usually form complexes with only one ribosome, with 40S ribosomal subunits, or with RNA - binding proteins. Translational status is often evaluated by fractionation of mRNA/ribosome complexes of different sizes through sucrose density gradients, and monitoring levels in individual fractions (2;100;105). This method is used extensively in this chapter.

Materials and Methods

Strains and media. *N. crassa* strains used in Chapter 4 are listed in Table 4.1. For collection of asexual spores or vegetative growth in liquid or solid culture, strains were cultured in Vogel's minimal medium (VM) (159), with 1% agar added for solid medium (BBL; Becton, Dickinson and Co., Franklin Lakes, NJ). Medium was supplemented with hygromycin at 200 µg/ml, where indicated.

Macroconidia (conidia) were propagated in VM agar medium flasks by incubation at 30ºC for three days in the dark, followed by five days at room temperature in constant light. Conidia were harvested as previously described (35).

Strain growth conditions and cellular extract preparation. A published protocol for ribosome sucrose density gradient profiling (105) was adapted for this work for *N. crassa*. Conidia from a 7 day-old culture of *N. crassa* strains grown in a foam-plugged, 125 ml flask filled with 30 ml of VM agar were collected with sterile water by agitation and filtered through sterile layer of shop towels to remove all tissue types except conidia, which flow through. The conidial solution was centrifuged at 2500 rpm for 5 min. The supernatant was poured out, and the conidial pellet resuspended in 25 ml of sterile water and concentrated by centrifugation at 2500 rpm for 5 min, with the supernatant poured off again. A volume of 1 ml, sterile water was added, and the conidial concentration was determined with a hemacytometer. Conidia collected from the strains were inoculated in 1 L VM liquid medium in a 2 L flask at 10^6 conidia/ml, and cultured at 30˚C for 16 hours

with shaking (200 rpm). Tissue was collected on filter paper using a vacuum system and cell pads were flash-frozen in liquid nitrogen prior to storage at –80°C. Tissue was pulverized in liquid nitrogen using a mortar and pestle. 4 ml of pulverized frozen tissue was thawed in 8 ml polysome extraction buffer [PEB: 0.2M Tris-HCl (pH 8.4), 0.2M KCl, 25 mM Ethylene glycol-bis(2-aminoethylether)-N,N,N',N'-tetraacetic acid (EGTA) (pH 8.4), 35 mM $MgCl_2$, 1% polyoxyethylene(23)lauryl ether (Brij-35), 1% Triton X-100, 1% octylphenyl-polyethylene glycol (Igepal CA 630), 1% polyoxyethylene sorbitan monolaurate 20 (Tween 20), 1% Sodium deoxycholate (DOC), 1% polyoxyethylene 10 tridecyl ether (PTE), 5mM dithiothreitol (DTT), 1 mM phenylmethylsulfonyl fluoride (PMSF), 100 µg/ml cycloheximide (CHX)], homogenized with glass homogenizer. The crude cell-extract was clarified by centrifugation at 16,000xg for 20 min at 4˚C. The supernatant was transferred to a new conical tube and either layered on top of a sucrose cushion, or directly on top of a sucrose gradient.

For EDTA treatment, EDTA (ethylenediaminetetraacetic acid) was substituted for EGTA in PEB buffer at a final concentration of 50 mM, MgCl was included at 5 mM, and no CHX was added. For RNAse treatment, RNAse A (#EN0531, Thermo Scientific) was added to clarified extracts at 100 µg/ml and the solution incubated at 37˚C for 30 min before loading on the sucrose gradient.

PEB was supplemented with heparin (#H-3149, Sigma) at 500 µg/ml, RNasin (#N2615, Promega) at 40 units/ml, and vanadyl ribonucleoside complex (VRC) (#S1402S, New England BioLabs) at 10 mM, where indicated.

Sucrose cushion. Clarified extracts were layered on top of an 8 ml 1.75 M sucrose cushion [0.4 M Tris–HCl (pH 8.4), 0.2 M KCl, 30 mM $MgCl_2$, 1.75 M sucrose, 5 mM DTT, 100 µg/ml cycloheximide], and centrifuged at 135000xg for 18 hours at 4˚C (70 Ti Rotor, Beckman, Brea, CA, USA) to obtain a crude ribosome pellet (105). The pellet was re-suspended in 250 µl of polysome resuspension buffer [PRB: 0.2 MTris–HCl (pH 8.4), 0.2 M KCl, 35 mM $MgCl_2$, 25 mM EGTA, 5 mM DTT, 100 µg/ml cycloheximide]. Approximately 2000 units (OD_{260}) were used for sucrose gradient fractionation.

Sucrose gradients and isolation of fractions. Equal units [15 – 30 units after cellular extraction or 2000 units after sucrose cushion (OD_{260})] for all samples (volume less than 450 µl) were layered on top of a 20–60% (w/v) sucrose gradient (105) and centrifuged at 275,000xg for 1.5 hours at 4˚C (SW55 Ti Rotor, Beckman), then passed through a UA-5 detector and 185 gradient fractionator (ISCO, Lincoln, NE, USA). Data were analyzed using Icruncher 2.2 (171). 12 fractions of equal volume were collected.

RNA extraction. Total RNA extraction was performed using two methods: the TRIzol reagent (Life Technologies) according to the manufacturer's protocol (Appendix A), and the Phenol-Chloroform method.

The Phenol-Chloroform method was adapted from a plant RNA isolation protocol (157) for extraction of RNAs from sucrose fractions of cell extracts derived from liquid cultures of *N. crassa*. Briefly, sucrose gradient fractions (each around 400 µl) were collected in 2 ml Eppendorf tubes containing the same volume of 8M guanidine HCl.

RNA was precipitated by adding two volumes of 100 % ethanol and incubating at -20°C for at least one hour. After centrifugation at 12,000g for 15 min at 4°C, pellet was washed with 70% ethanol. The pellet was resuspended by vortexing in 0.5 ml of RNA extraction buffer (100 mM Tris-HCl, pH 8.0, 10mM EDTA, 1% SDS) and 0.5 ml of water saturated phenol (pH 4.0) and incubated for 10 min at room temperature. After incubation, 0.5 ml of chloroform/isoamyl alcohol (24:1) was added, vortexed, and the solution centrifuged at 12,000g for 15 min at 4°C and the aqueous phase transferred to a clean 1.5 ml microcentrifuge tube. This step was repeated twice. To increase RNA recovery, glycogen (#R0551, Thermo Scientific) was added to a final concentration of 0.4 µg/µl. RNA was precipitated by adding 0.7 ml of 100 % ethanol and incubating at -20°C for at least one hour. If PEB contained heparin, LiCl precipitation was used to isolate RNA; 0.7 ml of 5M LiCl was added to each fraction, followed by overnight incubation 4°C. After centrifugation at 12,000g for 15 min at 4°C, 7 ml of 70% ethanol was added to the pellet and then briefly centrifuged for 1 min. The ethanol supernatant was discarded and pellet air dried for 15 min on ice and then resuspended in 35 – 50 µl of RNAse-free water.

The RNA concentration were measured by monitoring absorbance at A260 and protein contamination at 280 nm using a spectrophotometer (ND-2000, Nanodrop, Wilmington, DE, USA). The RNA integrity was examined using 1.2% (w/v) agarose gels run using TAE buffer (40 mM Tris-HCl, pH 8.0, 20 mM acetic acid, 1 mM EDTA) and then stained with 0.01% (w/v) ethidium bromide. RNA recovery was monitored by spiking fractions with 0.5 ng of a Luciferase Control mRNA (#L456A, Promega) before RNA extraction.

Evaluation of mRNA in tissues, cell extracts and gradient fractions. Transcript levels were evaluated using semi-quantitative reverse transcription-polymerase chain reactions (RT-PCR) or quantitative real-time reverse transcription-polymerase chain reactions (RT-qPCR). An aliquot (4-6 µl) of each fraction was treated with DNase (#M6101, Promega) according to manufacturer's protocol with addition of 40U/ µl of RNasin Plus (#N2615, Promega). The reverse transcription reaction was performed using 1 µg RNA of total RNA and the same volume with a maximum of 1 µg of RNA for sucrose gradient fractionated RNA using 2.5 µM oligo-dT (Integrated DNA Technologies, IDT) and ProtoScript II Reverse Transcriptase (#M0368, New England BioLabs, NEB) according to manufacturer's protocol.

PCR was performed in 20 µl of reaction volumes using *Taq 5X* Master Mix (#M0285, NEB) and 0.2 µM final concentration of forward and reverse primers (Table 4.2). PCR amplification was carried out with denaturation at 95°C for 1 min, annealing at 55°C for 30 sec and elongation at 68°C for 1 min for 30 cycles. RT-PCR samples were analyzed on 2% agarose gels (as was shown above) and images captured using a UVP Imaging system.

Quantitative real-time PCR was performed using iQ SYBR Green Supermix (#170-8880, BIO RAD). In total, 3 µl of 2x diluted original cDNA was mixed with 13 µl of iQ SYBR Green Supermix and 0.2 µM each forward and reverse primers. The sequence of the primers is listed in Table 4.2. Each gradient fraction was analyzed in triplicate. qPCR amplification was carried out with initial denaturation at 95°C for 3 min,

denaturation at 95°C for 20 sec, annealing at 55°C for 20 sec and elongation at 72°C for 20 sec for 45 cycles. Fluorescence emitted during each cycle was monitored using an iQ5 real-time PCR detection system (Bio Rad, Hercules, CA, USA). mRNA abundance was calculated using the comparative ΔCT method (129). The absence of non-specific products was determined by analysis of melting curves and the size of the PCR products by agarose gel electrophoresis.

Protein isolation and western blot. Preparation of PEB cell extracts and sucrose gradient fractionation are described above. Fractions were pooled according to ribosome populations: 40S, 60S ribosomal subunits, 80S monosomes, and polysomes. Pooled fractions were loaded in Amicon Ultra-15 Centrifugal Filter Units (#UFC900308, EMD Millipore) and centrifuged at 1000g for 10 min at 4°C. After addition of 1 ml of wash buffer (10 mM HEPES [pH 7.5], 0.5 mM EDTA, 0.5 mM PMSF and 0.1% fungal protease inhibitor cocktail; catalog no. P8215; Sigma-Aldrich, St. Louis, MO), filter units were centrifuged at 1500g for 10 min at 4°C. Concentrated protein samples (~50 μl) were subjected to western blot analysis (as described in Chapter 2).

Results

The low levels of G alpha proteins in mutants lacking the G beta subunit (GNB-1) or a cytosolic guanine nucleotide exchange factor (RIC8) results from a posttranscriptional mechanism.

Previously, experiments in our laboratory showed that GNB-1 and RIC8 proteins play very important role in maintenance of the level of G alpha proteins (82;174). Moreover, it was proposed that regulation of G alpha subunit proteins is due to posttranscriptional mechanism, since levels of mRNA are similar in wild type and Δ*gnb-1* and Δ*ric8* mutants (82;174). Based on these published results, I checked the level of mRNAs in wild type, Δ*gnb-1*, and Δ*ric8* backgrounds using RT-qPCR (Figure 4.1). In Δ*gnb*-1 mutant levels of *gna-1* and *gna-2* mRNA extracted directly from tissue were similar or slightly lower than in wild type. Levels of all three G alpha subunit mRNA were higher in Δ*ric8* mutant comparing with wild type (Figure 4.1). Interesting, *gnb-1* mRNA amount is the same in wild type and the *ric8* deletion mutant. On the other hand, levels of *ric8* mRNA are higher in Δ*gnb-1* than in wild type (Figure 4.1).

I also checked levels of G protein subunits and RIC8 in G protein subunit and *ric8* deletion mutants (Figure 4.2). GNA-1 protein cannot be detected in Δ*gnb-1* and Δ*ric8* mutants using western blots. Levels of GNA-2 and GNA-3 are decreased by approximately 30% and 50%, accordingly, in Δ*gnb-1* mutants, and they cannot be detected in the Δ*ric8* background (Figure 4.2). Interestingly, levels of GNB-1 are

decreased similarly in Δ*gna-1* and Δ*ric8* backgrounds, which may be explained by the very low level of GNA-1 in Δ*ric8* strains. In sum, the results confirmed previous findings that GNB-1 and RIC8 do not affect levels of G alpha subunit mRNA and regulation is due to a posttranscriptional mechanism.

Identification of ribosomal populations using ribosome sucrose density gradient profiles.

Based on the above results, I decided to focus my work on deciphering a possible mechanism to explain the low levels of G alpha subunit proteins in Δ*gnb-1* and Δ*ric8* backgrounds. First, I tried to identify ribosomal populations in sucrose gradient profiles. I tested treatment with RNAse to identify the 80S peak and EDTA to locate 40S and 60S peaks, and confirm polysome population (sensitive to RNAse and EDTA). The absorbance tracing at 254 nm of the typical control gradient of a cytoplasmic extract derived from wild type is shown in Figure 4.3 (Green line). It displays distinctive peaks for the 40S and 60S ribosomal subunits, a prominent peak of 80S single ribosomes, and a series of small peaks with maximum absorbance in heavy polysomes. The profile of an RNAse-treated extract in Figure 4.3 (Blue line) shows absorbance peaks of ribosomal subunits and single ribosome, but no peaks for polysomes. For confirming that peaks correspond to 40S and 60S, I used EDTA treatment: the graph clearly shows peaks for ribosomal subunits, and no peaks for 80S and polysomes (Figure 4.3 (Red line). These experiments allowed me to confirm that polysomes are sensitive to RNAse and EDTA,

and not arise by nonspecific aggregation. I also identified other ribosomal populations using sucrose gradient profiles.

Ribosome sucrose density gradient profiling reveals translational regulation of G protein subunits.

To determine whether translation of G protein mRNAs were affected in Δ*gnb-1* and Δ*ric8* backgrounds, I used a 1.7M sucrose cushion to concentrate mRNA/ribosome complexes from cellular extracts. Sucrose cushion centrifugation pellets most ribosomal particles and ribosomes, but does not enable the selective purification of monosomes from subunits and polysomes (11). The dissolved ribosomal pellet after sucrose cushion was loaded on a 20-60% sucrose gradient to separate and isolate 12 fractions. The profiles in Figure 4.4A show that peaks corresponding to 60S, 80S, and light polysomes are higher in Δ*gnb-1*, and Δ*ric8* strains extracts than in wild type. At the same time, deletion mutant strains demonstrate depletion of the heavy polysomes in comparison to wild type (Figure 4.4 A). The relative abundance of the G protein subunit mRNAs in each fraction was used to measure the degree of association of mRNAs with ribosomes. Loss of either the G beta subunit GNB-1 or the cytosolic GEF RIC8 reduced the amount of G alpha mRNA associated with polysomes (Figure 4.4 B-E). The most affected genes are *gna-1* and *gna-2*; the level of these mRNAs associated with polysomes was two-fold reduced in Δ*gnb-1* and Δ*ric8* backgrounds compared to wild type (Figure 4.4 B and C). All G alpha subunits show the lowest amount of mRNA associated with polysomes in the

Δ*gnb-1* background (Figure 4.4 B-D). A similar pattern was observed for *gnb-1* mRNA with polysomes collapsed in the Δ*ric8* background (Figure 4.4 E). Interestingly, the housekeeping control gene actin also demonstrated reduced levels of mRNA associated with polysomes in Δ*gnb-1*, and Δ*ric8* backgrounds (Figure 4.4 F). Taken together, results suggest that there is possible translation regulation of G protein subunits and housekeeping gene - actin. However, it is impossible to derive conclusion about the mechanism of the translational control.

Possible mechanism of translational control of G protein alpha subunits in mutants lacking the G beta subunit or a cytosolic guanine nucleotide exchange factor (RIC8) in *Neurospora crassa*

The majority of mutations or treatments, which could affect translation, are easily assessed by ribosome sucrose density gradient profiling experiments. Depending on the type of translational inhibition (initiation, elongation, etc.) affected mRNA redistributes from the polysomes to untranslated mRNA, 40S stalled ribosomal particles, or monosomes (80S) fractions, without change of total amount of mRNA of all fractions. In our case, levels of total mRNA of G protein subunits and actin mRNA are significantly reduced in Δ*gnb-1* and Δ*ric8* mutants (Figure 4.4 B-F). Our hypothesis was that either the mRNA formed RNA/protein complexes, such as stress granules, or that the mRNA was degraded during the experiment due to high activity of specific RNAses in Δ*gnb-1* and Δ*ric8* mutants.

After many experiments and troubleshooting (see Appendix C), I established a ribosome sucrose density gradient profiling protocol for *N. crassa*, which includes prevention of RNA degradation during the experiment by combining the effect of three RNAse inhibitors (RNasin, VRC, and heparin). In addition, I recommended using Phenol-Chloroform RNA extraction protocol instead of TRIzol.

I used the optimized ribosome sucrose density gradient profiling for several experiments and obtained reproducible profiles (Figure 4.5). The profile of the wild type strain has distinct peak in polysomes (light green line). The *gnb-1* deletion mutant (light blue lines) shows collapse of the polysome population. In case of Δ*ric8*, the profile shows polysome peaks that are slightly biased towards lighter molecular weight polysomes, in comparison to wild type. Introducing a constitutively active, GTPase-deficient allele of the *gna-1* gene in deletion mutants (dark blue and dark red lines) restores the polysomal population in Δ*gnb-1* mutants and increases it in Δ*ric8* background. Moreover, *gna-1*^{Q204L} in Δ*gnb-1* and Δ*ric8* backgrounds has higher polysomal peaks than wild type (Figure 4.5).

Total RNA extracted using Phenol-Chloroform protocol from the collected fractions showed the highest polysomal peak in wild type (Figure 4.6). In the case of Δ*gnb-1*, total RNA is apparently redistributed from polysomes to monosomes and untranslated mRNA (free mRNA) fractions. The total RNA distribution in Δ*ric8* mutants is similar to wild type. Expression of the constitutively active *gna-1*^{Q204L} allele in Δ*gnb-1* and Δ*ric8* backgrounds restores total RNA levels in polysomal populations to the level observed in wild type (Figure 4.6).

The next step will be to perform RT-qPCR to measure the abundance of *gna-1* mRNA in sucrose gradient fractions.

Association of G protein subunits and RIC8 with ribosomes.

The proteins associated with ribosomes are usually connected to global translational control. To determine whether G protein subunits or RIC8 were associated with ribosomes, I isolated total protein from sucrose gradient fractions. Western analysis showed that G alpha proteins could not be detected in any fractions (data not shown). In the case of GNB-1, I found that there is clear association with monosomes and the polysome population in wild type (Figure 4.7 first panel). I also determined that the GNB-1 protein shifted to the 40S and 60S subunit fractions in the Δ*ric8* strain. There were no GNB-1-specific bands in the Δ*gnb-1* strain (Figure 4.7 top panel), confirming the association with ribosomes in the other strains. In the case of RIC8, the protein exhibited association with all ribosomal populations in wild type and Δ*gnb-1* strains (Figure 4.7 second panel). Similar to the results with GNB-1, RIC8 protein was not detected in the samples from the Δ*ric8* strain.

Discussion

Heterotrimeric G proteins regulate multiple cellular processes in *N. crassa*. Many downstream effectors are activated by G proteins, including production of second messengers or direct physiological responses. Previous work from our lab, found that G alpha subunit protein levels are low in Δ*gnb-1* mutants and undetectable in Δ*ric8* backgrounds (Figure 4.2). At the same time, levels of the corresponding mRNAs are similar in wild type and deletion mutants (Figure 4.1) (82;173;174). In Chapter 3, I found that protein turnover is not the main mechanism for the low level of G alpha proteins observed in Δ*gnb-1* and Δ*ric8* backgrounds. In this chapter, I explored whether G proteins play a role in translational control.

For study of translation control in *N. crassa*, I adapted a plant ribosome sucrose density gradient profiling protocol (105). At first I tried to use preliminary sucrose cushion centrifugation which helps concentrate ribosomal particles and ribosomes, and proportionally increases the concentration of mRNA associated with ribosomal populations (11). The analysis of abundance of mRNA in sucrose gradient fractions could give a clue what type of control involved in the low level of G alpha proteins in Δ*gnb-1* and Δ*ric8* backgrounds. If there were affected common regulatory elements shared by many mRNAs, which could decrease translational activity of mRNA, I should observe redistribution of mRNA from polysomes to the light fractions, such as free mRNA, in Δ*gnb-1* and Δ*ric8* strains. Inhibition of the initiation translation step would increase the relative amount of mRNA in the 40S ribosome subunit fraction by forming 40S stall

complexes in deletion mutants. Halting of the elongation step would increase the relative amount of mRNA in 80S monosomes. My results show that there was a significant decrease in G protein subunit and actin mRNA associated with polysomes in Δ*gnb-1* and Δ*ric8* strains, which is consistent with translational inhibition (Figure 4.4 B-F). However, the mRNA for these genes was detected only in polysomes (fractions 6-12), with no redistribution of mRNA to other fractions. Based on these results, I could only conclude that there is possible inhibition of translation in Δ*gnb-1* and Δ*ric8* strains, but not the mechanism.

It was demonstrated in previous and this work that G alpha subunit mRNA extracted directly from tissue are not decreased in Δ*gnb-1* and Δ*ric8* mutants. However, in my experiments, I discovered a significant decrease in mRNA levels in deletion mutants, which could be explained by RNA degradation during the experiment or an RNA extraction method problem.

During troubleshooting, I found that there were two problems: a TRIzol specific phenomenon and RNAse activity (Appendix C). I changed the RNA extraction method from TRIzol to Phenol-Chloroform. I also started to use three RNAse inhibitors in the protocol. In sum, I established a reliable ribosome sucrose density gradient profiling protocol for *N. crassa*.

Using this protocol, I obtained sucrose gradient profiles of wild type, Δ*gna-1*, Δ*gnb-1*, and Δ*ric8*. RNA extracted from the fractions using the Phenol-Chloroform method exhibits good quality and integrity. Future experiments will be focused on determining mRNA abundance in ribosomal populations using RT-qPCR. If G alpha

subunit mRNA redistributes from polysomes to 40S or 80S fractions in Δ*gnb-1* or Δ*ric8* mutants, than we may suggest the type of translational regulation.

To investigate whether G beta or RIC8 proteins are a part of the translational machinery I investigated whether they associate with ribosomes. G alpha subunit proteins were not detected in ribosomal subunits, monosomes, or polysomes (Data not shown). GNB-1 associates with 80S and polysomal fractions in the wild type strain. In Δ*ric8* mutants, I observed redistribution of GNB-1 from 80S and polysomes to 40S and 60S ribosome subunits. In the case of RIC8, I could see strong bands in all ribosomal populations in wild type and Δ*gnb-1* strains (Figure 4.12). These results suggest that RIC8 is associated with 40S ribosomal subunits and may play a role in ribosome assembly and translational regulation. To confirm these results for GNB-1 and RIC8 in association with ribosomes, I would next check whether EDTA treatment could shift these two proteins from monosomes and polysomes to 40S and 60S subunits. In addition, it will be useful to determine whether GNB-1 or RIC8 could co-immunoprecipitate with ribosomes.

In sum, I established ribosome sucrose density gradient profiling protocol. In preliminary experiment I found decrease of mRNA associated with polysomes. I detected GNB-1 and RIC8 in ribosomal population fractions.

TABLE 4.1. *N. crassa* strains used in this work

Strain	Relevant genotype	Source or reference
74-OR23-IVA	Wild type, *mat A*	FGSC[a] 2489
ORS-SL6a	Wild type, *mat a*	FGSC 4200
1B4	Δ*gna-1::hph*$^{+}$ *mat A*	(66)
Δ2	Δ*gna-2::hph*$^{+}$ *mat a*	FGSC 12377
3lc2	Δ*gna-3::hph*$^{+}$ *mat A*	(77)
42-5-11	Δ*gnb-1::hph*$^{+}$ *mat A*	(173)
42-5-18	Δ*gnb-1::hph*$^{+}$ *mat A*	(177)
G1-F	Δ*gnb-1::hph*$^{+}$ *his-3*$^{+}$*::gna-1*^{Q204L} *mat a*	(173)
G2-C	Δ*gnb-1::hph*$^{+}$ *his-3*$^{+}$*::gna-2*^{Q205L} *mat a*	(173)
G3-C	Δ*gnb-1::hph*$^{+}$ *his-3*$^{+}$*::gna-3*^{Q208L} *mat a*	(173)
R81-5a	Δ*ric8::hph*$^{+}$ *mat a*	(174)
R81*	Δ*ric8::hph*$^{+}$ *his-3*$^{+}$*::gna-1*^{Q204L} *mat a*	(174)
R82*	Δ*ric8::hph*$^{+}$ *his-3*$^{+}$*::gna-2*^{Q205L} *mat a*	(174)
R83*	Δ*ric8::hph*$^{+}$ *his-3*$^{+}$*::gna-3*^{Q208L} *mat a*	(174)

[a]FGSC, Fungal Genetics Stock Center, Kansas City, MO.

TABLE 4.2 Oligonucleotides used in this study.

Name	Sequence
Q-GNA1-F	TCGATTCCATCTGCAACTCC
Q-GNA1-R	GGGGAAGTAGTTCTTCATCG
Q-GNA2-F	TCTCAGGTTACGATCAGTGC
Q-GNA2-R	TGTGAACCAGTGAGAATTGG
Q-GNA3-F	CCTGTTTCTCAACAAGGTCG
Q-GNA3-R	CTTGTTGACGTCGTTTCCAC
Q-GNB1-F	TTTGCGGCATTACCTCTGTC
Q-GNB1-R	AGTAAGATCCCAGACCTTGC
Q-RIC8-F	TTGTCTTGTTTGAGAGGGCG
Q-RIC8-R	GAATCCTCTTCGTAGTCGTC
Q-Act-F	TCCATCATGAAGTGCGATGTC
Q-Act-R	TTCTGCATACGGTCGGAGAGA
GADPH Fw	GTGCTACCTACGATGAGATCAAG
GADPH Rv	CGTTCATGTCGGAAGAGACAA
TUB2 Fw	TGGTACACTGGTGAGGGTAT
TUB2 Rv	ATCCTGGTACTGCTGGTACT
UBI4 Fw	GTCGAGTCTTCGGATACGATTG
UBI4 Rv	CCATCCTCCAACTGCTTACC

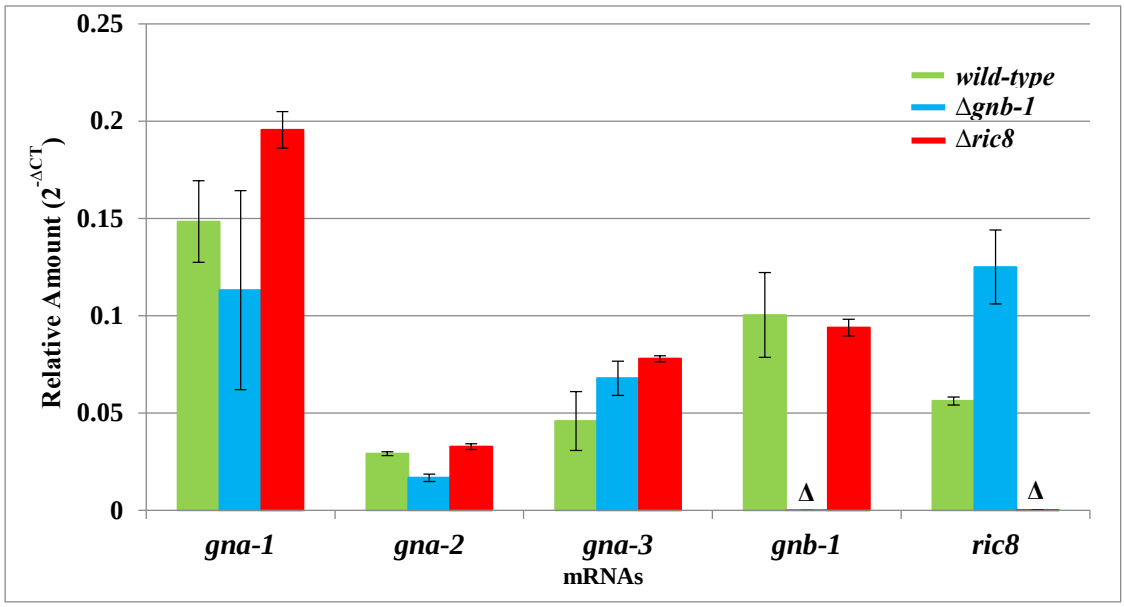

Figure 4.1 Relative levels of G protein subunit mRNAs in wild type, Δ*gnb-1*, and Δ*ric8* backgrounds. Strains are *wild type* (ORS-SL6a), Δ*gnb-1* (42-5-18), and Δ*ric8* (R81-5a). Strains were cultured in liquid VM medium with shaking at 200 rpm for 16 hours in the dark at 30˚C. RNA was extracted from tissue using the TRIzol reagent according manufacturer's protocol. RT-qPCR for the indicated genes (x-axis) was performed as described in the Methods.

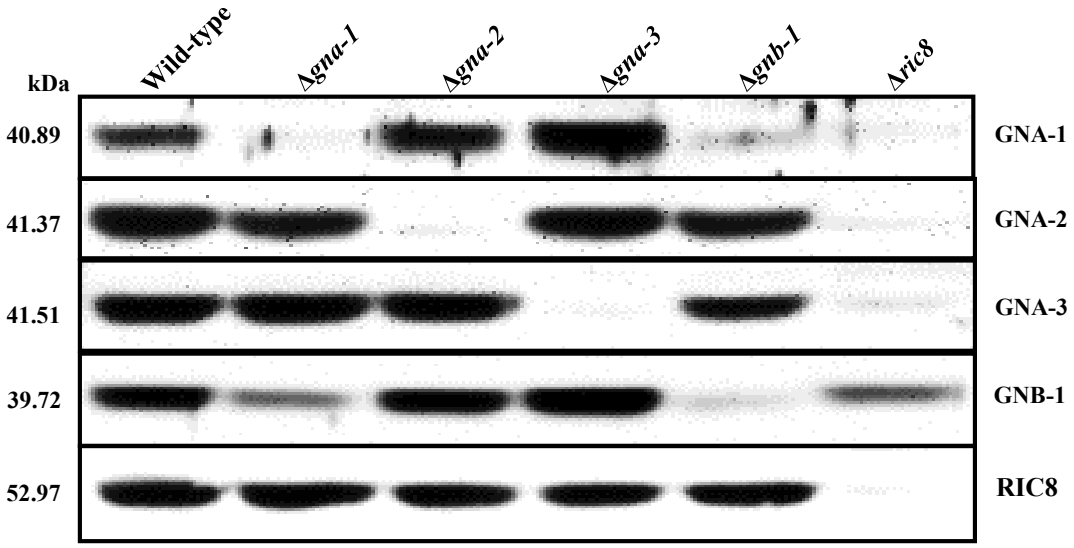

Figure 4.2 G protein levels are reduced in Δ*gnb-1* and Δ*ric8* mutants. Strains are wild type (ORS-SL6a), Δ*gna-1* (1B4), Δ*gna-2* (Δ2), Δ*gna-3* (3lc2), Δ*gnb-1* (42-5-18), and Δ*ric8* (R81-5a). Strains were cultured in liquid VM medium with shaking at 200 rpm for 16 hours in the dark at 30˚C. Whole cell extracts were isolated and 100 µg of total protein subjected to western analysis using GNA-1, GNA-1, GNA-3, GNB-1, and RIC8 polyclonal antibodies.

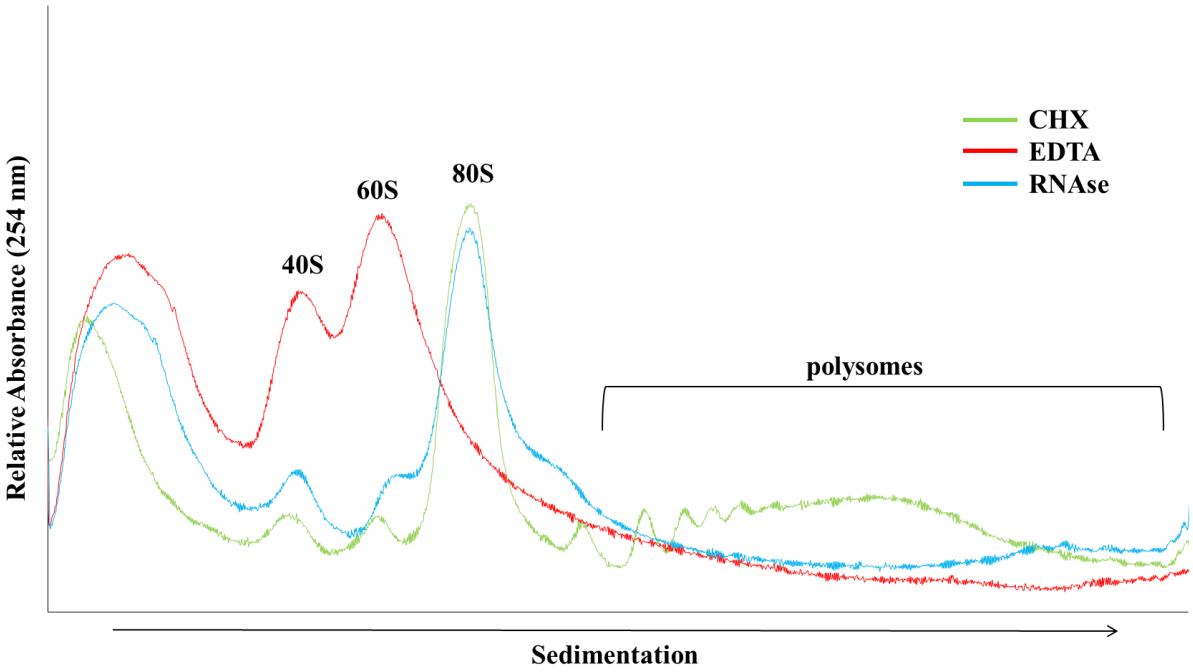

Figure 4.3 Identification of 40S, 60S ribosomal subunits, 80S single ribosome, and polysomes peaks. Absorbance profiles of rRNA complexes obtained from cytosolic extracts of submerged cultures of the wild type strain (ORS-SL6a) treated with cycloheximide (CHX) in extraction buffer (green line), with ethylenediaminetetraacetic acid (EDTA) in extraction buffer (red line), and 100 µg/ml of RNAse A for 30 min at 37˚C before loading on sucrose gradient (blue line). Traces represent absorbance after subtraction of the baseline of a blank sucrose gradient. Position of the free ribosomal subunits (40S and 60S), monosomes (80S) and polysomes, are indicated.

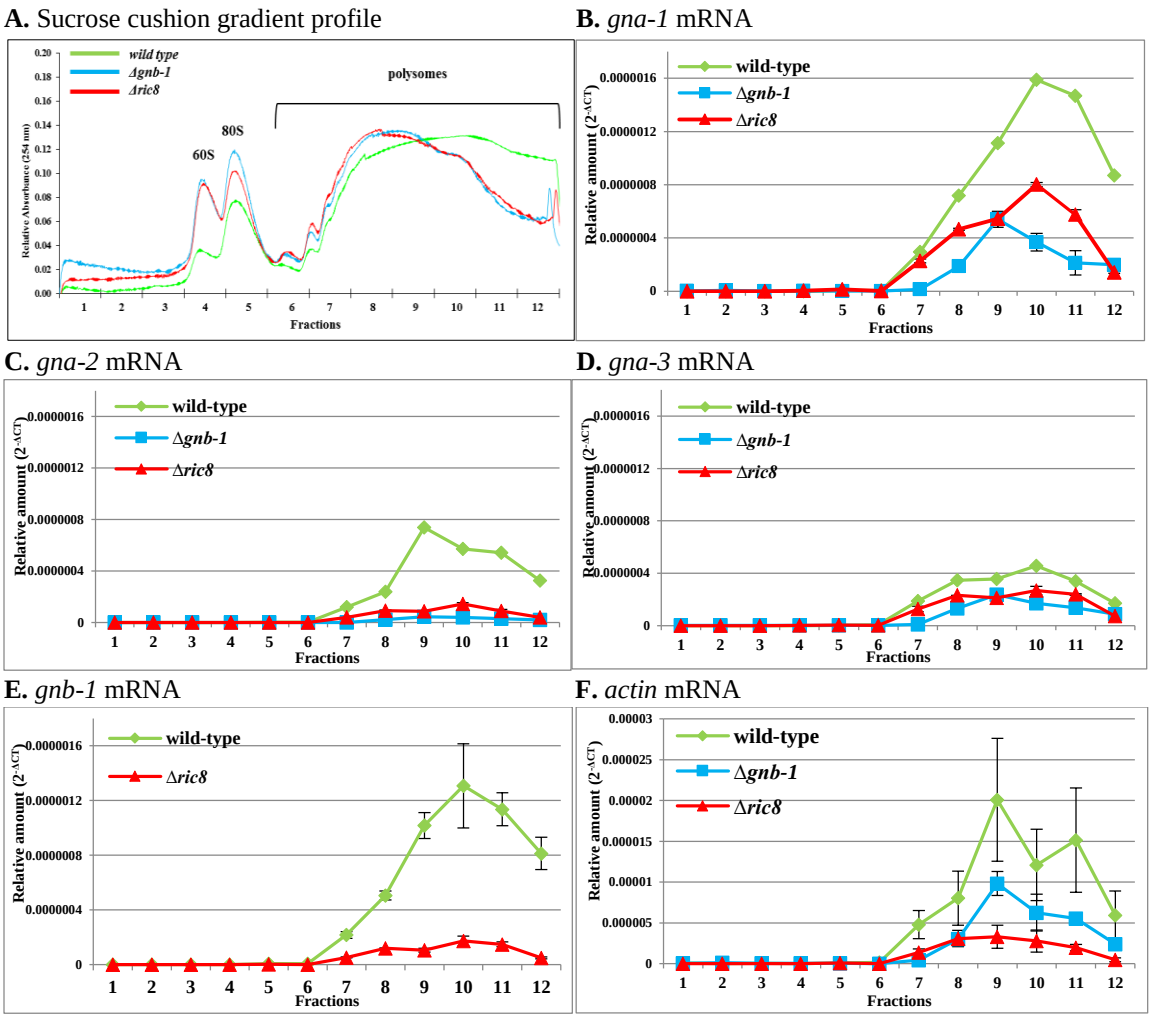

Figure 4.4 Analysis of the G protein subunits mRNAs associated with ribosomes in wild type, Δ*gnb-1*, and Δ*ric8* backgrounds. Strains are wild type (ORS-SL6a), Δ*gnb-1* (42-5-18), and Δ*ric8* (R81-5a). Strains were cultured in liquid VM medium with shaking at 200 rpm for 16 hours in the dark at 30˚C. Extracts were prepared and mRNP complexes were concentrated by 1.7M sucrose cushion. 20-60% sucrose gradient was used to separate mRNA/ribosome populations. RNA was extracted from sucrose fractions by TRIzol reagent according manufacturer protocol. mRNA relative amounts were examined by qPCR using SYBR Green Supermix (#170-8880, Bio-Rad). **A.** Sucrose gradient profile after sucrose cushion. **B.** *gna-1* mRNA distribution in different backgrounds. **C.** *gna-2* mRNA. **D.** *gna-3* mRNA. **E.** *gnb-1* mRNA. **F.** Housekeeping actin mRNA in wild type, Δ*gnb-1*, and Δ*ric8* backgrounds. Free ribosomal subunit (60S), monosomes (80S), and polysomes are indicated. Distribution of mRNAs in wild type (green line, diamonds), Δ*gnb-1* (blue line, squares), and Δ*ric8* (red line, triangles) backgrounds.

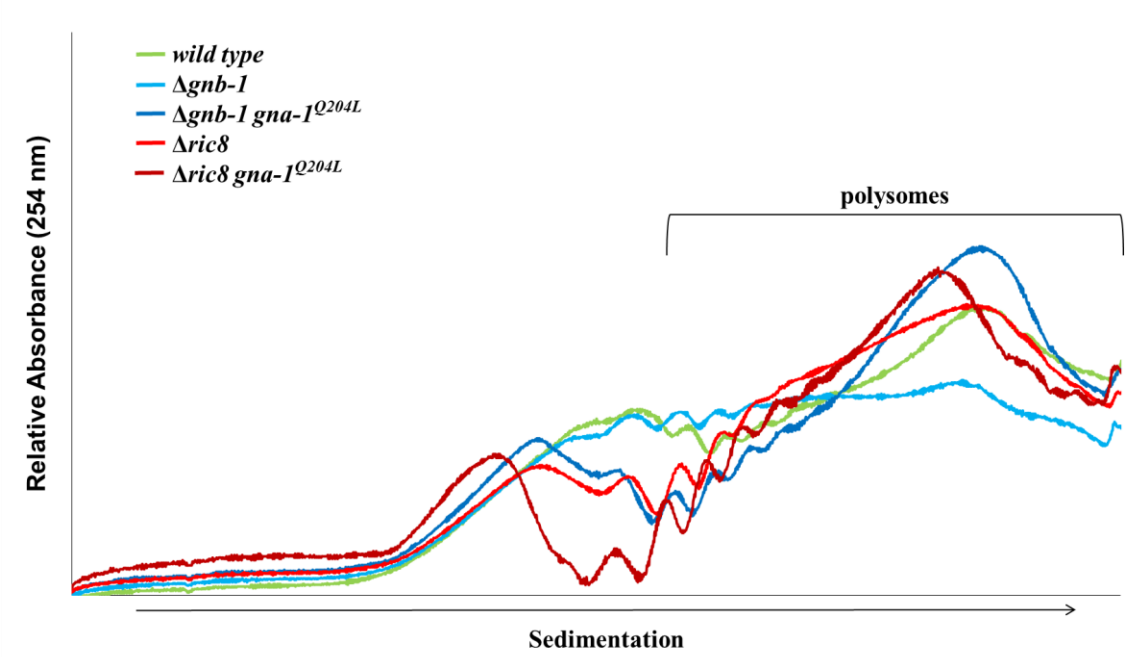

Figure 4.5 Ribosome sucrose density gradient profiling. Strains are shown in Table 4.1. Strains were cultivated as described in Figure 4.1. Cell extracts were prepared using PEB with heparin, VRC and RNasin, and directly loaded onto 4.5 ml 20 -60% (w/v) sucrose gradients. Traces represent absorbance after subtraction of the baseline from a blank sucrose gradient using iCruncher v. 2.2.

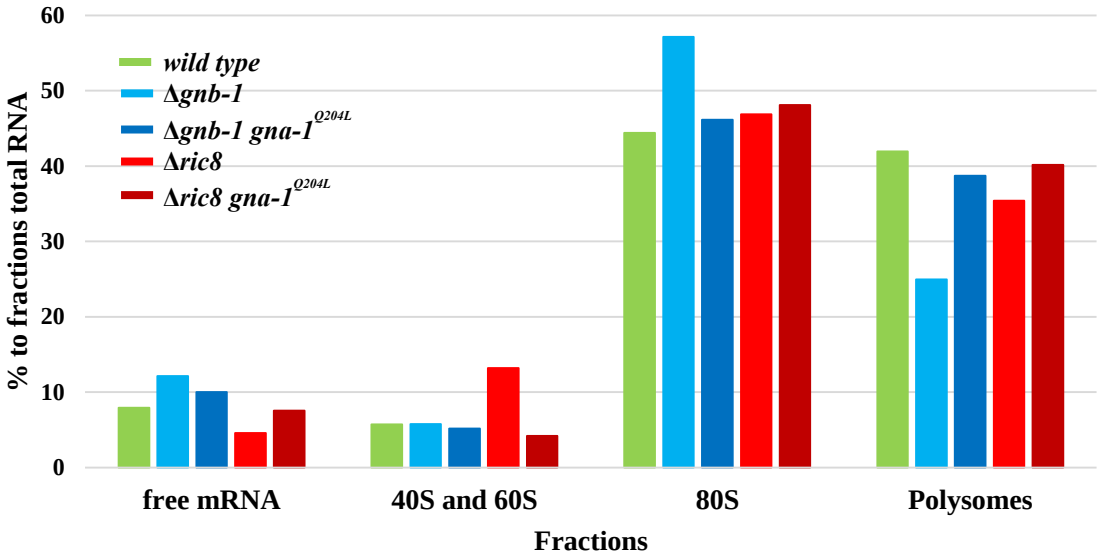

Figure 4.6 Total RNA extracted from sucrose gradient fractions. 12 fractions were collected from 20 - 60% (w/v) sucrose gradients and pooled into four fractions according to ribosomal population. Total RNA were extracted using Phenol-Chloroform protocol. OD of extracted total RNA was measured as shown in Methods. Results were calculated as % to all fractions total RNA for each strain.

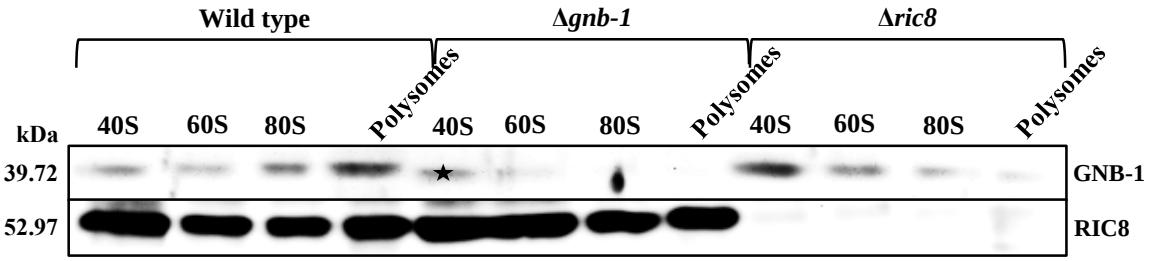

Figure 4.7 The GNB-1 and RIC8 proteins associate with ribosomes. Strains are wild type (ORS-SL6a), Δ*gnb-1* (42-5-18), and Δ*ric8* (R81-5a). Strains were cultured as described in Figure 4.1. Cell extracts were prepared using PEB and directly loaded on 4.5 ml 20 -60% (w/v) sucrose gradients. A total of 12 fractions were collected, and fractions corresponding to ribosomal subunits, monosomes and polysomes were pooled together, as indicated. Protein was isolated and concentrated using Amicon Ultra-15 Centrifugal Filter Units (#UFC900308, EMD Millipore). A volume corresponding to 50 µl of concentrated fractions was subjected to western analysis using GNB-1, and RIC8 antibody. The black star indicates a background band in the Δ*gnb-1* background.

Chapter 5

Conclusions and Future Directions

I am very proud to be a part of the team, which over time pioneered the discovery, and characterization of G proteins in filamentous fungi. This dissertation takes another step forward in understanding the regulation of G alpha subunits, which are an important part of the G protein signal transduction system.

Chapter 2 showed that G alpha and G beta subunits have genetic epistasis relationships for least for one function (173). This conclusion was supported by the finding that G alpha subunits physically interact with the G beta gamma dimer. At the same time, the G beta subunit has been demonstrated to positively regulate G alpha subunit protein levels (82;173). Moreover, the *N. crassa* cytosolic guanine exchange factor RIC8 regulates not only G alpha protein levels but also G beta subunit amount (174). It was not clear whether RIC8 regulates G alpha protein levels directly or through the action of the G beta subunit. The results presented in this dissertation showed that GNB-1 and RIC8 regulate levels of G alpha proteins independently from each other. However, there are still many remaining questions. For example, constructing *ric8* and *gnb-1* double mutants will give the opportunity to do genetic analysis and confirm the relationship between these genes. The observation that the Δ*gnb-1* Δ*ric8* double mutant does not resemble Δ*gnb-1* or Δ*ric8* single mutants will support the conclusion that *gnb-1*

and *ric8* are independent. Also, the finding that the Δ*gnb-1* Δ*ric8* double mutant has the same phenotype as the Δ*gnb-1* single mutant and overexpression of *ric8* does not suppress Δ*gnb-1* phenotypes and vice versa would indicate that the *gnb-1* and *ric8* genes are at least partially independent with regards to the cellular function being assayed. The interpretation of any other combinations of results from genetic analysis supports epistatic relationships between *gnb-1* and *ric8* genes in *N. crassa*.

In Chapter 3, I used epitope-tagged GNA-1 as a bait in two independent preliminary coimmunoprecipitation/mass spectrometry experiments, I identified cytosolic protein-protein interactions with RIC8 and several proteins in the Protein Fate category that could affect the G alpha subunit protein life cycle. I found that eukaryotic translational initiation factor (eIF-3f) deletion mutant and two 19S regulation proteasomal subunits (SEM-1 and RPN13) positively regulate GNA-1 protein levels. In the future, these results need to be followed up to confirm the associations. A system designed in our laboratory for high throughput protein-protein interaction allows not only check protein association by CoIP, but also investigates in real time *in vivo* co-localization of proteins. This system is comprised of two vectors with identical multiple cloning sites, bearing either the inositol auxotrophic marker, S-tag, and RFP or the pantothenate auxotrophic marker, V5-tag, and GFP. Strains expressing both a GFP and RFP tagged protein are created by fusing auxotrophic transformants that express only one tagged protein. If GNA-1 and a putative interacting protein from the CoIP/MS experiment can be detected by both CoIP and co-localization, it will confirm my results from CoIP/MS.

Also in Chapter 3, I obtained evidence that protein turnover is not major mechanism for regulating G alpha protein levels in Δ*gnb-1* and Δ*ric8* mutants. However, these results need to be followed up by pulse-chase studies. For these experiments, I already made strains containing the ^{V56His}*gna-1* allele in the wild type and Δ*ric8* backgrounds, but would need to make a strain expressing the ^{V56His}*gna-1* allele in the Δ*gnb-1* mutant. By measuring incorporation of ^{35}S into ^{V56His}GNA-1 protein at various times (through immunoprecipitation and scintillation counting) and under different treatments, we could quantitate turnover rates. For ^{V56His}*gna-1* in wild type background, I expect that the results will show similar ^{35}S levels in ^{V56His}GNA-1 in control and PMSF treated samples, but a higher concentration in MG132-treated samples, since I propose degradation via the 26S proteasome for GNA-1. For ^{V56His}*gna-1* in in the Δ*gnb-1* and Δ*ric8* backgrounds, there should be no significant change in MG132 or PMSF treated samples. These studies will establish the degradation pathway and rates of protein turnover for the G alpha subunit protein and confirm that the low level of GNA-1 is not due to protein turnover in Δ*gnb-1* and Δ*ric8* mutants.

In Chapter 4, I investigated the hypothesis that loss of *gnb-1* or *ric8* affects translation of G alpha transcripts. For these experiments, I established a ribosome sucrose density gradient profiling protocol. My preliminary results showed a significant decrease in G alpha mRNA levels associated with polysomes in Δ*gnb-1* and Δ*ric8* mutants. These preliminary findings must be followed up by ribosome sucrose density gradient profiling experiments to investigate the nature of translational regulation in Δ*gnb-1* and Δ*ric8* backgrounds. If RT-qPCR results show redistribution of mRNA from polysomes to the

40S fraction, it will suggest inhibition of initiation and formation of 43S stalled complexes. The finding that mRNA migrates from polysomes to 80S (monosomes) fractions in Δ*gnb-1* and Δ*ric8* backgrounds would be consistent with elongation inhibition . If we do not observe redistribution of mRNA, but just decreased levels in polysomes, we need to check for localization in mRNP complexes, such as Stress Granules (SG) or P-bodies (PB). The high throughput protein-protein interaction proposed for future experiments (see above) also could be used for tagging of SG and PB proteins. For example, V5 and GFP tagged alleles of *pab1*, and *pub1* (SG proteins) could be used to visualize formation of SG in different backgrounds. Detection of mRNA in the immunoprecipitated SG will confirm sequestration in mRNP complexes.

Also in Chapter 4, I showed that GNB-1 was present in monosomes and polysomes in wild type and that RIC8 was found in all ribosomal populations. These preliminary results can be followed up by analysis of sucrose gradients from EDTA treated cell extracts. If GNB-1 and RIC8 translocate to the 40S or 60S fractions, it will suggest that they associate with ribosomes. Another method to confirm results is CoIP with epitope-tagged ribosomal protein. If GNB-1 or RIC8 co-immunoprecipitate with ribosomes, it will confirm my preliminary results.

This dissertation has made attempts toward understanding G protein signaling in *N. crassa*, and by doing so, opened even more avenues for future studies of G alpha subunits and their regulation by G beta subunits and the RIC8 GEF.

Appendix A

Extraction of RNA from *N. crassa* tissue using TRIzol Reagent.

Sample preparation.

1. 100 mg of tissue from *N. crassa* liquid culture prepared as shown in Chapter 2 Methods was homogenized with 1 ml of TRIzol Reagent using pellet pestle in 1.7 ml Eppendorf tube.

Phase separation.

1. Homogenized samples incubated for 5 minutes at room temperature.
2. Added 0.2 ml of chloroform.
3. Tube was vortexed vigorously for 15 seconds.
4. Incubated for 2-3 minutes at room temperature.
5. The samples centrifuged at 12000 x g for 15 minutes at 4°C.
6. The aqueous phase of the sample removed by pipetting the solution out.
7. The aqueous phase placed into a new tube.

RNA precipitation.

1. Added 5 µg of RNase-free glycogen as a carrier to the aqueous phase.
2. Added 0.5 ml of 100% isopropanol to the aqueous phase.
3. Incubated at room temperature for 10 minutes.
4. Centrifuged at 12000 x g for 10 minutes at 4°C.

RNA wash.

1. The supernatant removed from the tube, leaving only the RNA pellet.
2. Pellet was washed with 1 ml of 75% ethanol.
3. Samples was vortexed briefly, then centrifuged at 7500 x g for 5 minutes at 4°C. The wash was discarded.
4. The RNA pellet was air dried for 10 minutes.

RNA resuspension

1. The RNA pellet was resuspended in 50 µl of RNase-free water by passing the solution up and down several times through a pipette tip.
2. Incubated in heat block set at 55°C for 10 minutes.
3. The RNA concentration, quality, and integrity was examined as was shown in Chapter 4.
4. Proceeded to downstream application, or stored at -70°C.

Extraction of RNA from *N. crassa* cell extracts or sucrose gradient fractions using TRIzol LS Reagent.

Sample preparation.

1. 400 µl of cell extract prepared as shown in Chapter 4 or 400 µl of sucrose gradient fraction was collected 2.0 ml Eppendorf tube containing 1.2 ml of TRIzol LS reagent.

Phase separation.

1. After brief vortexing, samples incubated for 5 minutes at room temperature.

2. Added 0.2 ml of chloroform.
3. Tube was vortexed vigorously for 15 seconds.
4. Incubated for 2-3 minutes at room temperature.
5. The samples centrifuged at 12000 x g for 15 minutes at 4°C.
6. The aqueous phase of the sample removed by pipetting the solution out.
7. The aqueous phase placed into a new tube.

RNA precipitation.

1. Added 5 µg of RNase-free glycogen as a carrier to the aqueous phase.
2. Added 0.5 ml of 100% isopropanol to the aqueous phase.
3. Incubated at room temperature for 10 minutes.
4. Centrifuged at 12000 x g for 10 minutes at 4°C.

RNA wash.

1. The supernatant removed from the tube, leaving only the RNA pellet.
2. Pellet was washed with 1 ml of 75% ethanol.
3. Samples was vortexed briefly, then centrifuged at 7500 x g for 5 minutes at 4°C. The wash was discarded.
4. The RNA pellet was air dried for 10 minutes.

RNA resuspension

1. The RNA pellet was resuspended in 50 µl of RNase-free water by passing the solution up and down several times through a pipette tip.
2. Incubated in heat block set at 55°C for 10 minutes.

3. The RNA concentration, quality, and integrity was examined as was shown in Chapter 4.
4. Proceeded to downstream application, or stored at -70°C.

Appendix B

N-terminal tagging of GNA-1 at native locus using V5 epitope tag

Introduction

Heterotrimeric G protein signaling pathways are important for eukaryotic cells to respond to various environmental signals. It has been previously reported that GNA-1, in the *N. crassa*, is required for female fertility, vegetative growth and stress responses. Such a wide impact for GNA-1 suggests that there are multiple proteins with which it interacts.

One of the goals of my research work was to identify cytosolic proteins that interacts with GNA-1. Therefore, I constructed two different epitope tagged GNA-1 strains: ^{V56His}GNA-1 and ^{V5}GNA-1. The ^{V56His}GNA-1 strain was discussed in Chapter 3, here I report about second strain ^{V5}GNA-1 properties and findings.

Materials and Methods

Strains and media. *N. crassa* strains used in this study are listed in Table B.1. Growing conditions and media for *N. crassa*, and *S. cerevisiae* are discussed in Chapter 3. Medium where indicated was supplemented with 400 µg/ml Ignite.

Strain construction. Used scheme for N-terminal epitope tagging of GNA-1 protein in native locus shown in Figure 3.1. All fragments for knock-in cassette were amplified from N. crassa genomic DNA by PCR with primers shown in Table B.2. For this construct the *bar* selectable marker (confers resistance to Ignite) was used obtained from pTJK1 by PCR (30) using *bar* primers (Table B.2). Detailed protocol is described in Chapter 3. ^{V5}*gna-1* in Δ*gnb-1* and Δ*ric8* background strains were obtained by a sexual cross using ^{V5}*gna-1* in wild type background as female. Female strain was inoculated on a SCM supplemented with Ignite, and grow until protoperithecia were formed. Then, a conidial suspension of the strains Δ*gnb-1* and Δ*ric8* used as a male was prepared by collecting conidia with a sterile stick and re-suspending into 500 µl of sterile water. The suspension was washed two times by centrifuging at 3,000 RPM for 1 minute, aspirating the supernatant, and re-suspending the conidia in 500 µl of sterile water. A sterile swab was then dipped in this conidial suspension, and rubbed over the surface of the slant. The slant was then returned to the light for at least 2 weeks for ascospores to be ejected. Ascospores were collected using a wet sterile swab, and re-suspended in sterile water. To isolate progeny, a 100 µl aliquot of spores is heat shocked in a 60°C water bath for 45 minutes, and then cooled to room temperature. Spores are plated on FGS (Δ*gnb-1* crosses) and VM (Δ*ric8* crosses) with Ignite. The spores were incubated for 24 hours, and then picked, and transferred to a VM slant supplemented with hygromycin. Successful crosses were examined by PCR using hygromycin, *bar*, and gene specific primers.

Western analysis and co-immunoprecipitation. Described in Chapter 2 and Chapter 3.

Mass spectrometry analysis, controls, and data analysis. Described in details in Materials and Methods in Chapter 3.

Results and Discussion

Phenotypic analysis of the ^{V5}*gna-1* strain showed complete identity to wild type strain: apical extension rates, male and female fertility, etc. Taken together it suggest that highly charged six histidine tag could affect tagged protein more than V5 epitope tag.

Western analysis using GNA-1 antibody showed presence of ^{V5}GNA-1 in cytosolic and doubled band in particulate fraction (Figure B.1 A). On the other hand, wild type GNA-1 is the most of the time is membrane associated and detected only in particulate fraction. Since G alpha subunit proteins undergo posttranslational modification such as palmitoylation, reversible depalmitoylation could explain release of ^{V5}GNA-1 into cytosol and doubled band in particulate fraction (96).

Introducing ^{V5}*gna-1* in Δ*gnb-1* and Δ*ric8* backgrounds did not change phenotype and resembles phenotype of Δ*gnb-1* and Δ*ric8*. Interestingly, I found that level of ^{V5}GNA-1 is similar in wild type, Δ*gnb-1* and Δ*ric8* backgrounds (Figure B.1 B). In sum, tagging of GNA-1 only with V5 epitope tag showed altered functionality of the protein, and it will be interesting to investigate this mechanism.

CoIP/Mass spectrometry analysis was done once with this strain. I identified 32 unique hits for ^{V5}GNA-1 CoIP sample after subtracting all protein detected in control samples (Table B.3). Proteins identified in both preliminary CoIP/MS runs are in bold.

TABLE B.1 *N. crassa* strains used in this study

Strain	Relevant genotype	Source or reference
74-OR23-IVA	Wild type, *mat A*	FGSC[a] 2489
ORS-SL6a	Wild type, *mat a*	FGSC 4200
42-5-12	Δ*gnb-1::hph*$^{+}$ *mat a*	(173)
42-5-18	Δ*gnb-1::hph*$^{+}$ *mat A*	(177)
R81-5a	Δ*ric8::hph*$^{+}$ *mat a*	(174)
mus-51 a	Δ*mus-51::hph*$^{+}$ *mat a*	FGSC 20277
mus-51 A	Δ*mus-51::hph*$^{+}$ *mat A*	FGSC 20278
27	^{V5}*gna-1 mat A*	This study
27B1	^{V5}*gna-1* Δ*gnb-1::hph*$^{+}$ *mat a*	This study
27R8	^{V5}*gna-1* Δ*ric8::hph*$^{+}$ *mat a*	This study

[a]FGSC, Fungal Genetics Stock Center, Kansas City, MO.

TABLE B.2 Oligonucleotides used in Chapter 3

Name	Sequence
[b]gna1 5'UTR V5 NT Fw	GTAACGCCAGGGTTTTCCCAGTCACGACGAGTGCCGTCTAGCG TAGTGCC
[a]gna1 5UTR V5 NT Rv	TAGAATCGAGACCGAGGAGAGGGTTAGGGATAGGCTTACCCA TTTTGGCGACTTGTTGTAGCTCGTAGC
[a]gna1 ORF V5 NT Fw	TCCCTAACCCTCTCCTCGGTCTCGATTCTACGGGCGGAGGCGG CGGAGGTTGCGGAATGAGTACAGAGG
[c]gna1 ORF V5 NT Rv	GCTCCTTCAATATCATCTTCTGTCGATCAAATCAAACCGCAGA GACGCAGG
[c]gna1 BAR V5 NT Fw	CCTGCGTCTCTGCGGTTTGATTTGATCGACAGAAGATGATATTG AAGGAGC
[c]gna1 BAR V5 NCT Rv	CTGATGAAAAAATTAGAAAGATTGCGTTCAGTGCGACGGATCA GATCTCGGTGACG
[c]gna1 3UTR V5 NCT Fw	CGTCACCGAGATCTGATCCGTCGCACTGAACGCAATCTTTCTA ATTTTTTCATCAG
[b]gna1 3UTR V5 NCT Rv	GCGGATAACAATTTCACACAGGAAACAGCAGACAAATCCAAC CGTTGCGTTGCCC
[f]BAR FW	TCGACAGAAGATGATATTGAAGGAGC
[f]BAR RV	GACGGATCAGATCTCGGTGACG
[d] V5 SC FW	GGTAAGCCTATCCCTAACCCTCTCC
[e] V5 SC RV	CGTAGAATCGAGACCGAGGAGAGGG

[a]V5 and 5 poly glycine included in oligonucleotide sequence for yeast recombination
[b]pRS426 sequences included in oligonucleotide sequence for yeast recombination with shuttle vector
[c]*bar* resistant gene sequences included in oligonucleotide sequence for yeast recombination
[d]Screening primer forward, include V5 tag sequence
[e]Screening primers reverse, include *bar* ORF sequence
[f]Primers for amplifying bar selectable marker from pTJK1

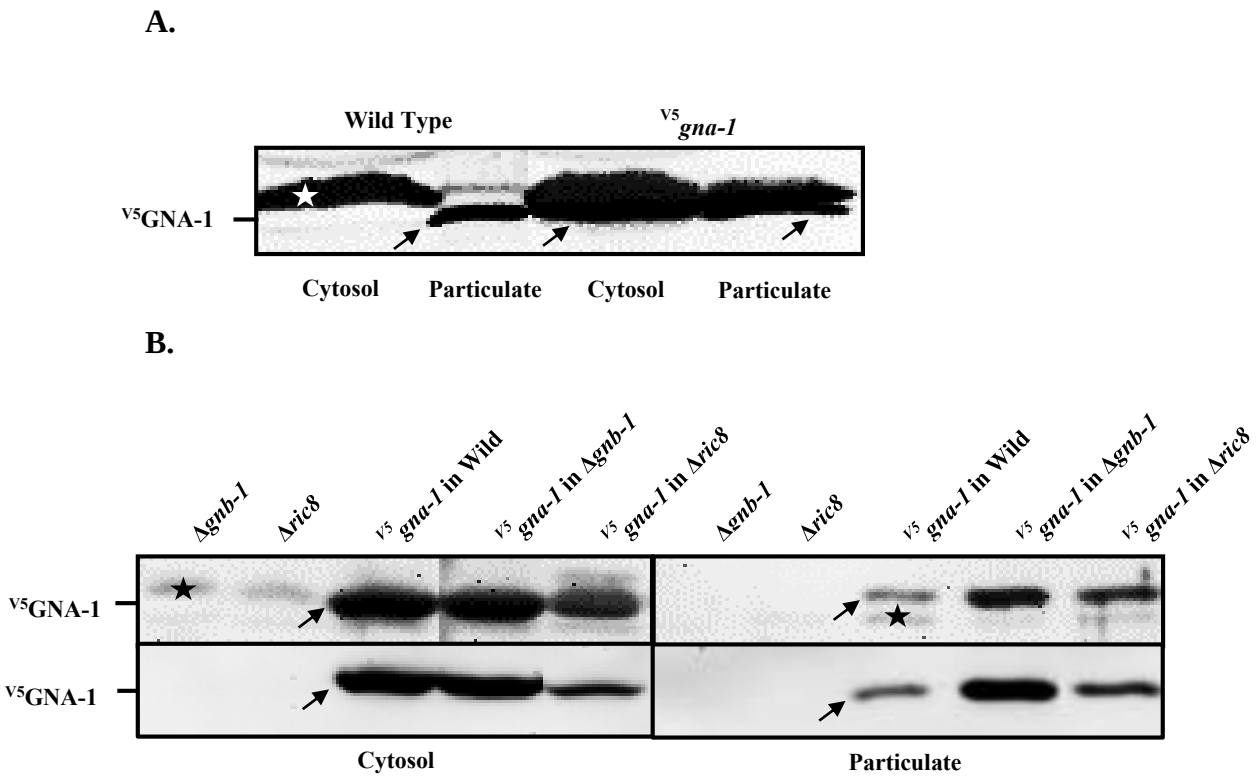

Figure B.1 Expression and Localization of ^{V5}GNA-1 protein. A. Detection and localization of the ^{V5}GNA-1 protein. Strains were cultured in liquid VM medium with shaking at 200 rpm for 16 hours in the dark at 30˚C. Cytosolic and particulate (membrane) fractions were isolated, and 100 µg of total protein subjected to western analysis using GNA-1 antibody. **B. Detection of the ^{V5}GNA-1 protein in Δ*gnb-1* and Δ*ric8* backgrounds.** Strains were cultured as described in (A). Top panel western blot with GNA-1 antibody, second panel V5 epitope tag antibody. White and black stars denotes background bands and black arrows indicate GNA-1 protein.

Table B.3 Putative ^{V5}GNA-1 cytosolic interacting proteins identified from CoIP/MS

Nº	NCU	Protein	Score
1	NCU06493	guanine nucleotide-binding protein alpha-1 (354 aa)	1933
2	NCU05390	mitochondrial phosphate carrier protein (320 aa)	231
3	NCU09132	alpha tubulin (455 aa)	136
4	NCU02788	RIC8 (480 aa)	110
5	NCU00106	glutamate 5-kinase (469 aa)	97
6	NCU00629	6-phosphofructokinase (846 aa)	88
7	**NCU07567**	**T-complex protein 1 subunit theta (548 aa)**	88
8	NCU03139	histidine-3 (871 aa)	81
9	NCU04331	cytoplasmic ribosomal protein-4 (302 aa)	81
10	NCU09222	hypothetical protein (117 aa)	74
11	NCU05526	lysine-5 (426 aa)	71
12	NCU07922	elongation factor 3 (1057 aa)	68
13	NCU11350	glucosamine-fructose-6-phosphate aminotransferase (701 aa)	65
14	NCU03980	T-complex protein 1 subunit epsilon (551 aa)	56
15	NCU07721	26S proteasome regulatory subunit rpn1 (903 aa)	55
16	NCU11181	Ras superfamily GTPase (190 aa)	35
17	NCU09817	DAHP synthase (377 aa)	35
18	NCU02393	mitogen-activated protein kinase-2 (353 aa)	32
19	NCU03608	ketol-acid reductoisomerase (403 aa)	31
20	NCU04945	mitochondrial intermembrane space protein Mia40 (299 aa)	31
21	NCU06512	methionine synthase (770 aa)	30
22	NCU07697	isocitrate dehydrogenase subunit 2 (380 aa)	29
23	NCU03311	polyadenylation factor subunit CstF64 (323 aa)	29
24	NCU06520	ATP-dependent RNA helicase dbp-7 (815 aa)	28
25	NCU06785	ATP-citrate synthase subunit 1 (671 aa)	28
26	NCU04414	hypothetical protein (461 aa)	28
27	NCU11202	cytoskeleton assembly control protein Sla2 (1054 aa)	27
28	NCU09376	hypothetical protein (390 aa)	22
29	NCU00633	hypothetical protein (371 aa)	22
30	NCU00502	ATP synthase subunit 4 (242 aa)	21
31	NCU06549	pyridoxine 2 (253 aa)	21
32	NCU01213	superoxide dismutase-2 (246 aa)	20

Score threshold for Mascot >30, which indicate identity or extensive homology ($p<0.05$)
Score threshold for Mascot >15, which indicate homology ($p<0.05$)
Proteins identified in both CoIP/MS are highlighted.

Appendix C

Establishing and troubleshooting ribosome sucrose density gradient profiling protocol in *Neurospora crassa*.

Materials and Methods. All material and methods, including strains and media, growth conditions, extract preparation and sucrose gradient profiling, RNA extraction and mRNA abundance measurement are described in Chapter 4.

Results

Cycloheximide treatment of living cell cultures before harvesting can result in cycloheximide-inflicted artifacts in *N. crassa*.

To study translation in *N. crassa* I adapted a plant ribosome sucrose density gradient profiling protocol (105). All protocols used previously for *S. cerevisiae* and *N. crassa* include pretreatment of living cells with cycloheximide (CHX) before harvesting (39;94;164). Recent studies indicate that using CHX in the culture medium can result in cycloheximide-inflicted artifacts in *S. cerevisiae*. These include slower elongation at the beginning of the open reading frame, resulting in increased levels of monosomes and light polysomes in the sucrose gradient profile (46). Before including CHX pretreatment in the protocol, I checked *N. crassa* liquid cultures for CHX-inflicted artifacts. I

determined that sucrose gradient profile with CHX pretreatment of living cell of wild type shows not only higher light polysomes but also rise of heavy polysomes and 60S ribosomal subunits comparing with using CHX in polysomes extraction buffer (PEB) only (Figure C.1). Interestingly, eliminating CHX in extraction buffer during preparation of cell extracts shows the same profile as using CHX in PEB (Figure C.1). In summary, the final adapted protocol did not include CHX pretreatment of living cells before harvesting, but CHX is included in PEB, to prevent ribosomes disassembly during cell extract preparation.

Levels of mRNA in tissue, cell extract, and sucrose gradient fractions derived from wild type, Δ*gnb-1*, and Δ*ric8* strains

Since level of *gna-1* mRNA (Figure 4.4.B) and level of GNA-1 protein (Figure 4.2 top panel) were the most affected in Δ*gnb-1* and Δ*ric8* backgrounds, I used this gene to trouble shoot the possible causes of reduction of G protein subunit mRNAs in the two mutants. Total RNA was extracted from tissue and PEB cell extracts of wild type, Δ*gnb-1*, and Δ*ric8* strains. Levels of *gna-1* and actin mRNAs were determined using RT - qPCR (Figure C.2). Levels of *gna-1* and actin mRNAs in cell extract derived with PEB from Δ*gnb-1* and Δ*ric8* strains were dramatically lower compared to wild type (Figure C.2 A and B, blue bars). In contrast, the level of *gna-1* and actin mRNA extracted directly from tissue shows a different pattern, with similar levels in all genetic backgrounds (Figure C.2 A and B, orange bars). Thus, levels of mRNAs were higher in

samples extracted directly from tissue. In case of sucrose gradient fractions, *gna-1* mRNA was in polysomes (fractions 7-12) in wild type, but not detectable in the two mutants (Figure C.2.C). These results all point to a potential problem with RNase activity in the cell extracts.

To determine whether the effect on mRNA stability is more global, I checked mRNA levels for other housekeeping genes, including tubulin (*tub-2*), ubiquitin (*ubi4*), and glyceraldehyde 3-phosphate dehydrogenase (*gpd-1*) in tissue and PEB cell extract-derived mRNA. The top panel of Figure C.3 shows actin bands corresponding to RNA extracted directly from tissue (left three lanes) or cell extracts (right three lanes) in wild type, Δ*gnb-1* and Δ*ric8* backgrounds. Levels of actin mRNA were similar in tissue for all backgrounds, and for the wild type strain in PEB cell extracts. I could not detect *actin* mRNA in Δ*gnb-1* and Δ*ric8* backgrounds. The same pattern was observed for the other housekeeping mRNAs (Figure C.3).

Since there is difference between RNA extraction from tissue and cell extract, the issue could be RNAse activity during cell extract preparation, or method-specific. If I could not detect mRNAs in any sucrose gradient fractions of cell extracts derived from Δ*gnb-1* and Δ*ric8* strains, including pellets after cell extract preparation and free mRNA fractions, the most likely these mRNAs form complexes or aggregates which could not be extracted with used TRIzol method. A recent publication states that there is TRIzol-specific phenomenon for very young *Arabidopsis* tissues RNA extraction. They found that TRIzol extracts the same amount of 18S ribosome RNA during seedling growth, but *β-TUBULIN* mRNA amount grew from undetectable in point zero to normal level during

12 days (18). The same samples were extracted using Phenol-Chloroform method showed the same level of *β-TUBULIN* mRNA during all 12 days (18).To investigate this issue I prepared cell extracts using PEB, and extracted RNA using two different methods: TRIzol and Phenol-Chloroform (Figure C.4 A). In Figure C.4.A, in the left three lanes, I could see that level of *gpd-1* mRNA with TRIzol extraction is the same as in previous experiments (Figure C.3): normal in wild type, and nearly undetectable in deletion mutants. In contrast, Phenol-Chloroform extraction shows similar levels of *gpd-1* mRNA in wild type, Δ*gnb-1* and Δ*ric8* backgrounds. In sum, TRIzol Reagent could not extract the same amount of RNA as Phenol-Chloroform extraction from tissue and cell extracts of the deletion mutants.

To find out if there is a high RNAse activity during cell extracts preparation I used a combination of three RNAse inhibitors: heparin, vanadyl ribonucleoside complex (VRC), and RNasin. RNasin was always used together with VRC, which later will be indicated as "VRC". I checked *gna-1* and *gpd-1* mRNA levels in cell extracts prepared with PEB with or without RNAse inhibitors and extracted using the Phenol-Chloroform method (Figure C.4.B). Levels of *gpd-1* and *gna-1* mRNA are similar in wild type, Δ*gnb-1* and Δ*ric8* strains (Figure C.4.B, left three lanes). On the other hand, in cell extracts prepared without RNAse inhibitors, the most affected mRNAs were in the wild type background and the least in Δ*ric8* (Figure C.4.B, right three lanes). To confirm these results future experiments should be include direct measurement of RNAse activity in PEB extracts before and after sucrose gradient fractionation for wild type and Δ*gnb-1* and Δ*ric8* strains.

Using heparin in PEB for sucrose gradients did not change the profile for cell extracts of wild type, Δ*gnb-1* and Δ*ric8* strains (Figure C.5.A), which suggests that heparin by itself could not inhibit all types of RNAses. In case of VRC in PEB, there were significant changes in the sucrose gradient profiles, including the higher level of polysomes in Δ*ric8* than in wild type and lower levels in Δ*gnb-1* (Figure C.5.B). To check how much the polysome population changed in wild type and Δ*gnb-1* profiled with heparin or VRC treatment, I prepared cell extracts with different treatments from the same sucrose gradient run (Figure C.5.C). VRC seems to decrease absorbance in the polysome region of wild type, and increase absorbance profile of polysomes for Δ*gnb-1* and Δ*ric8* strains (Figure C.5.C). Combination of all three inhibitors resemble only VRC treatment (Figure C.5.D). The high background of VRC absorbance makes it impossible to interpret sucrose gradient profiles. I recommend using total RNA abundance and rRNA analyzed by agarose gel in collected sucrose gradient fractions to identify ribosomal populations on profiles.

Conclusion

I am not recommend to use CHX pretreatment of living cell before harvesting in *N. crassa*. Using CHX pretreatment could causes cycloheximide-inflicted artifacts and alter ribosome sucrose density gradient profiling experiment results.

I also found that RNA TRIzol extraction from cell extracts could have TRIzol-specific phenomenon. To avoid a method specific bias I recommend using Phenol-Chloroform method.

I investigated the effect of different RNAse inhibitors on sucrose gradient profiles and found that VRC gives good inhibition of RNAse activity. To prevent RNAse activity I recommend using combination of inhibitors (heparin, VRC, and RNasin).

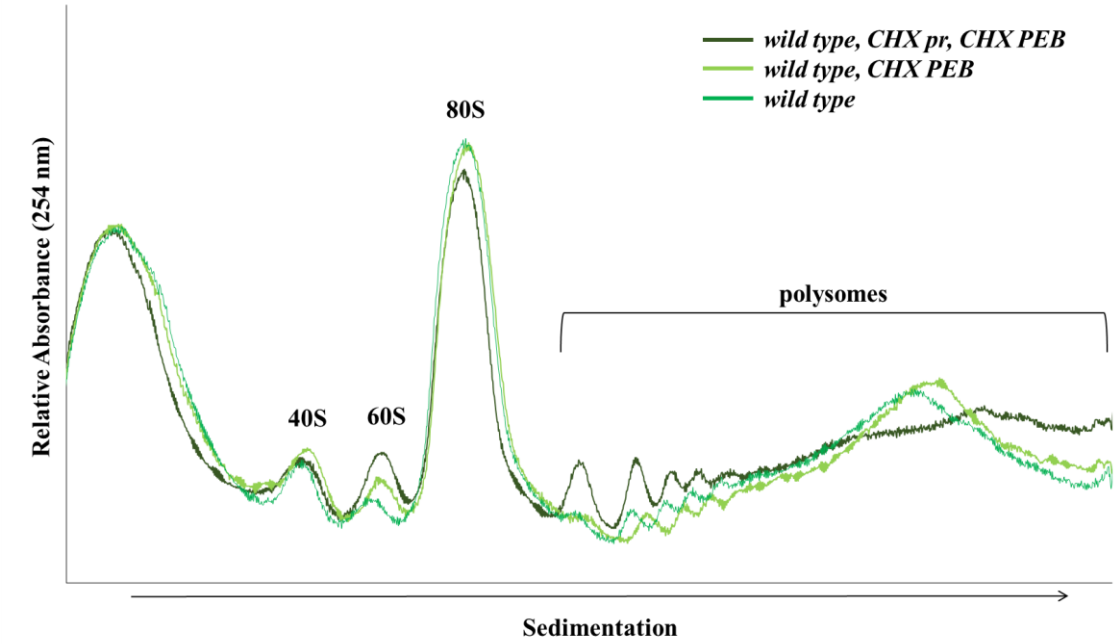

Figure C.1. Effect of using cycloheximide on sucrose gradient profile of wild type strain. Strain wild type (ORS-SL6a) was cultivated as shown in Methods Chapter 4. One of the liquid culture of wild type was pretreated with cycloheximide (100 µg/ml) 5 minutes before harvesting (CHX pr, dark green line). Cell extract prepared using PEB with adding cycloheximide (100 µg/ml) (CHX PEB) or without cycloheximide (not indicated, medium dark green line) and directly loaded on 4.5 ml 20 -60% (w/v) sucrose gradient. Traces represent absorbance after subtraction of the baseline of a blank sucrose gradient using iCruncher v. 2.2. Positions of free ribosomal subunits (40S and 60S), monosomes (80S) and polysomes are indicated.

A. *gna-1* mRNA

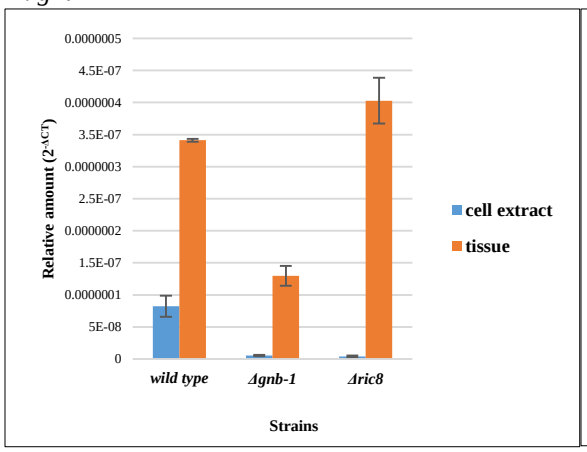

B. *actin* mRNA

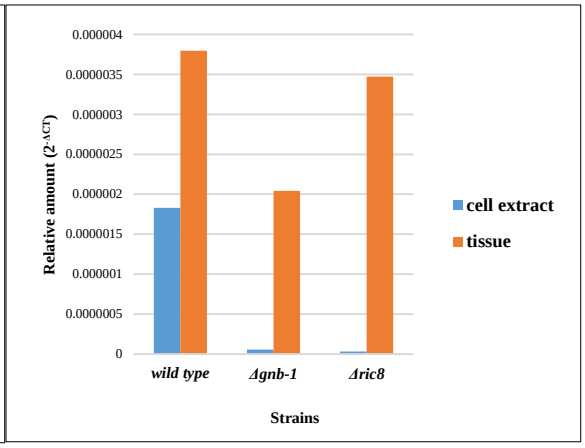

C. *gna-1* mRNA in fractions

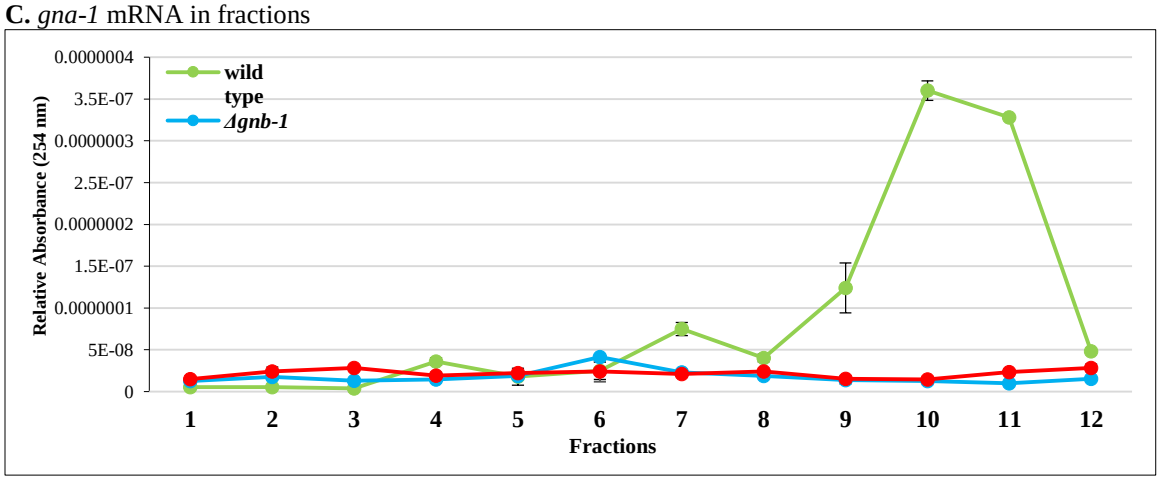

Figure C.2. Analysis of the *gna-1* and *actin* mRNAs in tissue, cell extracts, and sucrose gradients. Strains are wild type (ORS-SL6a), Δ*gnb-1* (42-5-18), and Δ*ric8* (R81-5a). Cell extracts were prepared, the one from two equal volumes was used for RNA extraction, and another was loaded on 20-60% sucrose gradient. RNA was extracted directly from tissue, cell extracts, and sucrose gradient fractions using TRIzol reagent according manufacturer protocol. mRNA relative amounts were examined by qPCR using SYBR Green Supermix (#170-8880, Bio-Rad). **A.** *gna-1* mRNA in cell extract and tissue. **B.** Housekeeping *actin* mRNA in cell extract and tissue. **C.** *gna-1* mRNA distribution through sucrose gradient fractions in wild type, Δ*gnb-1*, and Δ*ric8* backgrounds.
Distribution of mRNAs in wild type (green line), Δ*gnb-1* (blue line), and Δ*ric8* (red line) backgrounds.

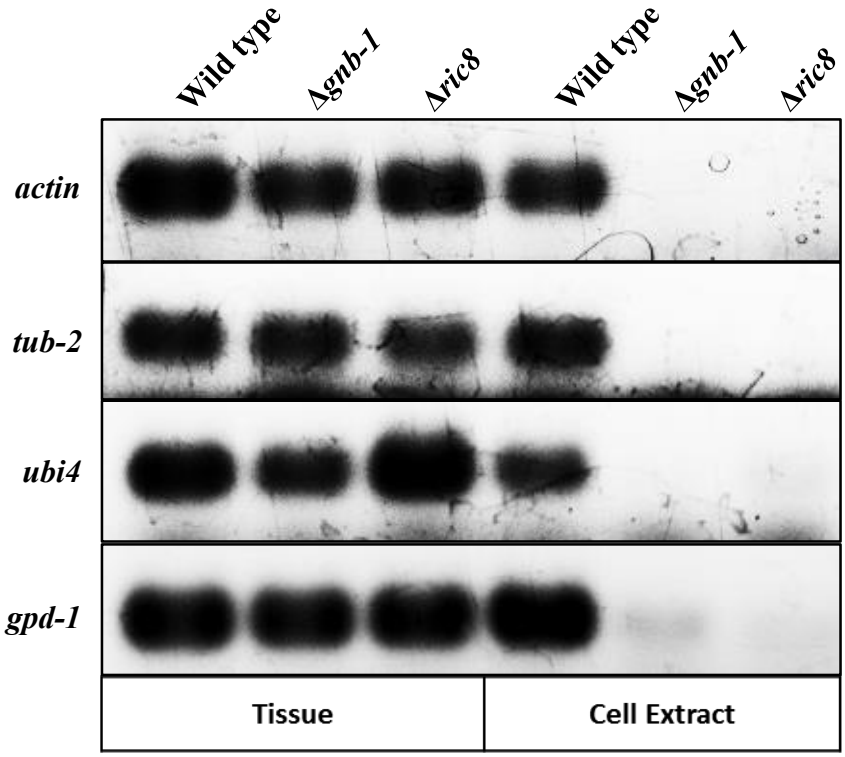

Figure C.3. Analysis of housekeeping gene mRNAs in tissues and cell extracts. Strains are wild type (ORS-SL6a), Δ*gnb-1* (42-5-18), and Δ*ric8* (R81-5a). Cell extracts were prepared from the tissue using PEB. RNA was extracted directly from tissue or cell extracts using TRIzol reagent according manufacturer protocol. After RT-PCR samples were resolved by agarose gel. From the top: *actin*; tubulin (*tub-2*); ubiquitin (*ubi4*); and glyceraldehyde 3-phosphate dehydrogenase (*gpd-1*).

A.

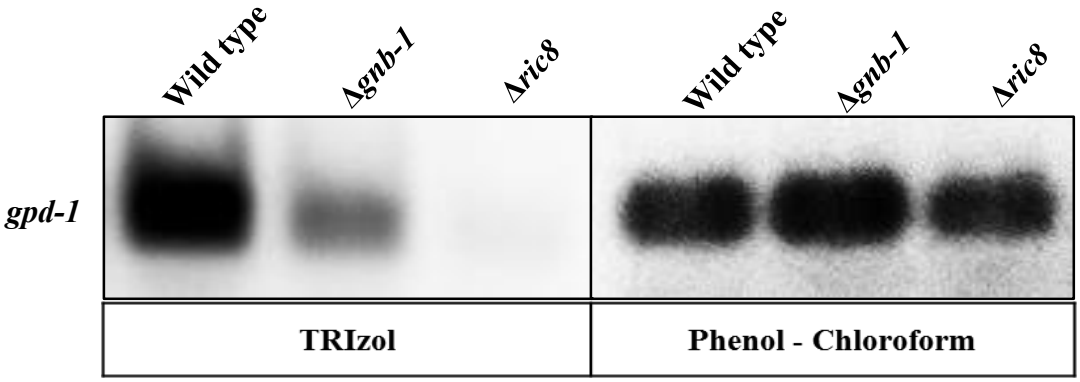

B.

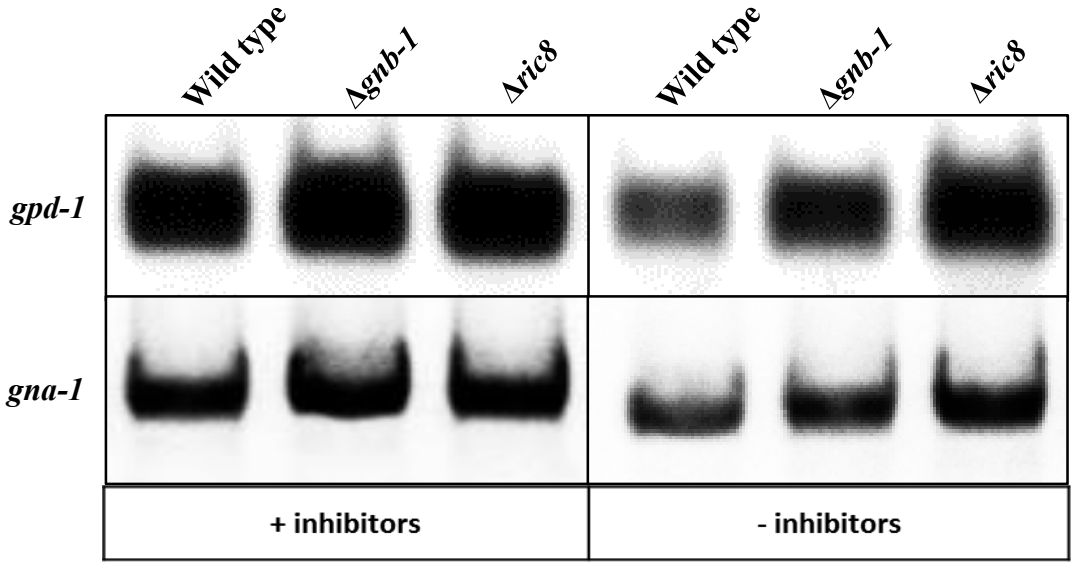

Figure C.4. Analysis of the mRNAs in cell extract. Strains are wild type (ORS-SL6a), Δ*gnb-1* (42-5-18), and Δ*ric8* (R81-5a). Cell extracts were prepared from the tissue using PEB and inhibitors were added where indicated (Vanadil ribonucleoside complex, heparin, and RNAsin). After RT-PCR, samples were resolved on agarose gels. **A.** glyceraldehyde 3-phosphate dehydrogenase (*gpd-1*) mRNA in tissue extracted using the TRIzol and Phenol-Chloroform methods. **B.** *gpd-1* and *gna-1* in tissue extracted using Phenol-Chloroform method with or without inhibitors in PEB.

A.

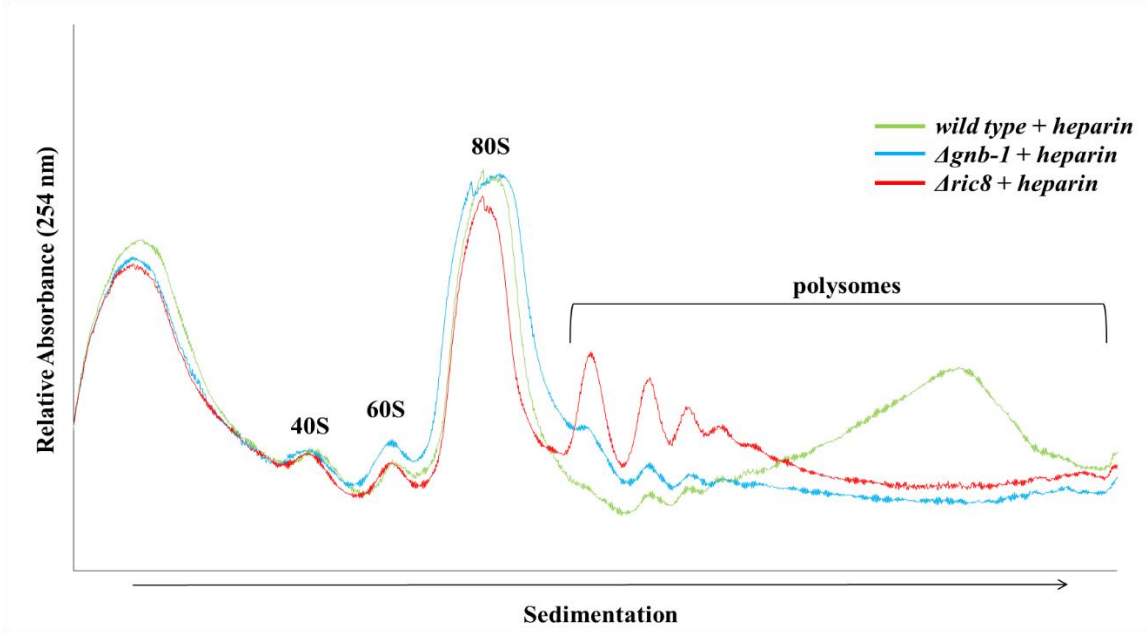
Relative Absorbance (254 nm)
80S
40S
60S
polysomes
wild type + heparin
Δgnb-1 + heparin
Δric8 + heparin
Sedimentation

B.

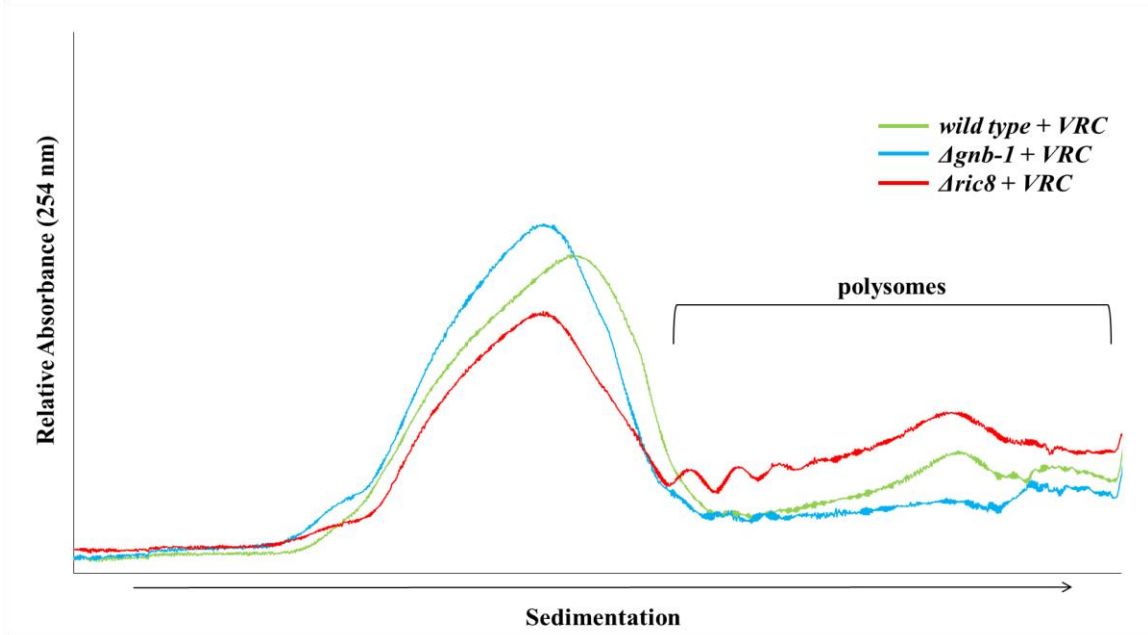
Relative Absorbance (254 nm)
polysomes
wild type + VRC
Δgnb-1 + VRC
Δric8 + VRC
Sedimentation

C.

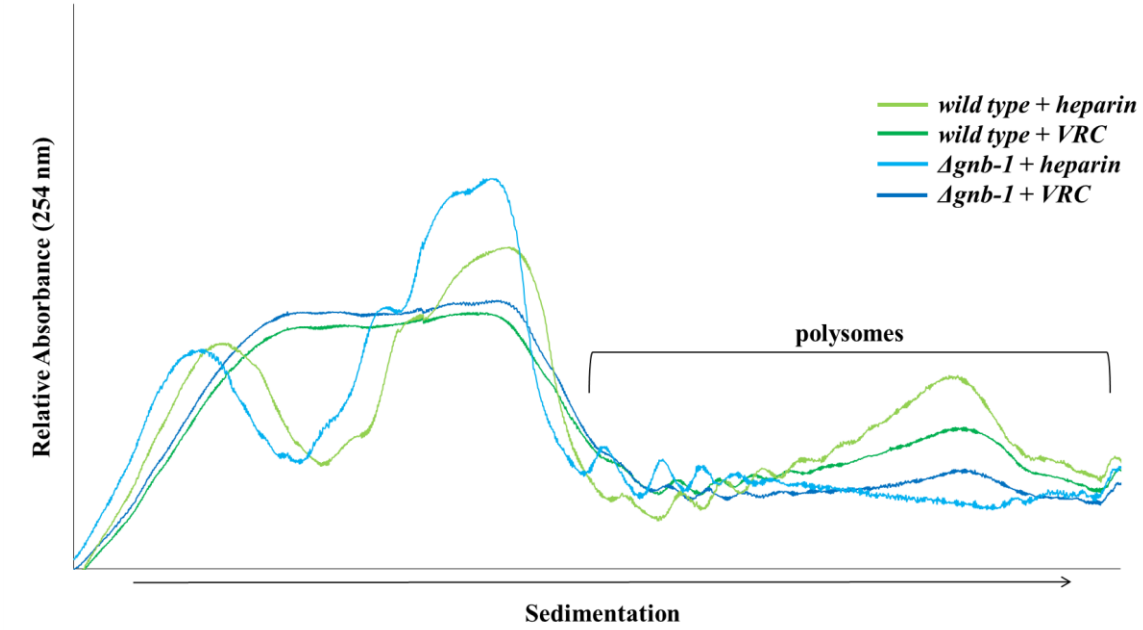
wild type + heparin
wild type + VRC
Δgnb-1 + heparin
Δgnb-1 + VRC
polysomes
Relative Absorbance (254 nm)
Sedimentation

D.

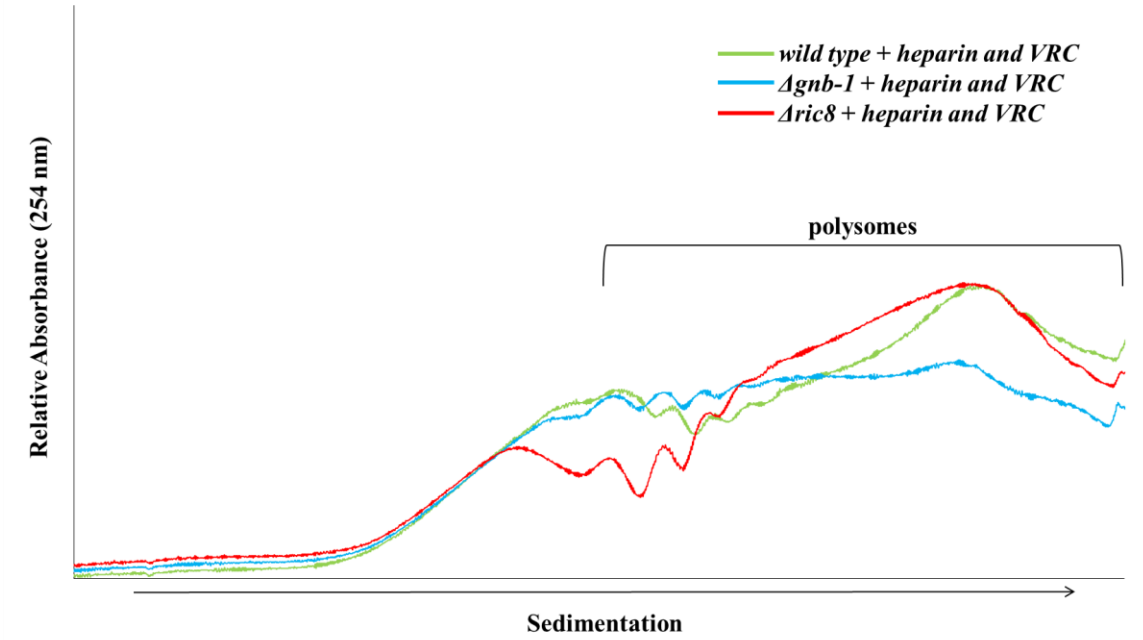
wild type + heparin and VRC
Δgnb-1 + heparin and VRC
Δric8 + heparin and VRC
polysomes
Relative Absorbance (254 nm)
Sedimentation

Figure C.5. Effect of RNAse inhibitors (heparin and VRC) on sucrose gradient profiles of wild type, Δ*gnb-1* and Δ*ric8* strains. Strains are wild type (ORS-SL6a), Δ*gnb-1* (42-5-18), and Δ*ric8* (R81-5a). Strains were cultivated as shown in Methods Chapter 4. Cell extracts were prepared using PEB with addition, where indicated, of the RNAse inhibitors heparin or VRC. Cell extracts were directly loaded on 4.5 ml 20 -60% (w/v) sucrose gradients. Traces represent absorbance after subtraction of the baseline of a blank sucrose gradient using iCruncher v. 2.2. **A.** Profile of cell extracts prepared with addition of heparin in PEB. **B.** Sucrose gradient profile of cell extracts prepared with addition of VRC. **C.** Profile of cell extracts prepared with heparin or VRC. D. Sucrose gradient profiles of cell extracts prepared with heparin and VRC. The positions of free ribosomal subunits (40S and 60S), monosomes (80S) and polysomes are indicated.

References

1. **Afshar,K., Willard,F.S., Colombo,K., Johnston,C.A., McCudden,C.R., Siderovski,D.P., and Gonczy,P.**, 2004. RIC-8 is required for GPR-1/2-dependent Galpha function during asymmetric division of C. elegans embryos. **119**, 219-230.

2. **Anthony,D.D. and Merrick,W.C.**, 1992. Analysis of 40 S and 80 S complexes with mRNA as measured by sucrose density gradients and primer extension inhibition. **267**, 1554-1562.

3. **Aramayo,R. and Metzenberg,R.L.**, 1996. Gene replacements at the his-3 locus of Neurospora crassa. **43**, 9-13.

4. **Asano,K., Kinzy,T.G., Merrick,W.C., and Hershey,J.W.**, 1997. Conservation and diversity of eukaryotic translation initiation factor eIF3. **272**, 1101-1109.

5. **Avery,L. and Wasserman,S.**, 1992. Ordering gene function: the interpretation of epistasis in regulatory hierarchies. **8**, 312-316.

6. **Baasiri,R.A., Lu,X., Rowley,P.S., Turner,G.E., and Borkovich,K.A.**, 1997. Overlapping functions for two G protein alpha subunits in Neurospora crassa. **147**, 137-145.

7. **Babitzke,P., Baker,C.S., and Romeo,T.**, 2009. Regulation of translation initiation by RNA binding proteins. **63**, 27-44.

8. **Bailly,E. and Reed,S.I.**, 1999. Functional characterization of rpn3 uncovers a distinct 19S proteasomal subunit requirement for ubiquitin-dependent proteolysis of cell cycle regulatory proteins in budding yeast. **19**, 6872-6890.

9. **Balagopal,V. and Parker,R.**, 2011. Stm1 modulates translation after 80S formation in Saccharomyces cerevisiae. **17**, 835-842.

10. **Beadle,G.W. and Tatum,E.L.**, 1941. Genetic Control of Biochemical Reactions in Neurospora. **27**, 499-506.

11. **Becker,A.H., Oh,E., Weissman,J.S., Kramer,G., and Bukau,B.**, 2013. Selective ribosome profiling as a tool for studying the interaction of chaperones and targeting factors with nascent polypeptide chains and ribosomes. **8**, 2212-2239.

12. **Bell-Pedersen,D., Dunlap,J.C., and Loros,J.J.**, 1992. The Neurospora circadian clock-controlled gene, ccg-2, is allelic to eas and encodes a fungal hydrophobin required for formation of the conidial rodlet layer. **6**, 2382-2394.

13. **BIANCHI,D.E.**, 1964. An Endogenous Circadian Rhythm in Neurospora Crassa. **35**, 437-445.

14. **Bistis,G.N.**, 1981. Chemotropic interactions between trichogyenes and conidia of opposite mating-type in Neurospora crassa. **73**, 959-975.

15. Bistis, G. N. Different cell types in Neurospora crassa. David D.Perkins and Nick D.Read. 50, 17-19. 1-3-2003. Fungal Genet. Newsl., Fungal Genet. Newsl.
Ref Type: Generic

16. **Bohn,S., Sakata,E., Beck,F., Pathare,G.R., Schnitger,J., Nagy,I., Baumeister,W., and Forster,F.**, 2013. Localization of the regulatory particle subunit Sem1 in the 26S proteasome. **435**, 250-254.

17. **Borkovich,K.A., Alex,L.A., Yarden,O., Freitag,M., Turner,G.E., Read,N.D., Seiler,S., Bell-Pedersen,D., Paietta,J., Plesofsky,N., Plamann,M., Goodrich-Tanrikulu,M., Schulte,U., Mannhaupt,G., Nargang,F.E., Radford,A., Selitrennikoff,C., Galagan,J.E., Dunlap,J.C., Loros,J.J., Catcheside,D., Inoue,H., Aramayo,R., Polymenis,M., Selker,E.U., Sachs,M.S., Marzluf,G.A., Paulsen,I., Davis,R., Ebbole,D.J., Zelter,A., Kalkman,E.R., O'Rourke,R., Bowring,F., Yeadon,J., Ishii,C., Suzuki,K., Sakai,W., and Pratt,R.**, 2004. Lessons from the genome sequence of Neurospora crassa: tracing the path from genomic blueprint to multicellular organism. **68**, 1-108.

18. **Box,M.S., Coustham,V., Dean,C., and Mylne,J.S.**, 2011. Protocol: A simple phenol-based method for 96-well extraction of high quality RNA from Arabidopsis. **7**, 7.

19. **Bramley,P.M. and Mackenzie,A.**, 1988. Regulation of carotenoid biosynthesis. **29**, 291-343.

20. **Buchan,J.R. and Parker,R.**, 2009. Eukaryotic stress granules: the ins and outs of translation. **36**, 932-941.

21. **Buttgereit,F. and Brand,M.D.**, 1995. A hierarchy of ATP-consuming processes in mammalian cells. **312 (Pt 1)**, 163-167.

22. **Cappell,S.D., Baker,R., Skowyra,D., and Dohlman,H.G.**, 2010. Systematic analysis of essential genes reveals important regulators of G protein signaling. **38**, 746-757.

23. **Carter,C., Pan,S., Zouhar,J., Avila,E.L., Girke,T., and Raikhel,N.V.**, 2004. The vegetative vacuole proteome of Arabidopsis thaliana reveals predicted and unexpected proteins. **16**, 3285-3303.

24. **Case,M.E. and Giles,N.H.**, 1958. EVIDENCE FROM TETRAD ANALYSIS FOR BOTH NORMAL AND ABERRANT RECOMBINATION BETWEEN ALLELIC MUTANTS IN Neurospora Crassa. **44**, 378-390.

25. **Case,M.E., Schweizer,M., Kushner,S.R., and Giles,N.H.**, 1979. Efficient transformation of Neurospora crassa by utilizing hybrid plasmid DNA. **76**, 5259-5263.

26. **Chan,P., Thomas,C.J., Sprang,S.R., and Tall,G.G.**, 2013. Molecular chaperoning function of Ric-8 is to fold nascent heterotrimeric G protein alpha subunits. **110**, 3794-3799.

27. **Chen,C.H., Dunlap,J.C., and Loros,J.J.**, 2010. Neurospora illuminates fungal photoreception. **47**, 922-929.

28. **Christianson,T.W., Sikorski,R.S., Dante,M., Shero,J.H., and Hieter,P.**, 1992. Multifunctional yeast high-copy-number shuttle vectors. **110**, 119-122.

29. **Collopy,P.D., Colot,H.V., Park,G., Ringelberg,C., Crew,C.M., Borkovich,K.A., and Dunlap,J.C.**, 2010. High-throughput construction of gene deletion cassettes for generation of Neurospora crassa knockout strains. **638**, 33-40.

30. **Colot,H.V., Park,G., Turner,G.E., Ringelberg,C., Crew,C.M., Litvinkova,L., Weiss,R.L., Borkovich,K.A., and Dunlap,J.C.**, 2006. A high-throughput gene knockout procedure for Neurospora reveals functions for multiple transcription factors. **103**, 10352-10357.

31. **Costache,A., Bucurenci,N., and Onu,A.**, 2013. Adenylate cyclases involvement in pathogenicity, a minireview. **72**, 63-86.

32. **Crouthamel,M., Thiyagarajan,M.M., Evanko,D.S., and Wedegaertner,P.B.**, 2008. N-terminal polybasic motifs are required for plasma membrane localization of Galpha(s) and Galpha(q). **20**, 1900-1910.

33. **Csibi,A., Cornille,K., Leibovitch,M.P., Poupon,A., Tintignac,L.A., Sanchez,A.M., and Leibovitch,S.A.**, 2010. The translation regulatory subunit eIF3f controls the kinase-dependent mTOR signaling required for muscle differentiation and hypertrophy in mouse. **5**, e8994.

34. **Cyr,D.M. and Douglas,M.G.**, 1994. Differential regulation of Hsp70 subfamilies by the eukaryotic DnaJ homologue YDJ1. **269**, 9798-9804.

35. **Davis,R.H. and de Serres,F.J.**, 1970. Genetic and microbiological research techniques for Neurospora. **17**, 79-143.

36. **Davis,R.H. and Perkins,D.D.**, 2002. Timeline: Neurospora: a model of model microbes. **3**, 397-403.

37. **Dever,T.E. and Green,R.**, 2012. The elongation, termination, and recycling phases of translation in eukaryotes. **4**, a013706.

38. **Dunlap,J.C., Borkovich,K.A., Henn,M.R., Turner,G.E., Sachs,M.S., Glass,N.L., McCluskey,K., Plamann,M., Galagan,J.E., Birren,B.W., Weiss,R.L., Townsend,J.P., Loros,J.J., Nelson,M.A., Lambreghts,R., Colot,H.V., Park,G., Collopy,P., Ringelberg,C., Crew,C., Litvinkova,L., DeCaprio,D., Hood,H.M., Curilla,S., Shi,M., Crawford,M., Koerhsen,M., Montgomery,P., Larson,L., Pearson,M., Kasuga,T., Tian,C., Basturkmen,M., Altamirano,L., and Xu,J.**, 2007. Enabling a community to dissect an organism: overview of the Neurospora functional genomics project. **57**, 49-96.

39. **Esposito,A.M., Mateyak,M., He,D., Lewis,M., Sasikumar,A.N., Hutton,J., Copeland,P.R., and Kinzy,T.G.**, 2010. Eukaryotic polyribosome profile analysis.

40. **Fleissner,A., Simonin,A.R., and Glass,N.L.**, 2008. Cell fusion in the filamentous fungus, Neurospora crassa. **475**, 21-38.

41. **Fleming,J.A., Lightcap,E.S., Sadis,S., Thoroddsen,V., Bulawa,C.E., and Blackman,R.K.**, 2002. Complementary whole-genome technologies reveal the cellular response to proteasome inhibition by PS-341. **99**, 1461-1466.

42. **Gaber,R.F., Copple,D.M., Kennedy,B.K., Vidal,M., and Bard,M.**, 1989. The yeast gene ERG6 is required for normal membrane function but is not essential for biosynthesis of the cell-cycle-sparking sterol. **9**, 3447-3456.

43. **Galagan,J.E., Calvo,S.E., Borkovich,K.A., Selker,E.U., Read,N.D., Jaffe,D., FitzHugh,W., Ma,L.J., Smirnov,S., Purcell,S., Rehman,B., Elkins,T., Engels,R., Wang,S., Nielsen,C.B., Butler,J., Endrizzi,M., Qui,D., Ianakiev,P., Bell-Pedersen,D., Nelson,M.A., Werner-Washburne,M., Selitrennikoff,C.P., Kinsey,J.A., Braun,E.L., Zelter,A., Schulte,U., Kothe,G.O., Jedd,G., Mewes,W., Staben,C., Marcotte,E., Greenberg,D., Roy,A., Foley,K., Naylor,J., Stange-Thomann,N., Barrett,R., Gnerre,S., Kamal,M., Kamvysselis,M., Mauceli,E., Bielke,C., Rudd,S., Frishman,D., Krystofova,S., Rasmussen,C., Metzenberg,R.L., Perkins,D.D., Kroken,S., Cogoni,C., Macino,G., Catcheside,D., Li,W., Pratt,R.J., Osmani,S.A., DeSouza,C.P., Glass,L., Orbach,M.J., Berglund,J.A., Voelker,R., Yarden,O., Plamann,M., Seiler,S., Dunlap,J., Radford,A., Aramayo,R., Natvig,D.O., Alex,L.A., Mannhaupt,G., Ebbole,D.J., Freitag,M., Paulsen,I., Sachs,M.S., Lander,E.S., Nusbaum,C., and Birren,B.**, 2003. The genome sequence of the filamentous fungus Neurospora crassa. **422**, 859-868.

44. **Gallie,D.R.**, 1991. The cap and poly(A) tail function synergistically to regulate mRNA translational efficiency. **5**, 2108-2116.

45. **Gebauer,F., Preiss,T., and Hentze,M.W.**, 2012. From cis-regulatory elements to complex RNPs and back. **4**, a012245.

46. **Gerashchenko,M.V. and Gladyshev,V.N.**, 2014. Translation inhibitors cause abnormalities in ribosome profiling experiments. **42**, e134.

47. **Glickman,M.H., Rubin,D.M., Fu,H., Larsen,C.N., Coux,O., Wefes,I., Pfeifer,G., Cjeka,Z., Vierstra,R., Baumeister,W., Fried,V., and Finley,D.**, 1999. Functional analysis of the proteasome regulatory particle. **26**, 21-28.

48. **Hampoelz,B., Hoeller,O., Bowman,S.K., Dunican,D., and Knoblich,J.A.**, 2005. Drosophila Ric-8 is essential for plasma-membrane localization of heterotrimeric G proteins. **7**, 1099-1105.

49. **Hanna,J. and Finley,D.**, 2007. A proteasome for all occasions. **581**, 2854-2861.

50. **Harris,S.D. and Momany,M.**, 2004. Polarity in filamentous fungi: moving beyond the yeast paradigm. **41**, 391-400.

51. **Harris,T.E., Chi,A., Shabanowitz,J., Hunt,D.F., Rhoads,R.E., and Lawrence,J.C., Jr.**, 2006. mTOR-dependent stimulation of the association of eIF4G and eIF3 by insulin. **25**, 1659-1668.

52. **Hay,N. and Sonenberg,N.**, 2004. Upstream and downstream of mTOR. **18**, 1926-1945.

53. **Hershey,J.W., Asano,K., Naranda,T., Vornlocher,H.P., Hanachi,P., and Merrick,W.C.**, 1996. Conservation and diversity in the structure of translation initiation factor EIF3 from humans and yeast. **78**, 903-907.

54. **Hershey,J.W., Sonenberg,N., and Mathews,M.B.**, 2012. Principles of translational control: an overview. **4**.

55. **Hickey,P.C., Jacobson,D., Read,N.D., and Louise Glass,N.L.**, 2002. Live-cell imaging of vegetative hyphal fusion in Neurospora crassa. **37**, 109-119.

56. **Hinnebusch,A.G. and Lorsch,J.R.**, 2012. The mechanism of eukaryotic translation initiation: new insights and challenges. **4**.

57. **Ho,Y., Gruhler,A., Heilbut,A., Bader,G.D., Moore,L., Adams,S.L., Millar,A., Taylor,P., Bennett,K., Boutilier,K., Yang,L., Wolting,C., Donaldson,I., Schandorff,S., Shewnarane,J., Vo,M., Taggart,J., Goudreault,M., Muskat,B., Alfarano,C., Dewar,D., Lin,Z., Michalickova,K., Willems,A.R., Sassi,H.,**

Nielsen,P.A., Rasmussen,K.J., Andersen,J.R., Johansen,L.E., Hansen,L.H., Jespersen,H., Podtelejnikov,A., Nielsen,E., Crawford,J., Poulsen,V., Sorensen,B.D., Matthiesen,J., Hendrickson,R.C., Gleeson,F., Pawson,T., Moran,M.F., Durocher,D., Mann,M., Hogue,C.W., Figeys,D., and Tyers,M., 2002. Systematic identification of protein complexes in Saccharomyces cerevisiae by mass spectrometry. **415**, 180-183.

58. **Holcik,M. and Sonenberg,N.**, 2005. Translational control in stress and apoptosis. **6**, 318-327.

59. **Holz,M.K., Ballif,B.A., Gygi,S.P., and Blenis,J.**, 2005. mTOR and S6K1 mediate assembly of the translation preinitiation complex through dynamic protein interchange and ordered phosphorylation events. **123**, 569-580.

60. **Hsueh,Y.P., Xue,C., and Heitman,J.**, 2007. G protein signaling governing cell fate decisions involves opposing Galpha subunits in Cryptococcus neoformans. **18**, 3237-3249.

61. **Hughes,T.E., Zhang,H., Logothetis,D.E., and Berlot,C.H.**, 2001. Visualization of a functional Galpha q-green fluorescent protein fusion in living cells. Association with the plasma membrane is disrupted by mutational activation and by elimination of palmitoylation sites, but not be activation mediated by receptors or AlF4-. **276**, 4227-4235.

62. **Husnjak,K., Elsasser,S., Zhang,N., Chen,X., Randles,L., Shi,Y., Hofmann,K., Walters,K.J., Finley,D., and Dikic,I.**, 2008. Proteasome subunit Rpn13 is a novel ubiquitin receptor. **453**, 481-488.

63. **Ito,T., Ota,K., Kubota,H., Yamaguchi,Y., Chiba,T., Sakuraba,K., and Yoshida,M.**, 2002. Roles for the two-hybrid system in exploration of the yeast protein interactome. **1**, 561-566.

64. **Ivey,F.D., Hodge,P.N., Turner,G.E., and Borkovich,K.A.**, 1996. The G alpha i homologue gna-1 controls multiple differentiation pathways in Neurospora crassa. **7**, 1283-1297.

65. **Ivey,F.D., Kays,A.M., and Borkovich,K.A.**, 2002. Shared and independent roles for a Galpha(i) protein and adenylyl cyclase in regulating development and stress responses in Neurospora crassa. **1**, 634-642.

66. **Ivey,F.D., Yang,Q., and Borkovich,K.A.**, 1999. Positive regulation of adenylyl cyclase activity by a galphai homolog in Neurospora crassa. **26**, 48-61.

67. **Jacobson,D.J., Dettman,J.R., Adams,R.I., Boesl,C., Sultana,S., Roenneberg,T., Merrow,M., Duarte,M., Marques,I., Ushakova,A.,**

Carneiro,P., Videira,A., Navarro-Sampedro,L., Olmedo,M., Corrochano,L.M., and Taylor,J.W., 2006. New findings of Neurospora in Europe and comparisons of diversity in temperate climates on continental scales. **98**, 550-559.

68. **Jacobson,D.J., Powell,A.J., Dettman,J.R., Saenz,G.S., Barton,M.M., Hiltz,M.D., Dvorachek,W.H., Jr., Glass,N.L., Taylor,J.W., and Natvig,D.O.**, 2004. Neurospora in temperate forests of western North America. **96**, 66-74.

69. **Jacobson,K.A., Costanzi,S., and Deflorian,F.**, 2013. Probing GPCR structure: adenosine and P2Y nucleotide receptors. **520**, 199-217.

70. **Janetopoulos,C., Jin,T., and Devreotes,P.**, 2001. Receptor-mediated activation of heterotrimeric G-proteins in living cells. **291**, 2408-2411.

71. **Johansson,B.B., Minsaas,L., and Aragay,A.M.**, 2005. Proteasome involvement in the degradation of the G(q) family of Galpha subunits. **272**, 5365-5377.

72. **Johnston,C.A., Afshar,K., Snyder,J.T., Tall,G.G., Gonczy,P., Siderovski,D.P., and Willard,F.S.**, 2008. Structural determinants underlying the temperature-sensitive nature of a Galpha mutant in asymmetric cell division of Caenorhabditis elegans. **283**, 21550-21558.

73. **Jones,E.W.**, 1991. Tackling the protease problem in Saccharomyces cerevisiae. **194**, 428-453.

74. **Kach,J., Sethakorn,N., and Dulin,N.O.**, 2012. A finer tuning of G-protein signaling through regulated control of RGS proteins. **303**, H19-H35.

75. **Kasahara,S., Wang,P., and Nuss,D.L.**, 2000. Identification of bdm-1, a gene involved in G protein beta-subunit function and alpha-subunit accumulation. **97**, 412-417.

76. **Kays,A.M. and Borkovich,K.A.**, 2004. Severe impairment of growth and differentiation in a Neurospora crassa mutant lacking all heterotrimeric G alpha proteins. **166**, 1229-1240.

77. **Kays,A.M., Rowley,P.S., Baasiri,R.A., and Borkovich,K.A.**, 2000. Regulation of conidiation and adenylyl cyclase levels by the Galpha protein GNA-3 in Neurospora crassa. **20**, 7693-7705.

78. **Kedersha,N. and Anderson,P.**, 2007. Mammalian stress granules and processing bodies. **431**, 61-81.

79. **Kim,H. and Borkovich,K.A.**, 2004. A pheromone receptor gene, pre-1, is essential for mating type-specific directional growth and fusion of trichogynes and female fertility in Neurospora crassa. **52**, 1781-1798.

80. **Kimura,Y., Yahara,I., and Lindquist,S.**, 1995. Role of the protein chaperone YDJ1 in establishing Hsp90-mediated signal transduction pathways. **268**, 1362-1365.

81. **Kritsky,M.S., Sokolovsky,V.Y., Belozerskaya,T.A., and Chernysheva,E.K.**, 1982. Relationship between cyclic AMP level and accumulation of carotenoid pigments in Neurospora crassa. **133**, 206-208.

82. **Krystofova,S. and Borkovich,K.A.**, 2005. The heterotrimeric G-protein subunits GNG-1 and GNB-1 form a Gbetagamma dimer required for normal female fertility, asexual development, and galpha protein levels in Neurospora crassa. **4**, 365-378.

83. **Kuck,U. and Hoff,B.**, 2006. Application of the nourseothricin acetyltransferase gene (nat1) as dominant marker for the transformation of filamentous fungi. **53**, 9-11.

84. **Lambreghts,R., Shi,M., Belden,W.J., DeCaprio,D., Park,D., Henn,M.R., Galagan,J.E., Basturkmen,M., Birren,B.W., Sachs,M.S., Dunlap,J.C., and Loros,J.J.**, 2009. A high-density single nucleotide polymorphism map for Neurospora crassa. **181**, 767-781.

85. **Lee,D.H. and Goldberg,A.L.**, 1996. Selective inhibitors of the proteasome-dependent and vacuolar pathways of protein degradation in Saccharomyces cerevisiae. **271**, 27280-27284.

86. **Li,D., Bobrowicz,P., Wilkinson,H.H., and Ebbole,D.J.**, 2005. A mitogen-activated protein kinase pathway essential for mating and contributing to vegetative growth in Neurospora crassa. **170**, 1091-1104.

87. **Li,L. and Borkovich,K.A.**, 2006. GPR-4 is a predicted G-protein-coupled receptor required for carbon source-dependent asexual growth and development in Neurospora crassa. **5**, 1287-1300.

88. **Li,L., Wright,S.J., Krystofova,S., Park,G., and Borkovich,K.A.**, 2007. Heterotrimeric G protein signaling in filamentous fungi. **61**, 423-452.

89. **Liu,C., Apodaca,J., Davis,L.E., and Rao,H.**, 2007. Proteasome inhibition in wild-type yeast Saccharomyces cerevisiae cells. **42**, 158, 160, 162.

90. **Lleres,D., Swift,S., and Lamond,A.I.**, 2007. Detecting protein-protein interactions in vivo with FRET using multiphoton fluorescence lifetime imaging microscopy (FLIM). **Chapter 12**, Unit12.

91. **Loros,J.J. and Dunlap,J.C.**, 1991. Neurospora crassa clock-controlled genes are regulated at the level of transcription. **11**, 558-563.

92. **Loros,J.J., Dunlap,J.C., Larrondo,L.F., Shi,M., Belden,W.J., Gooch,V.D., Chen,C.H., Baker,C.L., Mehra,A., Colot,H.V., Schwerdtfeger,C., Lambreghts,R., Collopy,P.D., Gamsby,J.J., and Hong,C.I.**, 2007. Circadian output, input, and intracellular oscillators: insights into the circadian systems of single cells. **72**, 201-214.

93. **Lu,Z. and Cyr,D.M.**, 1998. The conserved carboxyl terminus and zinc finger-like domain of the co-chaperone Ydj1 assist Hsp70 in protein folding. **273**, 5970-5978.

94. **Luo,Z., Freitag,M., and Sachs,M.S.**, 1995. Translational regulation in response to changes in amino acid availability in Neurospora crassa. **15**, 5235-5245.

95. **Maheshwari,R.**, 1999. Microconidia of Neurospora crassa. **26**, 1-18.

96. **Marrari,Y., Crouthamel,M., Irannejad,R., and Wedegaertner,P.B.**, 2007. Assembly and trafficking of heterotrimeric G proteins. **46**, 7665-7677.

97. **Martineau,Y., Wang,X., Alain,T., Petroulakis,E., Shahbazian,D., Fabre,B., Bousquet-Dubouch,M.P., Monsarrat,B., Pyronnet,S., and Sonenberg,N.**, 2014. Control of Paip1-eukayrotic translation initiation factor 3 interaction by amino acids through S6 kinase. **34**, 1046-1053.

98. **Mende,U., Zagrovic,B., Cohen,A., Li,Y., Valenzuela,D., Fishman,M.C., and Neer,E.J.**, 1998. Effect of deletion of the major brain G-protein alpha subunit (alpha(o)) on coordination of G-protein subunits and on adenylyl cyclase activity. **54**, 263-272.

99. **Mendoza,M.C., Er,E.E., and Blenis,J.**, 2011. The Ras-ERK and PI3K-mTOR pathways: cross-talk and compensation. **36**, 320-328.

100. **Merrick,W.C. and Hensold,J.O.**, 2001. Analysis of eukaryotic translation in purified and semipurified systems. **Chapter 11**, Unit.

101. **Miller,K.G., Emerson,M.D., McManus,J.R., and Rand,J.B.**, 2000. RIC-8 (Synembryn): a novel conserved protein that is required for G(q)alpha signaling in the C. elegans nervous system. **27**, 289-299.

102. **Miller,K.G. and Rand,J.B.**, 2000. A role for RIC-8 (Synembryn) and GOA-1 (G(o)alpha) in regulating a subset of centrosome movements during early embryogenesis in Caenorhabditis elegans. **156**, 1649-1660.

103. **Moresco,J.J., Carvalho,P.C., and Yates,J.R., III**, 2010. Identifying components of protein complexes in C. elegans using co-immunoprecipitation and mass spectrometry. **73**, 2198-2204.

104. **Munoz,A. and Castellano,M.M.**, 2012. Regulation of Translation Initiation under Abiotic Stress Conditions in Plants: Is It a Conserved or Not so Conserved Process among Eukaryotes? **2012**, 406357.

105. **Mustroph,A., Juntawong,P., and Bailey-Serres,J.**, 2009. Isolation of plant polysomal mRNA by differential centrifugation and ribosome immunopurification methods. **553**, 109-126.

106. **Nagai,Y., Nishimura,A., Tago,K., Mizuno,N., and Itoh,H.**, 2010. Ric-8B stabilizes the alpha subunit of stimulatory G protein by inhibiting its ubiquitination. **285**, 11114-11120.

107. **Ninomiya,Y., Suzuki,K., Ishii,C., and Inoue,H.**, 2004. Highly efficient gene replacements in Neurospora strains deficient for nonhomologous end-joining. **101**, 12248-12253.

108. **Oldham,W.M. and Hamm,H.E.**, 2008. Heterotrimeric G protein activation by G-protein-coupled receptors. **9**, 60-71.

109. **Pandey,A., Roca,M.G., Read,N.D., and Glass,N.L.**, 2004. Role of a mitogen-activated protein kinase pathway during conidial germination and hyphal fusion in Neurospora crassa. **3**, 348-358.

110. **Park,G., Colot,H.V., Collopy,P.D., Krystofova,S., Crew,C., Ringelberg,C., Litvinkova,L., Altamirano,L., Li,L., Curilla,S., Wang,W., Gorrochotegui-Escalante,N., Dunlap,J.C., and Borkovich,K.A.**, 2011. High-throughput production of gene replacement mutants in Neurospora crassa. **722**, 179-189.

111. **Park,G., Pan,S., and Borkovich,K.A.**, 2008. Mitogen-activated protein kinase cascade required for regulation of development and secondary metabolism in Neurospora crassa. **7**, 2113-2122.

112. **Parker,R. and Sheth,U.**, 2007. P bodies and the control of mRNA translation and degradation. **25**, 635-646.

113. **Perkins,D.D.**, 1984. Advantages of using the inactive-mating-type am1 strain as a helper component in heterokaryons. **31**, 41-42.

114. **Perlman,J. and Feldman,J.F.**, 1982. Cycloheximide and heat shock induce new polypeptide synthesis in Neurospora crassa. **2**, 1167-1173.

115. **Pickart,C.M. and Cohen,R.E.**, 2004. Proteasomes and their kin: proteases in the machine age. **5**, 177-187.

116. **Raghavan,A., Ogilvie,R.L., Reilly,C., Abelson,M.L., Raghavan,S., Vasdewani,J., Krathwohl,M., and Bohjanen,P.R.**, 2002. Genome-wide analysis of mRNA decay in resting and activated primary human T lymphocytes. **30**, 5529-5538.

117. **Raju,N.B.**, 1992. Genetic control of the sexual cycle in Neurospora. **96**, 241-262.

118. **Raju,N.B.**, 2009. Neurospora as a model fungus for studies in cytogenetics and sexual biology at Stanford. **34**, 139-159.

119. **Rao,V.S., Srinivas,K., Sujini,G.N., and Kumar,G.N.**, 2014. Protein-protein interaction detection: methods and analysis. **2014**, 147648.

120. **Rojo,E., Martin,R., Carter,C., Zouhar,J., Pan,S., Plotnikova,J., Jin,H., Paneque,M., Sanchez-Serrano,J.J., Baker,B., Ausubel,F.M., and Raikhel,N.V.**, 2004. VPEgamma exhibits a caspase-like activity that contributes to defense against pathogens. **14**, 1897-1906.

121. **Rosen,S., Yu,J.H., and Adams,T.H.**, 1999. The Aspergillus nidulans sfaD gene encodes a G protein beta subunit that is required for normal growth and repression of sporulation. **18**, 5592-5600.

122. **Rosenbaum,D.M., Rasmussen,S.G., and Kobilka,B.K.**, 2009. The structure and function of G-protein-coupled receptors. **459**, 356-363.

123. **Rosenberg,G. and Pall,M.L.**, 1979. Properties of two cyclic nucleotide-deficient mutants of Neurospora crassa. **137**, 1140-1144.

124. **Rosenberg,G.B. and Pall,M.L.**, 1983. Characterization of an ATP-Mg2+-dependent guanine nucleotide-stimulated adenylate cyclase from Neurospora crassa. **221**, 243-253.

125. **Roux,P.P. and Topisirovic,I.**, 2012. Regulation of mRNA translation by signaling pathways. **4**.

126. **Rubin,D.M., Glickman,M.H., Larsen,C.N., Dhruvakumar,S., and Finley,D.**, 1998. Active site mutants in the six regulatory particle ATPases reveal multiple roles for ATP in the proteasome. **17**, 4909-4919.

127. **Ruepp,A., Zollner,A., Maier,D., Albermann,K., Hani,J., Mokrejs,M., Tetko,I., Guldener,U., Mannhaupt,G., Munsterkotter,M., and Mewes,H.W.**, 2004. The FunCat, a functional annotation scheme for systematic classification of proteins from whole genomes. **32**, 5539-5545.

128. **Ryazanov,A.G. and Davydova,E.K.**, 1989. Mechanism of elongation factor 2 (EF-2) inactivation upon phosphorylation. Phosphorylated EF-2 is unable to catalyze translocation. **251**, 187-190.

129. **Schmittgen,T.D. and Livak,K.J.**, 2008. Analyzing real-time PCR data by the comparative C(T) method. **3**, 1101-1108.

130. **Semple,J.I., Sanderson,C.M., and Campbell,R.D.**, 2002. The jury is out on "guilt by association" trials. **1**, 40-52.

131. **Shalgi,R., Hurt,J.A., Krykbaeva,I., Taipale,M., Lindquist,S., and Burge,C.B.**, 2013. Widespread regulation of translation by elongation pausing in heat shock. **49**, 439-452.

132. **Sheikh,M.S. and Fornace,A.J., Jr.**, 1999. Regulation of translation initiation following stress. **18**, 6121-6128.

133. **Sherman,F.**, 1991. Getting started with yeast. **194**, 3-21.

134. **Shi,J., Feng,Y., Goulet,A.C., Vaillancourt,R.R., Sachs,N.A., Hershey,J.W., and Nelson,M.A.**, 2003. The p34cdc2-related cyclin-dependent kinase 11 interacts with the p47 subunit of eukaryotic initiation factor 3 during apoptosis. **278**, 5062-5071.

135. **Shi,J., Kahle,A., Hershey,J.W., Honchak,B.M., Warneke,J.A., Leong,S.P., and Nelson,M.A.**, 2006. Decreased expression of eukaryotic initiation factor 3f deregulates translation and apoptosis in tumor cells. **25**, 4923-4936.

136. **Shyu,A.B., Greenberg,M.E., and Belasco,J.G.**, 1989. The c-fos transcript is targeted for rapid decay by two distinct mRNA degradation pathways. **3**, 60-72.

137. **Siderovski,D.P. and Willard,F.S.**, 2005. The GAPs, GEFs, and GDIs of heterotrimeric G-protein alpha subunits. **1**, 51-66.

138. **Siegel,M.R. and Sisler,H.D.**, 1963. INHIBITION OF PROTEIN SYNTHESIS IN VITRO BY CYCLOHEXIMIDE. **200**, 675-676.

139. **Sikorski,R.S. and Hieter,P.**, 1989. A system of shuttle vectors and yeast host strains designed for efficient manipulation of DNA in Saccharomyces cerevisiae. **122**, 19-27.

140. **Smalle,J. and Vierstra,R.D.**, 2004. The ubiquitin 26S proteasome proteolytic pathway. **55**, 555-590.

141. **Sone,T., Saeki,Y., Toh-e A, and Yokosawa,H.**, 2004. Sem1p is a novel subunit of the 26 S proteasome from Saccharomyces cerevisiae. **279**, 28807-28816.

142. **Sonenberg,N. and Hinnebusch,A.G.**, 2009. Regulation of translation initiation in eukaryotes: mechanisms and biological targets. **136**, 731-745.

143. **Springer,M.L.**, 1993. Genetic control of fungal differentiation: the three sporulation pathways of Neurospora crassa. **15**, 365-374.

144. **Springer,M.L. and Yanofsky,C.**, 1989. A morphological and genetic analysis of conidiophore development in Neurospora crassa. **3**, 559-571.

145. **Stansfield,I., Jones,K.M., Kushnirov,V.V., Dagkesamanskaya,A.R., Poznyakovski,A.I., Paushkin,S.V., Nierras,C.R., Cox,B.S., Ter-Avanesyan,M.D., and Tuite,M.F.**, 1995. The products of the SUP45 (eRF1) and SUP35 genes interact to mediate translation termination in Saccharomyces cerevisiae. **14**, 4365-4373.

146. **Stoldt,V., Rademacher,F., Kehren,V., Ernst,J.F., Pearce,D.A., and Sherman,F.**, 1996. Review: the Cct eukaryotic chaperonin subunits of Saccharomyces cerevisiae and other yeasts. **12**, 523-529.

147. **Tall,G.G.**, 2013. Ric-8 regulation of heterotrimeric G proteins. **33**, 139-143.

148. **Tall,G.G., Krumins,A.M., and Gilman,A.G.**, 2003. Mammalian Ric-8A (synembryn) is a heterotrimeric Galpha protein guanine nucleotide exchange factor. **278**, 8356-8362.

149. **Tee,A.R., Blenis,J., and Proud,C.G.**, 2005. Analysis of mTOR signaling by the small G-proteins, Rheb and RhebL1. **579**, 4763-4768.

150. **Thomas,C.J., Tall,G.G., Adhikari,A., and Sprang,S.R.**, 2008. Ric-8A catalyzes guanine nucleotide exchange on G alphai1 bound to the GPR/GoLoco exchange inhibitor AGS3. **283**, 23150-23160.

151. **Tomko,R.J., Jr. and Hochstrasser,M.**, 2014. The intrinsically disordered Sem1 protein functions as a molecular tether during proteasome lid biogenesis. **53**, 433-443.

152. **Tonissoo,T., Lulla,S., Meier,R., Saare,M., Ruisu,K., Pooga,M., and Karis,A.**, 2010. Nucleotide exchange factor RIC-8 is indispensable in mammalian early development.

153. **Torres,M.P., Lee,M.J., Ding,F., Purbeck,C., Kuhlman,B., Dokholyan,N.V., and Dohlman,H.G.**, 2009. G Protein Mono-ubiquitination by the Rsp5 Ubiquitin Ligase. **284**, 8940-8950.

154. **Turner,B.C., Perkins,D.D., and Fairfield,A.**, 2001. Neurospora from natural populations: a global study. **32**, 67-92.

155. **Turner,G.E. and Borkovich,K.A.**, 1993. Identification of a G protein alpha subunit from Neurospora crassa that is a member of the Gi family. **268**, 14805-14811.

156. **Verma,R., Chen,S., Feldman,R., Schieltz,D., Yates,J., Dohmen,J., and Deshaies,R.J.**, 2000. Proteasomal proteomics: identification of nucleotide-sensitive proteasome-interacting proteins by mass spectrometric analysis of affinity-purified proteasomes. **11**, 3425-3439.

157. **Verwoerd,T.C., Dekker,B.M., and Hoekema,A.**, 1989. A small-scale procedure for the rapid isolation of plant RNAs. **17**, 2362.

158. **Vigfusson,N.V. and Cano,R.J.**, 1974. Artificial induction of the sexual cycle of Neurospora crassa. **249**, 383-385.

159. **Vogel,H.J.**, 1964. Distribution of lysine pathways among fungi: evolutionary implications. **98**, 435-436.

160. **Voges,D., Watzele,M., Nemetz,C., Wizemann,S., and Buchberger,B.**, 2004. Analyzing and enhancing mRNA translational efficiency in an Escherichia coli in vitro expression system. **318**, 601-614.

161. **Voges,D., Zwickl,P., and Baumeister,W.**, 1999. The 26S proteasome: a molecular machine designed for controlled proteolysis. **68**, 1015-1068.

162. **Wang,Y., Liu,C.L., Storey,J.D., Tibshirani,R.J., Herschlag,D., and Brown,P.O.**, 2002. Precision and functional specificity in mRNA decay. **99**, 5860-5865.

163. **Wang,Y., Marotti,L.A., Jr., Lee,M.J., and Dohlman,H.G.**, 2005. Differential regulation of G protein alpha subunit trafficking by mono- and polyubiquitination. **280**, 284-291.

164. **Wang,Z. and Sachs,M.S.**, 1997. Ribosome stalling is responsible for arginine-specific translational attenuation in Neurospora crassa. **17**, 4904-4913.

165. **Watson,N., Linder,M.E., Druey,K.M., Kehrl,J.H., and Blumer,K.J.**, 1996. RGS family members: GTPase-activating proteins for heterotrimeric G-protein alpha-subunits. **383**, 172-175.

166. **Welihinda,A.A., Beavis,A.D., and Trumbly,R.J.**, 1994. Mutations in LIS1 (ERG6) gene confer increased sodium and lithium uptake in Saccharomyces cerevisiae. **1193**, 107-117.

167. **Westergaard,M. and Mitchell,H.K.**, 1947. Neurospora V. A Synthetic Medium Favoring Sexual Reproduction.

168. **Westermarck,J., Ivaska,J., and Corthals,G.L.**, 2013. Identification of protein interactions involved in cellular signaling. **12**, 1752-1763.

169. **Wilkie,G.S., Dickson,K.S., and Gray,N.K.**, 2003. Regulation of mRNA translation by 5'- and 3'-UTR-binding factors. **28**, 182-188.

170. **Wilkie,T.M. and Kinch,L.**, 2005. New roles for Galpha and RGS proteins: communication continues despite pulling sisters apart. **15**, R843-R854.

171. **Williams,A.J., Werner-Fraczek,J., Chang,I.F., and Bailey-Serres,J.**, 2003. Regulated phosphorylation of 40S ribosomal protein S6 in root tips of maize. **132**, 2086-2097.

172. **Winston,F., Dollard,C., and Ricupero-Hovasse,S.L.**, 1995. Construction of a set of convenient Saccharomyces cerevisiae strains that are isogenic to S288C. **11**, 53-55.

173. **Won,S., Michkov,A.V., Krystofova,S., Garud,A.V., and Borkovich,K.A.**, 2012. Genetic and Physical Interactions between Galpha Subunits and Components of the Gbetagamma Dimer of Heterotrimeric G Proteins in Neurospora crassa. **11**, 1239-1248.

174. **Wright,S.J., Inchausti,R., Eaton,C.J., Krystofova,S., and Borkovich,K.A.**, 2011. RIC8 is a guanine-nucleotide exchange factor for Galpha subunits that regulates growth and development in Neurospora crassa. **189**, 165-176.

175. **Xu,B.E. and Kurjan,J.**, 1997. Evidence that mating by the Saccharomyces cerevisiae gpa1Val50 mutant occurs through the default mating pathway and a suggestion of a role for ubiquitin-mediated proteolysis. **8**, 1649-1664.

176. **Yang,Q. and Borkovich,K.A.**, 1999. Mutational activation of a Galphai causes uncontrolled proliferation of aerial hyphae and increased sensitivity to heat and oxidative stress in Neurospora crassa. **151**, 107-117.

177. **Yang,Q., Poole,S.I., and Borkovich,K.A.**, 2002. A G-protein beta subunit required for sexual and vegetative development and maintenance of normal G alpha protein levels in Neurospora crassa. **1**, 378-390.

178. **Zamborszky,J., Csikasz-Nagy,A., and Hong,C.I.**, 2014. Neurospora crassa as a model organism to explore the interconnected network of the cell cycle and the circadian clock. **71C**, 52-57.

179. **Zhouravleva,G., Frolova,L., Le,G., X, Le,G.R., Inge-Vechtomov,S., Kisselev,L., and Philippe,M.**, 1995. Termination of translation in eukaryotes is governed by two interacting polypeptide chain release factors, eRF1 and eRF3. **14**, 4065-4072.